Fakultät für Physik der Technischen Universität München, E15

The cosmogenic and anthropogenic ^{36}Cl in the environment

Vitali Lazarev

Vollständiger Abdruck der von der Fakultät für Physik
der Technischen Universität München
zur Erlangung des akademischen Grades eines

Doktors der Naturwissenschaften

(Dr. rer. nat.)

genehmigten Dissertation.

Vorsitzender:	Univ.-Prof. Dr. P. Ring
Prüfer der Dissertation:	1. Univ.-Prof. Dr. E. Nolte
	2. Univ.-Prof. Dr. R. Krücken

Die Dissertation wurde am 11.03.2003 bei der Technischen Universität München eingereicht und durch die Fakultät für Physik am 09.04.2003 angenommen.

Abstract

The origin of ^{36}Cl in the environment was investigated in this work. Together with its natural production due to cosmic rays, the anthropogenic input during nuclear weapon tests and due to the accident at Chernobyl nuclear power plant was considered. The hypothesis of the bomb-produced ^{36}Cl recycling via the biosphere was proved experimentally.

Water samples were collected from European, African, and Asian lakes and delivered to Technische Universität München. After a chemical treatment, ratio of $^{36}Cl/Cl$ was measured with accelerator mass spectrometry in Garching. The stable chlorine concentration was measured chromatographically. The obtained ^{36}Cl concentration was in the range from $0.6 \cdot 10^7$ at/l to $210 \cdot 10^7$ at/l.

High ^{36}Cl content in European lakes was assigned to the Chernobyl accident. The comparison of the ^{36}Cl and ^{137}Cs contamination showed that a ^{137}Cs activity of 1 kBq m^{-2} corresponds to a ^{36}Cl deposition of about $9 \cdot 10^{10}$ atoms per square meter. The total ^{36}Cl release from the Chernobyl accident was estimated to be 0.5±0.2 kg.

A box model was used to describe the atmospheric transport of radionuclides. The latitudinal distributions of the cosmogenic and bomb-produced ^{36}Cl were simulated. The ^{36}Cl concentration in African and Asian lakes was used to normalize the stratospheric release of ^{36}Cl from the near-water nuclear weapon tests. About 18% of the ^{36}Cl produced in the ocean reached the stratosphere. A total stratospheric emission of 24±9 kg of ^{36}Cl was obtained.

The results of the modeling were in a good agreement with the measurements for most of the lakes. This fact was used to estimate unknown hydrological parameters of lakes. The groundwater age of two lakes with short flushing times: Ammersee and Chiemsee was determined. The closure age of Issyk-Kul Lake was estimated to be about 270,000 years.

A part of the bomb ^{36}Cl was considered to be stored in the biosphere and to be released as $CH_3{}^{36}Cl$ to the troposphere. An experimental setup to determine the ^{36}Cl content in tropospheric CH_3Cl was developed. The measurements performed in Kranzberger Forst showed that the mean global recycled ^{36}Cl flux could be up to 70 at m^{-2} s^{-1}. The implementation of the recycling into the transport model explained the discrepancy of the simulated and measured ^{36}Cl flux, previously observed in modern precipitation.

Table of content

Introduction

^{36}Cl is a radioactive nuclide with a half-life of 301 kyr. It is produced naturally in spallation reactions on atmospheric argon induced by high-energy particles of cosmic rays (CR). The success of accelerator mass-spectrometry (AMS) allowed ^{36}Cl measurements with sensitivity better than 10^{-14} relative to the stable chlorine [1]. The ^{36}Cl concentration determined in dated samples could be used to reconstruct the CR intensity over 1 million years in the past if the conditions of its production and fallout were known [2]. ^{36}Cl proved to be a valuable tracer in hydrological studies and a useful dating tool for glaciers and ground water [3]. Interesting applications come up due to the anthropogenic ^{36}Cl released during nuclear weapon tests [4, 5] and the Chernobyl accident. Short ^{36}Cl pulses with large amplitude can be used as a marker and the time decrease of the ^{36}Cl concentration in environmental compartments can be used to study exchange processes.

However, a number of questions arise when the method of ^{36}Cl is applied. No study to determine the latitudinal distribution of the ^{36}Cl bomb pulse was performed until this work. The interpretation of local ^{36}Cl deposition based on the typical latitudinal distribution of cosmogenic radionuclide fallout obtained in [2] and normalized with the integral deposition of bomb ^{36}Cl in Greenland [5] failed to describe the measurements [6, 7]. A significant discrepancy was also observed when the calculated cosmogenic ^{36}Cl fluxes were compared with the measurements in modern precipitation [8].

Recycling of bomb-produced ^{36}Cl via the biosphere was suggested in [9] and in [8]. The main role of the ^{36}Cl back transfer to the troposphere was assigned to methyl chloride. However, no experimental confirmation of the recycling existed until this work.

The aim of this work was measurements of ^{36}Cl concentration in the environment with the following analysis of the ^{36}Cl sources.

- Lakes with long flushing time were chosen as environmental compartments to study the ^{36}Cl distribution. Due to its hydrophilic properties, chlorine from the catchment area of a lake remains attached to water and enters the lake. The only way of its removal from the reservoir is flow out with the water. The advantage of using large water systems is the natural averaging of the input signal over the catchment area and

the flushing time. Thus, the ^{36}Cl concentration in the lake is not influenced by small local effects. On the contrary, the influence of large-scale events with the total inventory much larger than the annual natural production of ^{36}Cl can be determined.

- The second environmental compartment to study the ^{36}Cl content was methyl chloride. Thus, the first direct experimental confirmation of the recycling was obtained.

The first chapter of the thesis gives a general overview of ^{36}Cl in the environment. Available information on the mechanisms of ^{36}Cl production and its transport is presented. In the second chapter, the models and the background of experiments are discussed. The atmospheric transport and the radionuclide injection into the stratosphere during the nuclear weapon tests are described there. The third chapter is dedicated to the experimental equipment, which was used for the measurements. The facility of accelerator mass spectrometry in Garching, the high performance liquid chromatography, and the setup for the CH_3Cl collection are described. The results of the measurements and modeling are discussed in the forth chapter. The ^{36}Cl input due to Chernobyl accident and due to nuclear bomb tests is estimated. A ^{36}Cl application for hydrology is illustrated for a few examples. A mean groundwater age in basins of European lakes with flushing times below 5 years and the closure age of Issyk-Kul Lake are quantified.

CHAPTER 1. Radioactive chlorine-36 in the environment

1.1. *Cosmogenic isotopes*

The modern science of cosmogenic isotopes (CI) was founded in 1967, when the classical paper of *D. Lal and B. Peters* [2] appeared. Some other attempts to determine cosmic ray (CR) fluxes by measuring radionuclide concentrations had been performed before [2] but *D. Lal and B. Peters* were the first who managed to systemize available data, to describe the most important features of CI production, and to point out the main problems to be solved.

The largest difficulty in the 60s of the last century was the sensitivity of the experimental setup, which was not sufficient to measure reliably small amounts of radioactivity. That is why many conclusions about long-lived radioisotopes (e.g. ^{26}Al) were based on assumptions and estimations. A significant step forward was done, when accelerator mass spectrometry (AMS) was developed. First attempts to measure ^{3}He with the help of a cyclotron were performed in 1939 [10]. In 1977, Muller suggested using a cyclotron for radiocarbon dating in case it would be possible to separate the isobars ^{14}C and ^{14}N [11]. In the same year, it became clear that nitrogen did not produce negative ions [12] and shortly afterwards an accelerator with negative ion injection was used for the ^{14}C determination [13].

At present, much data combining the concentrations of radionuclides in different compartments of the environment all over the globe is available. A number of models were developed to explain the production and distribution of CI. However, the main features, which were pointed out by *Lal and Peters*, are still correct and can be used successfully.

High-energy nuclei of hydrogen, helium and heavier elements, which compose Galactic Cosmic Rays (GCR), diffuse through the galaxy and penetrate into the solar system (see Figure 1). The interaction with the magnetic field frozen in solar wind leads to solar modulation, to which the low energetic part of GCR is especially sensitive. The Sun also emits Solar Cosmic Rays (SCR), which are known as Solar Energetic Particles (SEP) in the

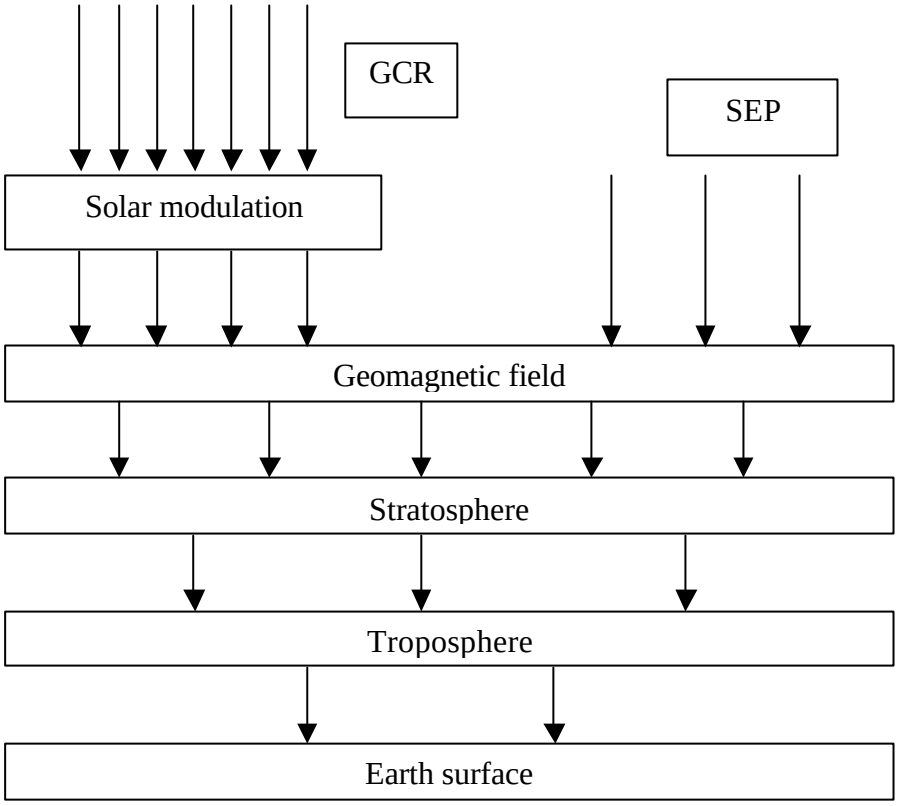

Figure 1. The penetration of Galactic Cosmic Rays (GCR) and of Solar Energetic Particles (SEP) into the atmosphere and to the Earth surface

modern literature [14]. Both GCR and SEP coming to the Earth interact with the geomagnetic field. Particles with low energy are reflected and only the high-energy nuclei are able to penetrate into the atmosphere. Thus, the geomagnetic cut-off takes place. It is stronger in equatorial region and weaker near the poles. The particles entering the atmosphere initiate nuclear, muon, and electron-photon cascades, which lead to the production of CI.

The produced isotopes are involved in the geochemical and geophysical cycles, which are specific for each element, and are transported to the surface of the Earth. Some of them are fixed in natural archives – closed systems, where the exchange with the environment is strongly suppressed (e.g. tree rings, polar glaciers, see sediments). Thus, the concentration of CI in the archive depends on

1) GCR intensity
2) Efficiency of solar modulation
3) SEP intensity
4) Geomagnetic dipole moment
5) Efficiency of the transport of particular CI from the place of production to this archive
6) Conditions of archive development

7) Time, which has passed since the archive became closed (the age of archive)
8) Non-cosmogenic sources, which influence the concentration of the isotope in the archive.

If one chooses a natural archive and measures the concentration of a nuclide in it, one gets a quantitative characteristic, which is a function of the 8 parameters mentioned above. Of special interest are those radionuclides, half-lives of which are small compared to the age of the Earth so that their primordial component can be neglected but large enough that their concentration remains measurable for a long time. Moreover, it is important that the cosmogenic production is the main source of this nuclide. In this case, the parameter (8) does not play any role. The possibility of archive dating solves the problem (7) and the information concerning (6) can be obtained from other sciences (dendrology, glaciology, etc.). Thus, we get a function of five unknown variables, which are related to the time of the archive closing. It is possible to solve a reverse problem and to find out how these 5 parameters were changing in time. This is a unique opportunity to look into the early history of the Earth, to find out if the environmental conditions remained the same or they were undergoing drastic changes.

To reconstruct the unknown parameters it is necessary to know how they depend on the concentration of CI in the archive and to have a sufficient data set. One way of their determination is the usage of a few nuclides, which react differently to the changes of these parameters. An alternative way is the detailed analysis of the variations of the concentration, their amplitude and frequency. For example, SEP are produced during solar flares, which last from seconds to hours. The solar modulation is connected with the activity of the Sun and has the main periodicity of 11 years (Schwabe cycle [15]). The longer time-scale variations have periodicities of 88 years (Gleissberg cycle [16, 17]) and 200 years (Suess cycle [18, 19, 20]). Until now no significant variation of GCR was discovered though according to simulations, an explosion of a supernova in the vicinity of the Solar system (at the distance of about 50 pc) could increase the charged particle fluxes by a factor of 2 for a few thousand years [21]. The long-term variations of the CI concentration induced by the fluctuations of the geomagnetic field are of the same order of magnitude, e.g. the Laschamp event about 38000 years ago [22, 23]. Till now not much is known about changes of the global atmospheric transport. It seems that deviations driven by local weather effects dominate compared to long-term changes. In order to get reliable and usable information it is necessary to perform multiple measurements with a following averaging over time and space. An exception is radiocarbon, which is naturally well mixed in the atmosphere in the form of $^{14}CO_2$.

In order to obtain information about the past:

I. *A CI should be chosen in a proper way. It means that its half-life should be between thousand and some tens of millions years. It should be produced in quantities large enough for measurements and there should be a suitable natural archive for it.*
II. *A theory or model, which connects the described above parameters and the rate of production of this isotope at different points of the atmosphere, should be developed*
III. *A transport model, which allows the calculation of the CI concentration in the archive from the known production rate, should be created.*
IV. *Calculations of the parameter of interest should be performed.*

I. Since the beginning of CI research, the most promising CI are considered to be ^{14}C ($T_{1/2}$=5730 yr), ^{10}Be ($T_{1/2}$=1.5 Myr), ^{26}Al ($T_{1/2}$=710 kyr), and ^{36}Cl ($T_{1/2}$=301 kyr). Among these nuclides only radiocarbon is mainly produced in an exothermal nuclear reaction ($^{14}N(n,p)^{14}C$). The rest are products of endothermic spallation nuclear reactions. The reactions as e.g. $^{35}Cl(n,\gamma)^{36}Cl$ and $^{36}Ar(n,p)^{36}Cl$ are also possible but neither ^{35}Cl nor ^{36}Ar are present in the atmosphere in sufficient quantities. These reactions do not make any significant contribution to the ^{36}Cl production. ^{14}C and ^{10}Be are produced on targets of nitrogen and oxygen, which are the most abundant elements in the atmosphere. ^{26}Al and ^{36}Cl are produced on argon, which atmospheric concentration is 1% only. Their production rates are low and the possibility to measure them is connected with the success of AMS. Typical natural archives for these radionuclides are tree rings (^{14}C), glaciers (^{10}Be, ^{36}Cl), and sea and lake sediments (^{10}Be, ^{14}C, ^{26}Al).

II. The first estimation of the CI production rate was made in [2]. The authors used the number of stars in nuclear emulsions exposed at different altitudes and latitudes and an experimentally determined yield of the isotope per star. The method was based on the similarity of the CR spectrum at different points of the atmosphere. This assumption is generally not valid and the estimation contained a large error. The method was also not suitable for the study of variations of the production rate in case of fluctuations of external parameters. To solve these problems, theoretical models were developed. For example in [24] a system of Boltzman equations with the CR spectrum as a boundary condition was solved. The latest simulations were based on the Monte-Carlo method with the usage of special software as e.g. LAHET and GEANT codes [25] and on the solution of transport equations, where the interactions of nuclei with matter were described with the help of analytical approximations of differential cross-sections [26].

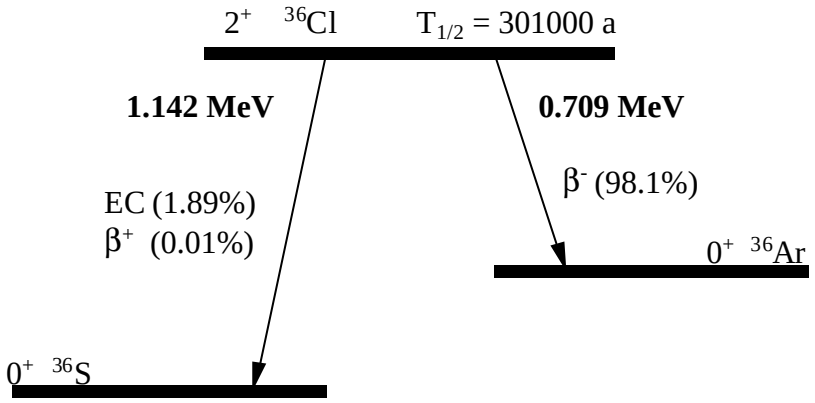

Figure 2 Decay scheme of ^{36}Cl [30]

Though the results of these calculations are in a good agreement, there are some evidences that the description of the ^{36}Cl production is not complete and it should be reviewed [27]. The main part of the present work is devoted to the consideration of this problem.

III. Until now, there is no agreement how the transport of elements in the environment should be described. Most authors use their original models for their specific tasks. Most of the models are developed for local conditions and they are obviously not suitable on the global scale. A way to solve this problem is presented in Chapter 2.

IV. The problems discussed in points II and III should be solved before the reconstruction of the time information would be possible. An attempt to solve the reverse problem was performed for radiocarbon [28], for which a transport model exists [29].

1.2. *General information about chlorine-36*

Chlorine belongs to the group of halogens. It is the 11th abundant element in the Earth's crust. Mostly it is bound to the following compounds: NaCl, $KClMgCl_2H_2O$, KCl, and $KClMgSO_43H_2O$ [31]. Chlorine has two stable isotopes: ^{35}Cl (75.77 %) and ^{37}Cl (24.23 %).

The radioactive ^{36}Cl ($T_{1/2}$= 301 ky) has 3 decay channels (see Figure 2): β^- (98.1%), EC (1.89%), and β^+ (0.01%):

$$^{36}Cl \rightarrow {}^{36}Ar + e^- + \bar{n}_e$$

$$^{36}Cl + e^- \rightarrow {}^{36}S + n_e$$

$$^{36}Cl \rightarrow ^{36}S + e^{+} + n_e$$

Because the half-life of ^{36}Cl is short compared to the age of the Earth, all primordial ^{36}Cl nuclei have already decayed. Thus, the ^{36}Cl abundance is completely determined by its modern production rate. The main source of ^{36}Cl in our environment is the spallation reactions on atmospheric ^{40}Ar induced by CR. The charge exchange reaction ^{36}Ar(n,p)^{36}Cl contributes less than 4% to its average production [32]. The global average ^{36}Cl production rate is estimated from 11 [2] to 22 at m^{-2} s^{-1} [33]. The latest results are within these limits. Unfortunately, there are no direct experiments able to prove the simulations. Available measurements [34, 35] give only the local fluxes of the isotope, which can differ strongly from the average value.

One of the natural sources of ^{36}Cl is neutron activation of stable ^{35}Cl in the lithosphere. When the chlorine abundance in a rock is low, the spallation reactions on potassium and calcium become important. At larger depths, the nucleonic component of the GCR fluxes is strongly reduced. The capture of negative muons by ^{40}Ca and reactions of showers produced by the interactions of fast muons with K and Ca become the main mechanism of ^{36}Cl production [36, 37]. At depths greater than about 100 m, the dominant ^{36}Cl production channel is the neutron capture reactions ^{36}Cl(n,γ) where the neutrons originate from decay of thorium and uranium.

The anthropogenic production of ^{36}Cl is of special importance. Because of the intensive tests of nuclear weapon performed in the 50-60s of the last century, the environment was affected by activation due to neutrons of fission (atom bombs) and fusion (hydrogen bombs). In case of barge tests, the neutrons activated ^{35}Cl of the seawater. High density of the released energy caused strong upward airflows, which brought a part of the produced ^{36}Cl to the upper layers of troposphere and into the stratosphere. Once being above the tropopause the chlorine was transported over large distances before falling down to the Earth's surface. Thus, the effect became global. The analysis of the bomb peak in Greenland [5] demonstrated a rapid increase of ^{36}Cl concentration in ice within the test years (the integral flux - fluence - was $2.4 \cdot 10^{12}$ at m^{-2}, which corresponds to about 2000 years of natural production). However, in the 80s the ^{36}Cl fluxes decreased to the natural level and it was assumed that no observable bomb produced ^{36}Cl should be present in modern precipitation.

Another anthropogenic source of ^{36}Cl is the production in civil and military reactors. In case of an accident (e.g. Chernobyl accident) or due to some regular releases this chlorine enters the environment. Though this source does not make a significant contribution to the global budget, it can temporally dominate in local ^{36}Cl fluxes [38].

1.3. *Natural production of chlorine-36 by cosmic rays (CR)*

Because the rate of the ^{36}Cl natural production plays a central role in this work, the most important parameters needed for its calculation are discussed below. The discussion is based on the method of solution of transport equations. Additional information can be found in [39].

1.3.1. CR spectrum in the vicinity of the Earth

The CR consist of protons (87%), alpha-particles (12%) and heavier nuclei (1%). The proton differential spectrum at the orbit of the Earth can be written in the form [40]:

$$f(E_0) = f_0 \frac{E_0(E_0 + 2m_p c^2)}{(E_0 + SF)(E_0 + 2m_p c^2 + SF)} (E_0 + \chi + SF)^{-\gamma} \qquad (1)$$

with

$$\chi = 780 \exp(-2.5 \cdot 10^{-4} E_0)$$

- g - spectral index. The used value is γ = -2.65,
- $m_p c^2$ - rest energy of the proton in MeV,
- SF - parameter of solar modulation, which varies from ~250 MeV during the minimal solar activity up to ~950 MeV during the maximum,
- f_0 - normalizing coefficient, f_0=1244000,
- E_0 - kinetic energy of a proton in MeV,
- $f(E_0)$ - proton spectrum in MeV^{-1} s^{-1} m^{-2}.

The equation (1) does not describe the spectrum correctly at energies below 100 MeV. In this energy range, the influence of SEP and anomalous CR should be considered. However, this part of the spectrum does not contribute significantly to the ^{36}Cl production rate because of the geomagnetic cut-off, strong ionization losses, and the threshold of the spallation reaction of about 20 MeV. Neither is this equation correct at very high energies (more than some TeV), at which the pair production becomes important. This part of the spectrum does not make any significant contribution to the bulk ^{36}Cl production because of the rapid decrease of the CR flux with energy. The maximum of the ^{36}Cl production is due to the particles of mean energies, spectrum of which is described by equation (1) quite well.

The spectra of heavier particles of the CR are assumed the same as for protons if E_0 corresponds to the energy per nucleon. Only the normalizing coefficient should be corrected for this case. The error made by this assumption cannot be large because heavy particles of the CR make a smaller contribution to the ^{36}Cl production than the proton component. For

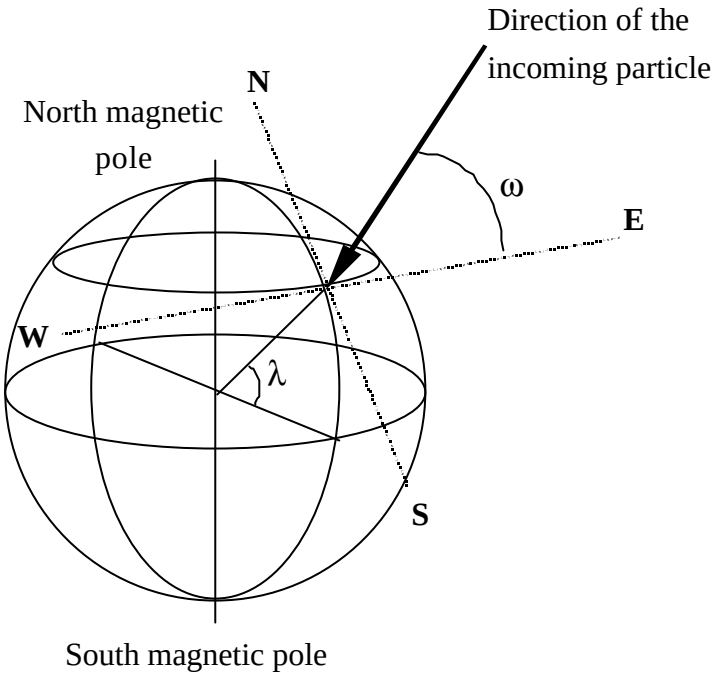

Figure 3 Schematic drawing of the geomagnetic sphere

example, the second most abundant CR component (alpha particles) contributes about 40% compared to primary protons [24].

1.3.2. Geomagnetic cut-off

The geomagnetic field leads to a shielding effect. The low energy particles are deflected by the geomagnetic field and they cannot penetrate into the atmosphere. In order to describe this effect Störmer introduced an analytical approximation [41]. In this theory, the magnetic field of the Earth is assumed a simple dipole without offset and tilt. A critical rigidity R_{cr} exists for every direction of the incoming particle. Particles with larger rigidity $R>R_{cr}$ can penetrate into the atmosphere and induce the nuclear cascade. Particles with lower rigidity $R<R_{cr}$ are reflected and do not enter the atmosphere. This critical rigidity is calculated as

$$R_{cr} = \frac{Ro \cdot \cos^4(l)}{\left(\sqrt{1-\cos(w)\cdot\cos^3(l)}+1\right)^2} \qquad (2)$$

where (see Figure 3)

λ - geomagnetic latitude

ω - angle between the direction of the primary incoming particle and the direction to the East

Ro - a constant related to the Earth's magnetic dipole moment. *Ro*=59.6 GV for dipole moment of $8.06 \cdot 10^{25}$ Gauss cm^3 (for the 1930s to the 1950s) and *Ro*=58 GV for dipole moment of $7.84 \cdot 10^{25}$ Gauss cm^3 (1990).

Precise calculation of the cut-off effect can be performed numerically.

1.3.3. Transport equations

The production rate of ^{36}Cl can be calculated if fluxes of particles in every point of the atmosphere and the corresponding cross-sections are known. In order to determine the fluxes a transport equation applied to the entire atmosphere should be solved. A boundary condition for this equation is the CR spectrum corrected for the geomagnetic shielding. With the use of particle conservation the transport equation can be written in a form

$$\cos\vartheta \cdot \frac{\partial}{\partial x} N_i(E,\Omega,x) + \frac{\partial N_i(E,\Omega,x)}{\partial E}\frac{dE_i}{dx}(E) = -\mu_i(E)N_i(E,\Omega,x) + \sum_k \iint\limits_{\substack{E_1>E \\ \Omega_1}} n_{k,i}(E,E_1,\Omega,\Omega_1)\mu_k(E_1)N_k(E_1,\Omega_1,x)dE_1 d\Omega_1 \quad (3)$$

where

$N_i(E,\Omega,x)$ - flux of the particles of type i with energy E in solid angle W at depth x,

$m_i(E) = s_{tot}(E)/m$ - mass absorption coefficient for the particle of type i,

$s^i_{tot}(E)$ - total inelastic cross-section of the particle of type i,

m - atomic mass of the target,

$\frac{dE_i}{dx}(E)$ - ionization losses of the particle of type i,

$n_{k,i}(E,E_1,W,W_1)$ - differential spectrum of the secondary particles of type i with energy E in the solid angle W, which are produced within the interaction of primary particle of type k with energy E_1 in the solid angle W_1, with the nuclei of the target,

J - angle between direction of the incoming particle and the normal to the target.

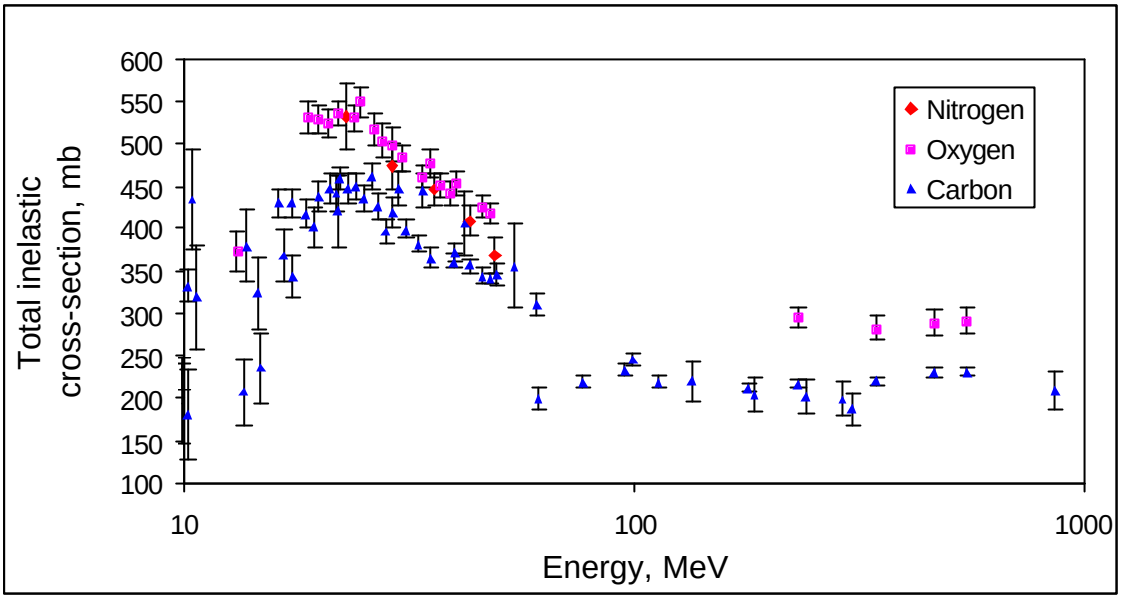

Figure 4 Total inelastic cross-section for protons in nitrogen (diamond), oxygen (square), and carbon (triangle) [43]

In this equation, it was assumed that only particles from a small solid angle around the normal to the target make a significant contribution to the flux. Thus, the convexity of the Earth can be neglected and the plane geometry is described by one variable.

Even if each function in the equation (3) were known exactly, only with the help of a powerful computer it would be possible to obtain results in the range of 1 percent uncertainty. However, the necessary cross-sections are still not measured with high precision and an error of the numerical calculation can be neglected.

1.3.4. Total inelastic cross-section

Some data on nuclear interaction of protons with matter can be found in [42, 43] (see Figure 4). There is little difference in the mass absorption coefficient for targets of carbon, nitrogen, and oxygen. Though there are not much data available in the high-energy range, the dependence of the cross-section on energy is weak there. At low energies, the uncertainty of measured values exceeds 10%. However, because the maximum of the ^{36}Cl production corresponds to primary particles with energy of about 1 GeV this error does not contribute significantly to the overall uncertainty. A larger difficulty originates from the lack of experimental cross-sections for energetic neutrons. However, at energies larger than about 100 MeV the Coulomb barrier can be neglected and neutron cross-sections can be assumed the same as the proton ones.

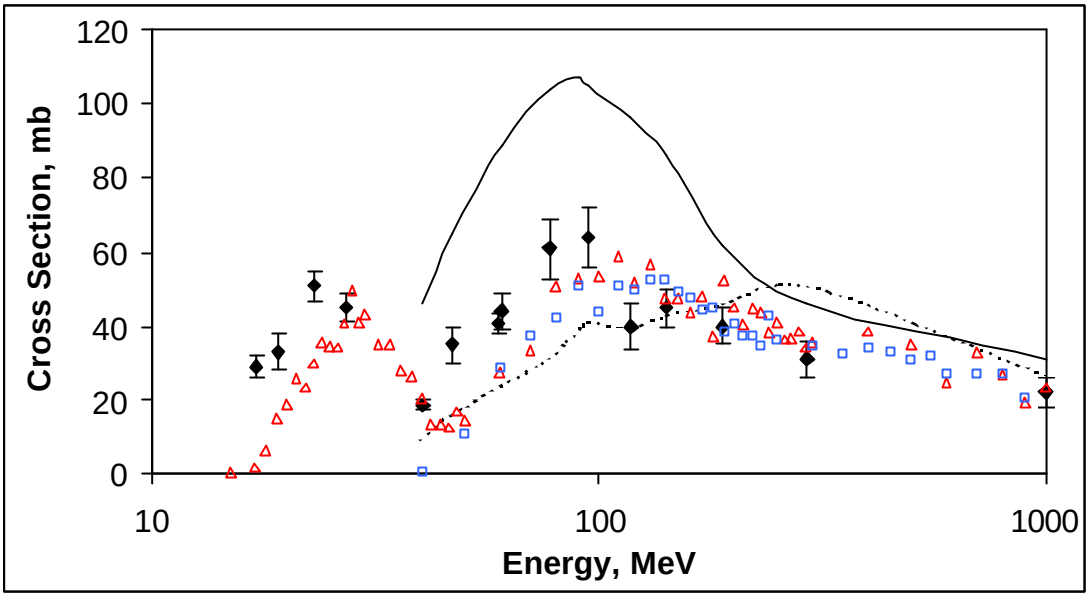

Figure 5 Energy dependence of the cross-section of ^{36}Cl production on ^{40}Ar
$^{40}Ar(p,X)^{36}Cl$:
diamonds – experimental points [51], solid line – Silberberg approximation [47], dashed line – Rudstam [48] approximation, triangles – CEM95 simulation [53]
$^{40}Ar(n,X)^{36}Cl$:
squares – CEM95 simulation [53].

1.3.5. A single nuclear interaction

In order to solve the transport equation (3) the knowledge of the differential spectrum of secondary particles produced in a nuclear reaction is necessary. This spectrum can be obtained by calculation of the internuclear cascade by Monte-Carlo method or by applying the analytical approximations [44]. Each of these methods has a relatively high uncertainty, which is one of the main sources of the resulting uncertainty in the production rate calculation.

1.3.6. Ionization losses

Ionization losses of a charged particle in matter are calculated according to Bethe-Bloch formula [45, 46]

$$\frac{dE}{dx} = -\frac{4\pi\, Z^2 e^4}{m_e c^2 \beta^2}\frac{z}{AM}\left[\ln\frac{2m_e c^2\beta^2\gamma^2}{\bar{I}} - \beta^2\right] \qquad (4)$$

where

Z - charge of the incoming ion,

z - charge of the target nucleus,

A - atomic mass of the target nucleus,

M - atomic mass unit,

$\bar{I}$ - average ionization potential of the target matter,

$m_e c^2$ - rest energy of the electron,

$?$ - speed of light,

b - velocity of the incoming particle in units of c,

$$g = \frac{1}{\sqrt{1 - b^2}}.$$

Alternatively, tabulated data [47] or simulation (http://www.srim.org) can be used.

1.3.7. Cross-sections of chlorine-36 production

The cross-section of ^{36}Cl production on ^{40}Ar can be estimated using Rudstam [48] or Silberberg and Tsao [49, 50] approximations. However, their accuracy is not sufficient and it is preferable to use the interpolated experimental data [51]. Unfortunately only the cross-sections of the reaction ^{40}Ar(p,X)^{36}Cl are measured while the reaction ^{40}Ar(n,X)^{36}C plays a dominant role for the ^{36}Cl production. It was claimed [52] that the cross-sections of proton and neutron induced reactions can be quite different, especially in the cases of similar masses of target and product. However, the simulations made with CEM95 [53] show that Coulomb interaction is important at the energies below 50 MeV only and at higher energies, no large difference between *n*- and *p*- reactions can be observed (see Figure 5).

It is difficult to estimate which error can arise from the uncertainty of the cross-section data. In the first estimations, when only approximations were available, it could be up to a factor of two. The usage of experimental data can reduce it to about 15% - the uncertainty of the measured cross-sections.

1.4. *Available data on chlorine-36*

The first measurements of ^{36}Cl were performed in the middle of the 50s by screen-wall counters [54], which had a sensitivity of about 10^{-12} for the ^{36}Cl/Cl ratio. This sensitivity was improved by a factor of 2 in the middle of the 60s when liquid scintillation was used [55]. However, measurements of most of the natural samples became possible only with development of AMS [56, 4], which combines a high sensitivity (about $1{\cdot}10^{-15}$ of ^{36}Cl/Cl) with small sizes of the sample (about few mg).

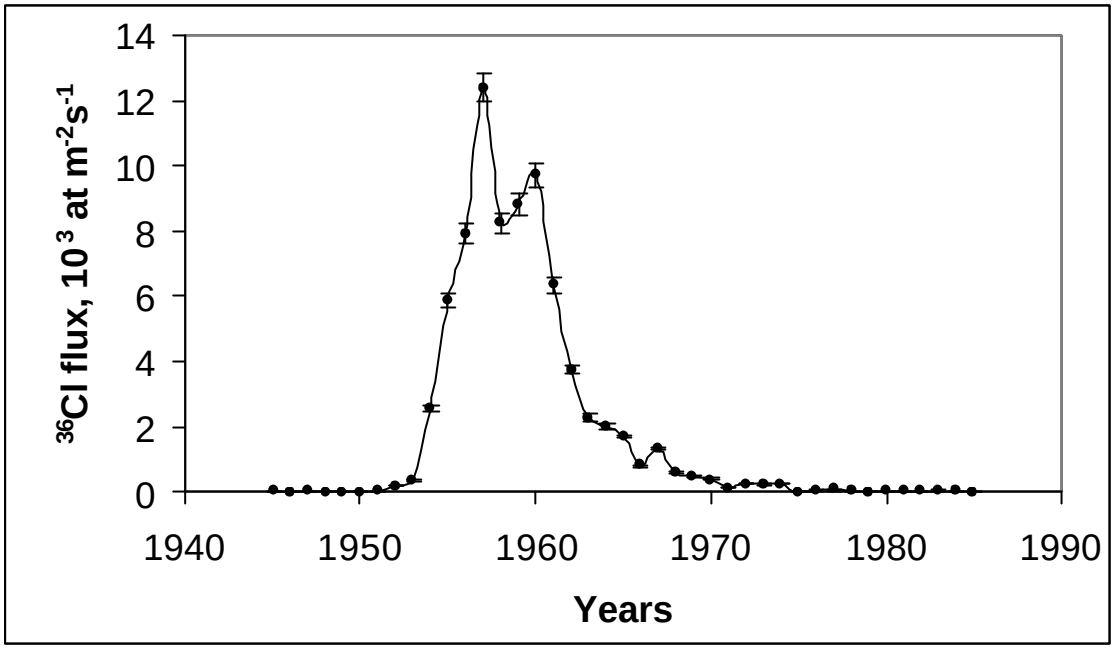

Figure 6 Bomb pulse of ^{36}Cl measured on Dye-3, Greenland [5]

The ^{36}Cl concentration in a number of samples from different parts of the globe was published. However, only few of the results can be used to obtain information on ^{36}Cl fluxes. These are the measurements in precipitation (snow and rain) when both the concentration of ^{36}Cl (in at m^{-3}) and the precipitation rate (in m per year) are known. Similar information can be obtained from measurements in glaciers. Another way of getting experimental data about fluxes is the measurement of ^{36}Cl in lakes with known hydrological parameters. In this case, the obtained fluxes are model dependent but their advantage is that they are naturally averaged over the catchment area and flushing time (the ratio of volume to outflow rate) of the lake.

The first measurements of ^{36}Cl in rainwater were performed in the end of the 50s [57]. A high ^{36}Cl concentration (between $2.4 \cdot 10^{8}$ and $1.8 \cdot 10^{9}$ at/l) demonstrated the influence of nuclear weapon tests. Until 1979, the ^{36}Cl concentration in precipitation had been reduced by 2-3 orders of magnitude [58]. Detailed information on bomb chlorine impact was achieved by measurements in Greenland ice [5] (Figure 6). Later on, the measurements of ^{36}Cl in precipitation were performed in [59, 60, 61, 62]. However, the most extensive study, which covered a wide latitudinal range, was done in [8]. The data calculated in these works are gathered in Table 29 and are presented in Figure 7. High amplitudes of the fluctuations demonstrate the importance of local effects. It is clear that no conclusion can be made upon a single measurement and only average fluxes should be used for data interpretation. In Figure

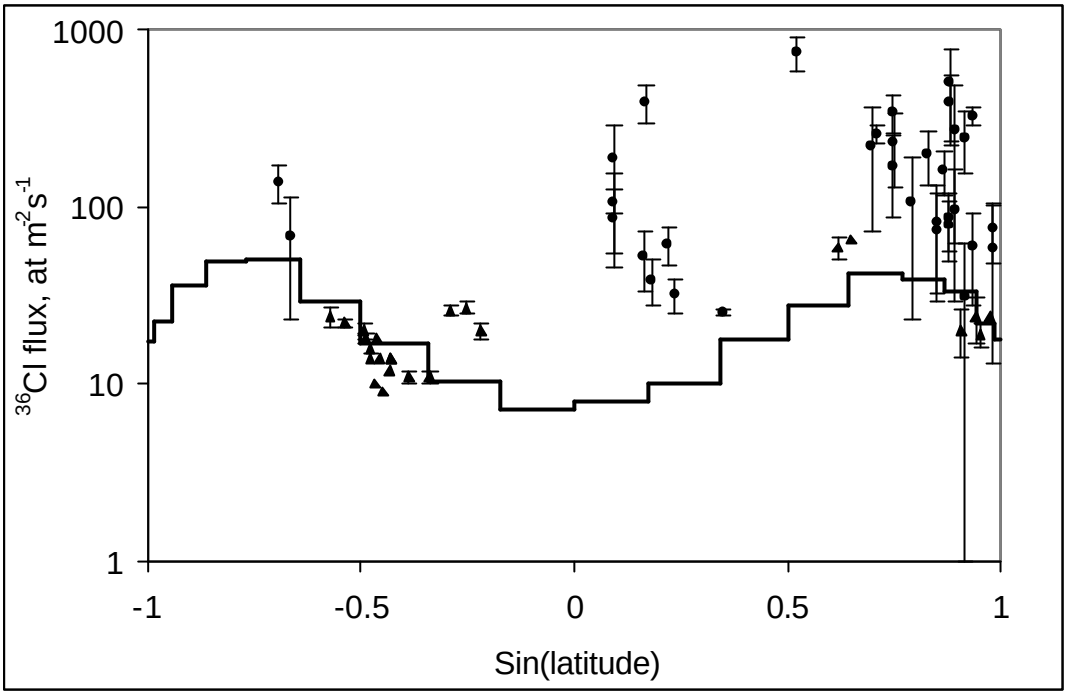

Figure 7 Calculated and measured ^{36}Cl fluxes in rainwater as functions of latitude [8]. The experimental points are presented by symbols with error bars; the solid line stands for the calculation.

7, the experimental fluxes are systematically higher than the simulated. This requires a revision of present understanding of ^{36}Cl sources [27].

Measurements of ^{36}Cl in water systems were usually performed in ground water with the purpose of their dating, e.g. [63]. In open reservoirs, ^{36}Cl was measured for the first time in Great Laurentian lakes in the beginning of the 90s [7]. Because of interpretation difficulties, these measurements were also discussed in the following works [64]. The most important conclusions done were the impossibility of explanation of high ^{36}Cl concentration without taking into account the input of the bomb-produced chlorine and importance of atomic power plants for local ^{36}Cl fallout [38]. In contrary, *Beasley et al.* [65] made a conclusion about the natural origin of ^{36}Cl in lake Baikal and rivers Yenisey and Kolyma.

Besides Dye-3, the measurements of ^{36}Cl in ice were performed for stations Milcent, SUMMIT, and Camp Century in Greenland [66], in Alpine glacier Fiescherhorn (Switzerland, 46N, 8E, altitude about 4000 m over sea level), in glacier Gulya in Himalayas (China, 35N, 81E, altitude about 6700 m), and in Huascaran in Ands (9S, 77W, altitude about 6000 m) [6]. In both works, the bomb peak of ^{36}Cl was measured and compared with [5]. The expected latitudinal distribution could not be confirmed on the base of these works. The ^{36}Cl fluences in Fiescherhorn and Guliya appeared to be lower than in Dye-3 though they were expected to be higher than that one in Dye-3 by a factor of 2. All attempts to explain this phenomenon by

blowing out of chlorine with snow from the glaciers contradicted the measured data on ^{18}O. It is likely that the ^{36}Cl fluxes decrease with the altitude (for example, the fluences of ^{36}Cl in Huascaran and Guliya, which are at about the same height, are of an order of magnitude lower than the fluence in Dye-3).

1.5. *The problem and its solution*

1.5.1. The problem

In section 1.1 it was shown that CI could be a very useful tool for obtaining information about the physical conditions of the Solar system and the Earth in the past. However, a detailed understanding of their sources is necessary. In section 1.2 it was mentioned that ^{36}Cl could also be effectively used as a tracer and it was a very important isotope for hydrology. The sources of ^{36}Cl were listed, among which the natural production prevailed. In section 1.3 the methods of calculation of the ^{36}Cl production rate by CR were briefly discussed. Though the uncertainties in cross-sections are high, the modern nuclear physics is able to describe the production of ^{36}Cl with accuracy better than 20%. Thus, enough information about ^{36}Cl is known and ^{36}Cl can be successfully used for different applications. However, the discrepancy of calculated and measured fluxes of ^{36}Cl stated in section 1.4 shows that either there is a problem in the simulation of ^{36}Cl production or there should be another important source of this isotope, which has not been taken into account until now. In the first case the nuclear modeling should be revised, in the second one a new environmental effect should be considered. In any way, the discrepancy points to a problem of high importance. An answer to the question of a "hidden source" is given in this work.

This source was neglected and it means that its influence was assumed improbable. That is why it is important to consider all possibilities, which can lead to the high ^{36}Cl fluxes even if they seem not realistic:

a) There was a systematic experimental error in the work [8].
b) ^{36}Cl production due to CR is higher than it was assumed.
c) ^{36}Cl enters the Earth atmosphere from the space.
d) ^{36}Cl from the Earth surface enters the atmosphere and increases the modern ^{36}Cl fluxes.
e) A part of the bomb-produced ^{36}Cl has been stored in the high atmosphere and is still falling out.
f) ^{36}Cl produced in reactors is released to the atmosphere in accidents or by nuclear reprocessing plants.

1.5.2. Possible solutions

a) A part of the samples measured at TUM was also measured at ETH Zurich , Switzerland. The results were in a good agreement [8].

b) Because the calculations of the production rate of other CI (^{10}Be, ^{14}C) are in a good agreement with experimental data, no large systematic error was done in nuclear modeling.

c) Indeed, there are indications that meteorites bring a significant amount of radioactive isotopes onto the Earth. Recently, it was shown that the flux of ^{26}Al due to meteorites could locally reach the same order of magnitude as the flux of atmospheric ^{26}Al [67]. However, this calculation did not get any experimental confirmation. Moreover, compared to ^{26}Al, ^{36}Cl has fewer targets to be produced in meteorites and its atmospheric production rate is a factor of 10 higher than for ^{26}Al.

d) The largest chlorine-containing reservoir on the Earth's surface is ocean. With a total mass of $1.4 \cdot 10^{21}$ kg and chlorine concentration of 1.9% it contains about $m_{Cl} = 2.7 \cdot 10^{19}$ kg of stable Cl. Using the global average flux of ^{36}Cl F=16 at m^{-2} s^{-1} we can find the burden of cosmogenic ^{36}Cl in the ocean is

$$m = \frac{FA\tau M}{N_A} = 6700 \text{ kg},$$

where

- $A = 5.1 \cdot 10^{14}$ m^2 - surface area of the Earth,
- $N_A = 6 \cdot 10^{23}$ mol^{-1} - Avogadro's number,
- M=36 g mol^{-1} - ^{36}Cl atom mass,
- t=434 kyr - life-time of ^{36}Cl.

According to [68], the flux Φ of sea salt into the atmosphere is estimated to be 6500 Tg yr^{-1}, a part η=55% of which is chlorine. Thus, we can estimate the flux of ^{36}Cl coming out of the ocean:

$$F_{ocean} = \frac{\Phi \eta N_A}{AM} \cdot \frac{m}{m_{Cl}} \approx 0.9 \frac{\text{at}}{\text{m}^2\text{s}}$$

This flux is small compared to the direct fallout of CR produced ^{36}Cl.

A little is known about chlorine, which falls on the land. Mainly it is washed out to lakes and later on to the ocean. However, a part of it can be captured by the biosphere. For example, the

measurements of ^{36}Cl in the region of the reprocessing facility *La Hague* indicate an increase of ^{36}Cl in grass [69].

e) Nuclear bomb tests increased the fluxes of ^{36}Cl by 3 orders of magnitude. However, the ^{36}Cl flux measured in Greenland (see section 1.4) reached its prebomb level at the beginning of the 80s, and no bomb ^{36}Cl is presumably observed in modern precipitation. On the other hand, due to high fluctuations of the annual fluxes it is hard to say if the measured postbomb fluxes reached their natural level or they were still higher by a factor of 2. It is possible that the chorine removal from the low stratosphere is a relatively fast process (that's why we see the rapid decrease of ^{36}Cl fluxes after the termination of atmospheric nuclear tests) and the removal from the high stratosphere is a slow process, which determines the decrease of the fluxes for longer time.

f) There is not much data available, which show the influence of the nuclear industry onto the ^{36}Cl budget. According to [38, 69] the reactors and reprocessing plants can increase the local inventory of ^{36}Cl but this effect is not observable on a large scale.

1.5.3. The aim of the work

The aims of this work were:

- Development of an atmospheric transport model for ^{36}Cl. The model suitable for long time scale was necessary to investigate the possibility of delayed fallout of ^{36}Cl. This model was also used for interpretation of the measurements.
- Analysis of the relation between different sources of ^{36}Cl. Natural production by the CR, bomb production, and input from the Chernobyl accident were studied. This analysis has been performed by the AMS measurements of ^{36}Cl concentration in lakes with long flushing times. Additionally, the study of the latitudinal dependence of bomb-produced ^{36}Cl fallout and contamination due to Chernobyl accident was performed.
- The possibility of chlorine reemission into the atmosphere from land was examined. Of a special interest were the bioactivity and a role of methyl chloride. In order to perform this task an experimental setup had to be developed.
- Combining the gained information for a conclusion about the reason for the ^{36}Cl discrepancy in modern precipitation.

CHAPTER 2. Chlorine in atmosphere and in lakes

2.1. *Chlorine-36 transport in the atmosphere*

2.1.1. The structure of troposphere

In the atmosphere, a low part called troposphere and a high part called stratosphere are distinguished. The troposphere is characterized by a negative gradient of the temperature with height and it is well mixed vertically. On the contrary, the stratosphere is stable because of positive temperature gradient and the vertical exchange is a slow process there. A tracer can be spread horizontally over large distances along the isentropes in the stratosphere and as soon as it enters the troposphere, it falls out rapidly. Thus, the stratosphere is responsible for the global mixing of species and the distribution of fallout depends on the features of stratospheric-tropospheric exchange (STE).

In equatorial regions, the troposphere absorbs more energy than it emits [70]. The warmed up air forms an upward flow and is replaced by a cooler air from the subtropics. These fluxes in the low troposphere are compensated by the poleward movements of the air masses in the high troposphere and their following sinking in subtropics. Thus, Hadley cells are created on both sides of the equator. The Hadley cells play an important role in atmospheric circulation because of the following reasons:

- The poleward movements of the air in the upper troposphere hinder the mixing between south and north hemispheres.
- The fast upward flows help the tropospheric air enter the stratosphere.
- Due to Coriolis force, the upward directed flows produce the east trade winds, which assist fast mixing within one latitudinal belt.

The position of the Hadley cells on both sides of the equator is not symmetrical and it changes within a year. The maximum deflection of zenith sun from the equator is 23 degrees. Accordingly, the boundary between the southern and the northern Hadley cells called

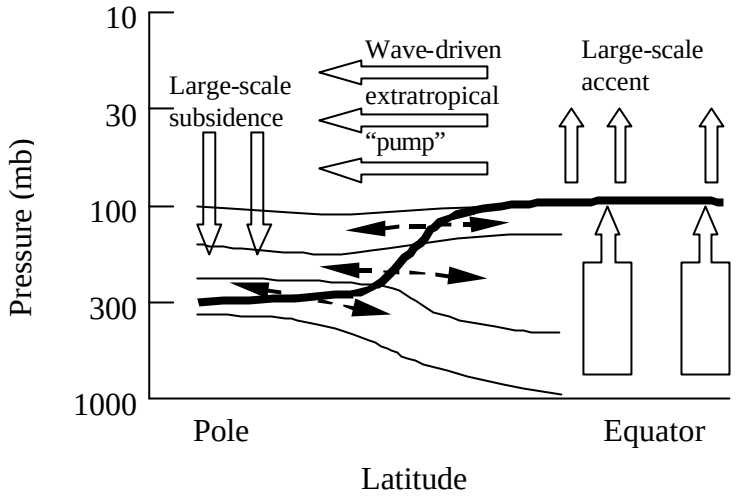

Figure 8 General scheme of STE from [74]. The tropopause is shown with a thick line. Thin lines are isentropic surfaces. Block arrows show the direction of the advective circulation. Double-arrowed lines indicate the exchange along isentropes at the places of the tropopause breaks.

Intertropical Convergence zone (ITC) can reach latitude 23° over land. Due to the high heat capacity of the ocean, the deflection of the ITC over it does not exceed 5 degrees.

There is no stable circulation between latitudes 35° and 70°. The meteorological conditions there are determined by collisions of cold polar and warm equatorial fronts and by cyclone and anticyclone production. The main wind direction (eastward) can be explained as a thermal wind, which is produced by the temperature gradient and Coriolis force [71].

In the pole regions, the air cools down by the ice and sinks. Thus, a circulation with equatorward airflow at low altitudes is formed. Coriolis force deflects this flow in west direction and circumpolar winds are generated.

2.1.2. Transport in the stratosphere and through the tropopause

The stratosphere is much more stable than the troposphere and the diffusivity is generally low there. The air parcels move slowly along the isenthropes and only a weak energy exchange takes place. In the presence of winds, instabilities might appear and eddy diffusion leads to a faster mixing.

The wind pattern in the stratosphere is determined by its heating. The summer hemisphere obtains more energy than the winter one. This leads to the formation of the thermal west winds in the winter hemisphere and the east winds in the summer hemisphere. The east winds have a regular structure and the diffusion in their regions is very slow. On the contrary, a number of instabilities and wave structures are created in the zone of west winds (*drift or surf zone*). The exchange there is much faster, especially in the end of winter –

beginning of spring. At this time of the year, daily oscillations of temperature can reach 30 degrees.

The wind strength is maximum at mid-latitudes. In the pole regions, the air movements are slow and have a regular structure. A so-called *polar vortex* is created there, which hinders the exchange of the polar air with the air of the middle latitudes. Only in the beginning of spring, this structure is disturbed by the irregularities of the winter hemisphere and fast mixing takes place.

The equatorial belt is situated between the regions with opposite directed airflows. The wind speed there is close to zero and the diffusion is strongly suppressed. Thus, one can speak about *tropic barriers*, which separate the northern hemisphere from the southern one.

Brewer circulation [72], which can be compared with Hadley cells, plays an important role for the longitudinal transport. The air rises up in the tropics (typically between 10 and 20 degrees [73]), moves to mid or high latitudes, and sinks down there (see Figure 8). The mechanism of this circulation is connected with the particularity of eddy motions coursed by so-called "breaking Rossby waves" [74].

It has been already noticed that the vertical transport above the tropopause is slow. However, the STE exists and three mechanisms are mainly responsible for it.

- Due to seasonal variations, the tropopause rises and sinks within a year. When this happens, a part of the stratospheric air appears in the troposphere and vice versa.
- Because of the fast upward flows in the tropics, a part of the tropospheric air is brought higher than the tropopause (Hadley circulation). Due to mass conservation, also some stratospheric air sinks down to the troposphere. This takes place at the mid-latitudes.
- Due to angular momentum conservation, an air parcel rotating around the Earth in east direction gets a higher speed moving polewards. Thus, at the latitude of about 30 degrees on both sides of equator the subtropical jets are formed. The tropopause has a fold at the place of these fast west winds and thus it is divided into the equatorial tropopause and the tropopause of high latitudes. Through the gap, air can diffuse along the isentropes from the stratosphere to the troposphere and vice versa.

Among these mechanisms, the first one is of the least importance. It is responsible for the exchange of about 10% of the stratospheric mass per year, whereas the contribution of the last two is of about 50-60% [71].

An important feature of the STE is its seasonal variability. The concentration of stratospheric gases in the troposphere increases in spring because:

- The tropopause rises in spring and sinks in autumn.
- Hadley circulation has seasonal fluctuations.
- The stratosphere is unstable in the end of wintertime.

2.2. *The modeling*

In the 60s, the processes of the ^{36}Cl transport were characterized as known and simple [2]. Once an atom of ^{36}Cl is produced, it is reduced to HCl. This molecule remains in the gas form or it stacks to aerosols. Because most of the aerosols have small masses and their gravitation settling is very slow, chlorine in both forms follow the air masses. In the low atmosphere, chlorine is scavenged by water droplets and is washed out with rain. For the description of the ^{36}Cl distribution, the following assumptions were used.

a) There is no longitudinal dependence within one latitude belt. This is because the strong east and west winds (e.g. trade winds in the equatorial belt and circumpolar winds in pole regions) mix air masses faster than they are washed out of the atmosphere.
b) Only high energetic particles, which are not sensible to the geomagnetic cutoff, are able to reach the low atmosphere. Thus, the production of ^{36}Cl in the troposphere and the fallout of "tropospheric" ^{36}Cl do not depend on the latitude.
c) Long-lived radionuclides like ^{36}Cl are well mixed in the stratosphere and the distribution of their fallout depends not on the distribution of its production but on the structure of the tropopause.
d) Because ^{36}Cl is washed out from the troposphere by rain, its local fluxes are proportional to the precipitation rate.

The ^{36}Cl data gained up to the middle of the 80s [3] confirmed these assumptions. However, the necessity of quantitative models was clear. In [75] the atmospheric transport was studied on the base of the ratio $^{7}Be/^{10}Be$ at different altitudes. A tropospheric residence time between 20 and 35 days was deduced in this work. An attempt to improve a 4-box model of ^{36}Cl transport suggested in [76] was performed in [5]. The stratospheric residence time was estimated to be 2 years and the tropospheric one 2 weeks. This model could describe Dye-3 data reasonably well but it was not suitable for the calculations of ^{36}Cl fluxes at variable places on the Earth.

A description of all air parcels on a long time scale is a hardly realizable work at present. A few general circulation models (GCM) were developed [77, 78] but they are too complicated for the description of average processes. Moreover, conditions in the atmosphere

change all the time and a too detailed program is wrong on the long scale. Ideally, a model of ^{36}Cl transport should satisfy following conditions.

- The model should use few free parameters but it should describe reasonably most of the available experimental data.
- It should take into account the main features of the atmospheric structure but it should not depend on frequently changing parameters.
- It should reproduce the observed latitudinal dependence of the fallout.
- It should describe a time dependence of a tracer decrease after an injection of radionuclides into the atmosphere
- An applicability of the model for different elements can be important for determination of free parameters and as a cross check.

An attempt to develop such a model was performed in [79] and later in [27, 80]. The atmosphere was divided in 18 latitudinal belts, 10 degrees each. Vertically a tropospheric and four stratospheric layers were used. Thus, the entire atmosphere was described by 90 boxes, each of them was properly mixed. The exchange rates were defined by the assumption of concentration equilibrium in the closed system. The exchange between the stratosphere and the troposphere took into account the tropopause breaks and seasonal variations. Moreover, a gravitational settling of aerosols was implemented into the model. The washout rate from the troposphere was estimated using the residence time from [75] and the ratio between dry and wet fallout [70]. Thus, tropospheric residence time of 19 days and 34 days were obtained for wet and dry deposition, respectively. The data on bomb-produced radionuclides were used for normalization of the parameters.

This model could reproduce the latitudinal distribution of radioisotopes well but it was not applicable for long timescale calculations. Another difficulty became apparent in the description of the stratospheric exchange. This was performed using uniform diffusion along isentropes and only the exchange through the equator was slower. The applied method contradicted the usage of the ^{14}C data [81, 82] for calibration of the model. Impossibility to describe eddy-transport barriers quantitatively in terms of diffusivities only was stated in [83]. The deduced from the model rates of diffusion appeared to be unrealistically large [84, 85]. Another weak point of the model was the necessity of different altitudinal distributions of the bomb ^{14}C and ^{90}Sr injection into the atmosphere, which did not depend on the bombs power.

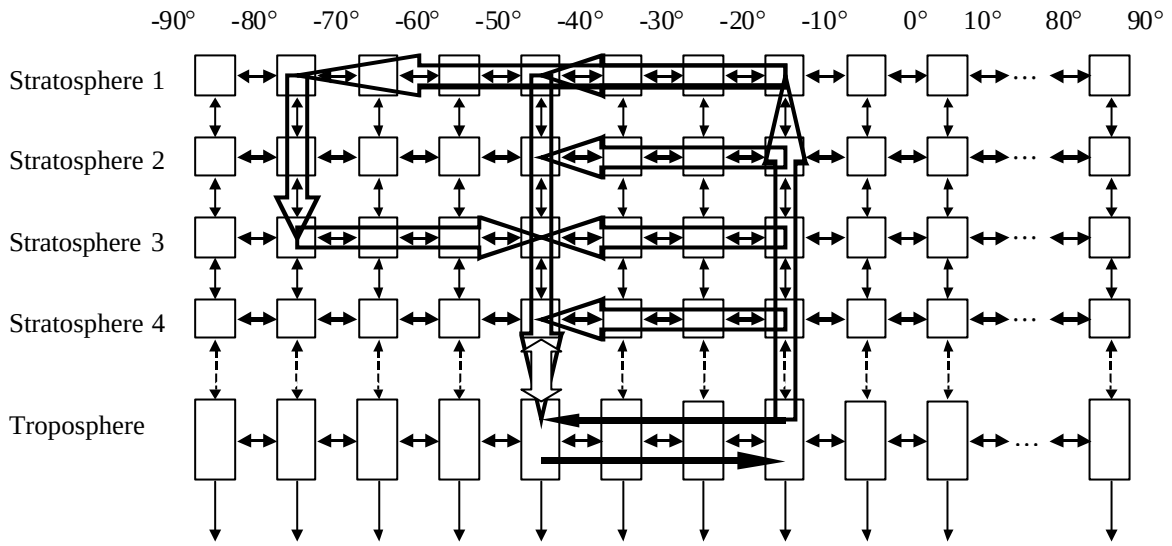

Figure 9 Scheme of the transport model. Double arrowed lines indicate the diffusive mixing. Block arrows show the advection in the stratosphere. The arrows in the troposphere between -10° and -50° demonstrate the Hadley circulation. The scheme is presented for the south hemisphere. The north hemisphere looks symmetrically.

2.3. *Transport model*

2.3.1. Box model

Though the model [27] has a few disadvantages (see Section 2.2), it has proved to be able to reproduce most of the available experimental data. That is why we have chosen it as a base of a new model and just improved it with a few additional features like advection and diffusion barriers.

Because the strong east and west winds, which exist in both the stratosphere and the troposphere, mix the air along a parallel rapidly, the longitudinal dependence of ^{36}Cl in the atmosphere was neglected. On the contrary, the latitudinal dependence of the nuclides fallout is observed and should be taken into account when the experimental data are interpreted. The size of a typical zone in the troposphere is 30° (see Section 2.1.1) but in order to improve the resolution the width of 10° was chosen. However, it should be noticed that due to different kinds of fluctuations (e.g. the difference “continent-ocean”) every single local point could differ from the averaged over its latitude value and correspond to the neighbor latitudinal belt.

Because of the fast vertical mixing in the troposphere, no altitude dependence of the concentration was considered there. On the contrary, the stratosphere is vertically stable. In order to be able to describe the slow exchange there, it was divided into 4 layers of equal depth in gcm^{-2}. The heights of the borders between these boxes can be seen in Table 1. The

Latitudinal belt	Troposphere		Stratosphere 4		Stratosphere 3		Stratosphere 2	
	depth, g×cm^{-2}	*altitude, km*	*depth, g×cm^{-2}*	*altitude, km*	*depth, g×cm^{-2}*	*altitude, km*	*depth, g×cm^{-2}*	*altitude, km*
0-10	151.3	16.0	113.5	18.4	75.7	21.8	37.8	27.5
10-20	152.2	15.9	114.2	18.3	76.1	21.7	38.1	27.5
20-30	157.9	15.6	118.4	18.0	78.9	21.4	39.5	27.2
30-40	182.2	14.5	136.7	16.8	91.1	20.2	45.6	26.0
40-50	229.2	12.5	171.9	14.9	114.6	18.3	57.3	24.1
50-60	274.8	11.0	206.1	13.4	137.4	16.8	68.7	22.6
60-70	300.1	10.3	225.1	12.7	150.0	16.1	75.0	21.8
70-80	311.4	10.0	233.5	12.4	155.7	15.8	77.8	21.5
80-90	318.2	9.8	238.6	12.2	159.1	15.6	79.5	21.4

Table 1 Position of the upper borders of the atmospheric boxes, which were used in the model.

relationship between the altitude h of every point and the column mass x above was calculated barometrically:

$$x = 1033 \frac{\mathrm{g}}{\mathrm{cm}^2} \cdot e^{-\frac{h}{8.33\ \mathrm{km}}}$$

Thus, the atmosphere was modeled as 90 boxes, which exchange gases. The change of nuclide content in the box number i can be described with the equation.

$$\frac{dN_i}{dt} = \sum_{j \neq i} \lambda_{ji} N_j - N_i \sum_{j \neq i} \lambda_{ij} - \frac{N_i}{\tau} + Q_i$$

where

N_i - content of the nuclide in the box number i,

l_{ij} - rate of transition from the box number i to the box number j,

Q_i - sum of all additional sources for the box number i,

τ - life time of the radionuclide. For stable and long-lived isotopes (e.g. ^{36}Cl) τ can be considered as infinitely large. However, for some isotopes (e.g. ^{7}Be) the radioactive decay might be important.

2.3.2. Diffusive mixing

The basic condition of the diffusive mixing is the equilibrium of every two boxes. It means that if l_{ij} is the rate of transport from the box number i with the mass M_i into the box number j with the mass M_j then the transport rate from the j to i is

$$l_{ji} = l_{ij} \frac{M_{ij}}{M_{ji}} \tag{5}$$

In the approach of the uniform atmosphere, the horizontal fluxes are proportional to the effective cross-section area. If *i-1*, *i*, *i+1* are three neighbor boxes at one vertical level and $S_{i-1,i}$, $S_{i,i+1}$ are the boundary areas between them then

$$\lambda_{i,i+1} = \lambda_{i,i-1} \frac{S_{i,i+1}}{S_{i,i-1}} \tag{6}$$

For the vertical exchange, a similar formula can be used. If *i* and *j* are the numbers of the boxes at one level and the boxes *i+1* and *j+1* are at the next level

$$\lambda_{i,i+1} = \lambda_{j,j+1} \frac{S_{i,i+1}}{S_{j,j+1}} \tag{7}$$

At different altitudinal levels, properties of the medium differ and the exchange rates at every level have to be assigned separately. Thus, in the first approximation the diffusion can be described by 8 free parameters

- 5 parameters T^{Hor}_i (4 layers of the stratosphere and one of the troposphere) describe the horizontal exchange from the equatorial belt to the neighbor one. The horizontal exchange rates for other latitudinal belts can be deduced with the equations (5) and (6).
- 3 parameters T^{Ver}_i describe the vertical exchange between the boxes of the stratosphere in the equatorial latitudinal belt. The exchange rates at other latitudes can be deduced with the equations (5) and (7).

In the middle-latitude region of the winter hemisphere the assumption of the uniform atmosphere is not fulfilled. At the end of winter, the mixing rate between 20° and 70° of the north hemisphere increases significantly. This range of latitudes is called the surf zone. To describe the mixing there, the exchange rate in each stratospheric layer was multiplied by a seasonal dependent coefficient sz_i. The time dependence was approximated by harmonic functions with the maximum in March for the northern hemisphere and in September for the southern one:

$$sz_i(month) = 1 + \frac{sz_i^0}{2}\left[1 \pm \cos\left(2\pi \frac{month - 3}{12}\right)\right]$$

The coefficients sz_i^0 for every layer of the stratosphere were chosen to reach the best agreement of the results of the simulation with the experimental data. The sign "+" is valid for the northern hemisphere and "- " for the southern one. The full cycle of season alternation takes 12 months and the maximum of the exchange for the northern hemisphere is reached in March (*month* number 3).

To take into account the reduction of the mixing at the tropic barriers (from equator to 20°) the diffusion rates in every layer were multiplied by coefficients tb_i. The numerical values of these coefficients were chosen to reach the best agreement between the experimental data and the results of the simulation.

2.3.3. Gravitational settling

Many nuclides in the atmosphere are bound to aerosols, which are sensitive to the gravitation and settle down. In the approximation of spherical form of the aerosols, the speed of their settling can be found from the equilibrium of the Stokes-Cunningham friction force

$$F = \frac{6\pi\eta r v}{1 + \beta\frac{\lambda}{r}}, \tag{8}$$

where

- v - speed of the aerosol,
- r - radius of the aerosol,
- η - viscosity of the air,
- λ - averaged path length of an air molecule,
- β - correction factor that can be calculated as $\beta = 1.26 + 0.4 \cdot e^{-1.1\frac{r}{\lambda}}$,

and the gravitational force

$$F_G = \frac{4\pi}{3} r^3 \rho g, \tag{9}$$

where

- r - density of the aerosol,
- g - gravitational acceleration.

The gravitational settling is not important in the troposphere because of its effective mixing. However, it cannot be neglected, when the transport in the stratosphere and through the

tropopause is considered. The size of the box number i is known and using (8), (9) to calculate the speed of the settling, it is easy to find the characteristic time t_i. Thus, the corrected transport rate from the box i into the box $i+1$ is

$$\tilde{\lambda}_{i\,i+1} = \lambda_{i\,i+i} + \frac{1}{\tau_i}.$$

Because the aerosols of different sizes are present in the atmosphere, r in the equations (8) and (9) has a meaning of an average value and it is used as a free parameter.

2.3.4. STE. Advection

In the Section 2.1.2, it was mentioned that diffusive STE takes place mainly at the tropopause folds. The tropopause is not stationary and its folds move within a year between 30° and 60°. Thus, in this range of these latitudes an exchange through the tropopause is the most effective. Rises and sinks of the tropopause lead to an additional exchange. The variations of the height of the equatorial tropopause are larger than of the polar tropopause. Thus, the exchange is more efficient at the low latitudes than at the polar regions. The rates of the diffusive exchange through the tropopause were calculated as:

$$STE_{\downarrow}(\lambda, month) = STE_0 \cdot \frac{p(5^o)}{p(\lambda)}\, f(\lambda)\, j(month)$$

$$STE_{\uparrow}(\lambda, month) = \frac{1}{4}\, STE_0 \cdot \frac{1033\,\frac{\mathrm{g}}{\mathrm{cm}^2} - p(5^o)}{1033\,\frac{\mathrm{g}}{\mathrm{cm}^2} - p(\lambda)}\, f(\lambda)\, j(month),$$

where

- STE^{-}, STE_{-} - the rate of transition from the *Stratosphere 4* to the *Troposphere* and from the *Troposphere* to the *Stratosphere 4* correspondingly,
- STE_0 - coefficient, which is determined by the comparison of experimental data and the simulation,
- l - latitude,
- $p(l)$ - column mass of the stratosphere at the latitude λ (see Table 1),
- $f(l)$ - efficiency of the transport though the tropopause at the latitude λ. The values shown in Table 2 were optimized to have maximum at mid-latitudes and to be constant far from the tropopause folds,

j(month) - coefficient, which shows the seasonal variations:

$$j(month) = 1 \pm a \cdot \cos\left(2\pi \frac{month - 3}{12}\right).$$

Here *a* is the amplitude of the seasonal oscillations, the sign "+" is used for the northern hemisphere and "-" for the southern one.

Latitudinal belt	0°-10°	10°-20°	20°-30°	30°-40°	40°-50°	50°-60°	60°-70°	70°-80°	80°-90°
f(l)	0.07	0.07	0.07	0.5	1.0	0.5	0.03	0.03	0.03

Table 2 Latitudinal distribution of the STE efficiency

The advection (see Figure 8) plays an important role in the mass transport and in the STE. In order to describe it, the horizontal exchange rates at the latitudinal belt 10°-20° for the layers *Stratosphere 1*, *Stratosphere 4*, and *Troposphere* were given as free parameters v_{St1}, v_{St4}, and v_{Tr} correspondingly. At the place of the tropopause breaks, the poleward flux bifurcates. A part *k* of the high stratospheric (the level *Stratosphere 1*) flux moves further to the pole region, where it sinks to the low stratosphere (the level *Stratosphere 3*) and moves back to the latitudinal belt 40°-50°. The rest of it and the flow of the low stratosphere sink down to the troposphere. The corresponding exchange rates in horizontal and vertical directions were obtained using the mass conservation condition. The poleward flow in the high troposphere and in the stratosphere is compensated by the equator directed flow in the low troposphere. Thus, both the circulations in the troposphere (Hadley cells) and in the stratosphere (Brewer circulation) were taken into account in the model.

2.3.5. Application of the model to different elements

Concentrations of the nuclides, in the transport of which we are interested, are very low. Thus, they cannot influence the atmospheric processes and their transport is determined by the movements of the air masses. The difference in the transport of different elements can be seen only if additional forces appear.

The elements, which are present in the atmosphere in a gas form (e.g. ^{14}C in form of CO_2), are in the equilibrium with the gravitational force and their transport repeats the movements of the air masses. The elements (e.g. Be, Sr, Cs), which are bound to aerosols, undergo gravitational settling in the stratosphere and through the tropopause (see 2.3.3).

In the troposphere, they are in the centers of water vapor condensation. Thus, together with the dry fallout they are effectively washed out with precipitation (*rain-out*). Highly

soluble gases are attached to water aerosols in the troposphere and they undergo the similar processes. The fact that a part of these gases remains in a free form is compensated by *washout* during rains from the layer below the clouds. In order to describe the fallout of Be, Cl, and Sr an additional box of so-called "wet troposphere" was introduced for every latitudinal belt. The nuclides of the "dry troposphere" can fall out onto the surface of the Earth or they can be transformed to the wet troposphere, from where the rate of removal is proportional to the precipitation rate *P*. The used parameters are given in Table 3

Direction of the flow			Residence times (days)
Dry troposphere	→	Wet troposphere	18
Dry troposphere	→	Surface of the Earth	36
Wet troposphere	→	Surface of the Earth	5/*P*

Table 3 Tropospheric residence times of nuclides, attached to aerosols (e.g. ^{36}Cl, ^{90}Sr, ^{137}Cs). P is precipitation rate in m\a^{-1}

The low soluble gases are removed from the troposphere after their decay (e.g. CH_3Cl after the interaction with OH) or by diffusion to other reservoirs (in the case of CO_2 these reservoirs are the surface layer of the ocean and the biosphere). The corresponding residence times can be often found in literature (e.g. [29], [86]).

In order to describe the transport of radiocarbon, the box model was extended to 8 boxes in every latitudinal belt, including *the biosphere*, *the surface* and *deep oceans.* The used residence times are shown in Table 4.

Direction of the flow			Residence times (years)
Troposphere	→	Surface ocean	2.6
Surface ocean	→	Troposphere	3.5
Troposphere	→	Biosphere	20
Biosphere	→	Troposphere	60
Surface ocean	→	Deep ocean	6

Table 4 Residence times in the radiocarbon transport model

In the pole regions, the biological activity is suppressed and no exchange between the troposphere and the biosphere was taken into account above 70°.

Figure 10 Explosion of the nuclear bomb of 14 kt TNT at the height of 345 m in 1951. This photo is the property of DoE and it is obtained from http://www.dreamlandresort.com

2.4. *Normalization of the transport parameters*

2.4.1. Nuclear explosion

In order to determine the parameters of the transport model it is convenient to use the data of bomb-produced radionuclide distribution [87, 88]. In the last years, detailed information about nuclear explosions became available [89, 90].

After a nuclear explosion, the prompt radiation (γ and neutrons) carries about 5% of the released energy. 50% of the energy is brought away by the spherical shock wave and for the rest 45% the delayed radiation is responsible (10% - delayed β and γ radiation, 35% - heating) [91]. The fireball created in the epicenter of the explosion is warmed up to a high temperature. The increased pressure expands it and the buoyancy force pushes it upward. Fission products (e.g. ^{90}Sr) being inside of the fireball are also lifted to high altitudes. The air under the fireball cools down and it becomes compressed under the atmospheric pressure around. Thus, the stem of the nuclear mushroom is created, and the air is sucked into its bottom. This air rises above the fireball, cools down and sinks forming the convective cells,

which look like a cap of a mushroom (see Figure 10). Thus, the gas from the vicinity of the explosion, e.g. ^{14}C that was produced in interaction of neutrons with nitrogen, has a similar altitudinal distribution as the fireball itself. Unfortunately, no reliable data exist on the heights of the fireballs and the injection of radioactive isotopes.

To describe this dependence it was assumed that an explosion of 1 Mt TNT creates a fireball, which rises up to 15 km and has a radius of 5 km. The height and the radius of the fireballs of the other nuclear explosions are scaled as a cubic root of the power in Mt. This corresponds to the general conclusion that a nuclear mushroom created by an explosion below hundreds of kt remains in the troposphere and the mushrooms of 1 Mt and higher enter the stratosphere and can reach high altitudes. For example, according to witnesses of the largest atmospheric test (50 Mt, 30. October 1961) the nuclear mushroom reached the altitude of 67 km [92].

In the calculations, a contribution of the injection to every box was assumed equal to the ratio of the geometrical volume of the fireball within this box to the entire volume of the fireball. The obtained altitude distribution for the explosions of different power was in a good agreement with [89], where the stratosphere was divided into two boxes only.

2.4.2. Number of injected radionuclides

The nuclear weapon tests caused the production of radionuclides of two types:

- the products of fission of heavy nuclei (e.g. ^{90}Sr).
- the products of the reactions induced by bomb neutrons (e.g. $^{14}N(n,p)^{14}C$).

To calculate the injection of a radionuclide it is necessary to know the power of the explosion (it can be found in [89]), the number of fissions and the number of released neutrons per 1 Mt TNT.

Two principles have been used for the energy production in the nuclear weapon: fission and fusion. In the first case, the explosive was ^{235}U or ^{239}Pu, which was brought into condition corresponding to the overcritical mass. The number of fission neutrons was enough to initiate at least one more fission, which released the energy of about 200 MeV and 2 or 3 neutrons. It is easy to estimate the number of fissions per 1 Mt TNT (about $4.2 \cdot 10^{15}$ J):

$$N = 4.2 \cdot 10^{15} J \cdot \frac{1}{1.6 \cdot 10^{-19} \frac{J}{eV}} \cdot \frac{1}{200 \cdot 10^{6} eV} = 1.3 \cdot 10^{26}$$

The number of released neutrons can be found, if the number of neutrons Ns, necessary for the induction of N fissions is subtracted from the number of produced neutrons Nn. Here s is

the ratio of the total inelastic cross-section of neutrons to the cross-section of the induced fission and n is the averaged number of neutrons, released per fission. The results of the estimation for uranium and plutonium are shown in Table 5. To compare, the integral fluxes of neutrons were $1.07 \cdot 10^{26}$ Mt^{-1} after the explosions in Hiroshima (^{235}U) and $1.65 \cdot 10^{26}$ Mt^{-1} in Nagasaki (^{239}Pu) [93]. In the calculation, the value of $1.8 \cdot 10^{26}$ neutrons per 1 Mt of fission was used. This corresponds to the theoretical estimate for ^{235}U and is close to the measured neutron release during ^{239}Pu bomb explosion.

Explosive	ν [91]	σ [91]	Number of neutrons per 1 Mt TNT
^{235}U	2.56	1.2	$1.8 \cdot 10^{26}$
^{239}Pu	3.08	1.12	$2.5 \cdot 10^{26}$

Table 5 Average number of neutrons per fission n, ratio of total inelastic cross-section of neutrons to the cross-section of the induced fission s, and estimated number of released neutrons for ^{235}U and ^{239}Pu.

In the case of fusion the main part of the energy was obtained by the collision of deuterium and tritium:

$$D + T \rightarrow a\,(3.5\,MeV) + n(14.1\,MeV)$$

Practically it is convenient to produce tritium “at the place”. The reaction

$$^{6}Li + n \rightarrow a + T + 4.8\,MeV$$

is used for this purpose. The sum of the reactions can be written as

$$^{6}Li + D \rightarrow 2a + 22.4\,MeV$$

It is easy to see that no neutron is emitted. Their production takes place during the burning of deuterium:

$$A: \begin{cases} D + D \rightarrow {}^{3}He + n + 3.25\,MeV \\ D + {}^{3}He \rightarrow {}^{4}He + p + 18.3\,MeV \end{cases}$$

$$B: \begin{cases} D + D \rightarrow T + p + 4\,MeV \\ D + T \rightarrow {}^{4}He + n + 17.6\,MeV \end{cases}$$

The realization of each of these two channels leads to a sum reaction

$$3D \rightarrow {}^{4}He + p + n + 21.6\,MeV$$

Thus, neglecting other possible reactions like $^{6}Li+^{6}Li$, $^{6}Li+p$, $^{6}Li+D$, etc. the number of the produced neutrons depends on the ratio of ^{6}LiD and DD cycles. The largest possible neutron

emission can be reached by the production of pure DT or DD bombs: $1.49 \cdot 10^{27}$ and $1.2 \cdot 10^{27}$ neutrons per 1 Mt TNT respectively.

There was only one pure fusion bomb exploded (Mike, 1952). Typically FFF (fission-fusion-fission) bomb were used. The explosion started with fission of ^{235}U or ^{239}Pu. The released neutrons produced tritium and initiated the fusion. For better efficiency, the bomb was surrounded by the natural uranium, which was used simultaneously as a neutron reflector, neutron multiplier, and a fast fission explosive. Thus, both processes fusion and fission must be considered when a FFF bomb is discussed.

According to [94], every Megaton explosion produces about $2 \cdot 10^{26}$ neutrons. Much higher estimates made in [91] ($1.49 \cdot 10^{27}$ Mt^{-1} neutrons for a fusion bomb and $2.95 \cdot 10^{26}$ Mt^{-1} for a fission bomb) seem to be unrealistic and they should be considered as an upper limit.

The most recent consideration of the radionuclides injection, which is in good agreement with the above estimations, was performed in [89]. According to this work the explosion of 1 Mt uranium or plutonium bomb leads to $1.45 \cdot 10^{26}$ fissions. With the ^{90}Sr yield of 3.5% the production of this isotope was calculated to be $5 \cdot 10^{24}$ atoms per Mt. The production of ^{14}C was pointed as 0.85 PBq/Mt, which corresponds to $2.2 \cdot 10^{26}$ atoms per Mt. Slightly different estimations of the injection were done in [80]:

- $4.2 \cdot 10^{24}$ atoms of ^{90}Sr per Mt of fission
- $1.95 \cdot 10^{26}$ atoms of ^{14}C per Mt of fission and $1.15 \cdot 10^{26}$ atoms of ^{14}C per Mt of fusion

The uncertainty appears because the technological data of nuclear bombs are not available. In Table 6 it can be seen that fission yields of ^{90}Sr for different explosives differ by a factor of 2. Moreover, they are sensitive to the neutron energy, which depend on the moderating properties of a bomb. However, we have assumed that the yield of 3.5% from [89] can be considered as an averaged value. Thus, each Mt TNT of fission produce about $4.5 \cdot 10^{24}$ atoms of ^{90}Sr.

	^{235}U	^{238}U	^{239}Pu
Spontaneous fission		5.43	
Thermal neutrons	5.78		2.1
Fission spectrum neutrons	5.47	3.25	2.05
High-energy neutrons (14 MeV)	4.59	3.19	2.1

Table 6 Cumulative yields of ^{90}Sr(%) in spontaneous and induced fission of ^{235}U, ^{238}U, and ^{239}Pu [95].

The neutron capture by nitrogen with the production of radiocarbon is the main channel of neutron absorption. According to [96] only about 17% of neutrons are absorbed in the reactions like *Fe(n,g)*, *Fe(n,p)*, and $^{14}N(n,T)^{12}C$. However, this estimation has a high uncertainty and in the limits of accuracy, the number of the produced ^{14}C can be assumed equal to the number of the released neutrons. In the calculation, 1Mt of fission or fusion produced $1.8 \cdot 10^{26}$ atoms of ^{14}C (see Table 7). The neutron release for fusion bombs was optimized for the total amount of ^{14}C observed in the atmosphere. If the explosion was performed near the surface of the Earth, half of the neutrons was absorbed by the lithosphere and did not produce ^{14}C.

Radionuclide	**Production by 1 Mt of fission bomb, 10^{26}**	**Production by 1 Mt of fusion bomb, 10^{26}**	**Remark**
^{14}C	1.8	1.8	*For the tests near the Earth surface it is 2 times less*
^{36}Cl	0.3	0.3	*Water tests only*
^{90}Sr	0.045		

Table 7 Production of radioisotopes per 1 Mt TNT due to the atmospheric nuclear weapon tests

The bomb ^{36}Cl was produced by neutron activation of ^{35}Cl. Because the concentration of stable chlorine in the atmosphere is very low, this channel of the ^{36}Cl production can be neglected. However, large quantities of stable chlorine are present in the ocean. Thus, the production of bomb ^{36}Cl was mainly due to explosion near the water (on barge, water, and underwater tests). If n_i is the concentration of the nuclide i in water and neutron absorption cross-section of this nuclide is s_i, the part

$$\eta = \frac{\sigma_{^{35}Cl \to ^{36}Cl}\, n_{^{35}Cl}}{\sum_i \sigma_i\, n_i} \qquad (10)$$

of neutrons produces ^{36}Cl. Analysis of the most abundant elements in the ocean (see Table 8) with the help of (10) shows that about 33% of the thermal neutron produced ^{36}Cl. However, some corrections should be applied to this estimation. A part of neutrons (about 50%) does not enter the water and does not produce ^{36}Cl. Moreover, not all produced ^{36}Cl atoms were injected into the atmosphere because some of them remained in the ocean. This reduction factor α was not known and was to be estimated. The production of ^{36}Cl per 1 Mt TNT in the "*near water*" tests with α=1 is shown in Table 7.

Element	Content, parts per thousand	Atom mass	Particle abundance, n_{rel}, $^{o}/_{oo}$	Cross-section of neutron absorption σ, b	$\frac{s\ n}{\sum_i s_i\ n_i}$, %
O	860	16	334	0.00027	0.03
H	106	1	659	0.332	65.70
Cl	19.4	35	2.6	43	33.05
		37	0.8	0.43	0.11
S	0.9	32.1	0.2	0.52	0.03
Na	10.8	23	2.9	0.53	0.46
Mg	1.3	24.3	0.3	0.063	0.01
Ca	0.4	40.1	0.1	0.43	0.01
K	0.4	39.1	0.1	2.1	0.04
B	0.0043	10.8	0.002	759	0.56

Table 8 The most abundant elements in the ocean and their contribution to the neutron absorption

2.4.3. Available experimental data

For the normalization of the model parameters the data on bomb produced radioactive fallout and the concentration of the radioisotopes in the atmosphere were used. Unfortunately, some authors used estimated data instead of the measured ones. At present, it is not always possible to distinguish, which of the "experimental points" are results of the measurements and which of them are products of simulation. For example, the integral latitudinal dependence of ^{90}Sr fallout in [89] repeats the data of [97], which were obtained from multiple measurements over the globe. However, in [89] it was not mentioned that no experimental data to the north of 70°N and to the south of 60°S were available and an extrapolation was used for the pole regions. Within these limits, this dependence can be used to study the relationship between vertical and horizontal transport. In particular, it can be seen that the strontium exchange between the hemispheres takes place mainly in the stratosphere. Into the troposphere, ^{90}Sr enters in the middle latitude zone and then it diffuses in both directions.

In the works mentioned above, also the annual integral fallouts over the northern and southern hemispheres for the periods of 1945 – 1992 and 1951 – 1991 correspondingly were published. The phase shift between two data sets gives the information about the rate of the horizontal transport. The phase shift between the fallout in the northern hemisphere and the injection of ^{90}Sr gives the information about the rate of the vertical transport.

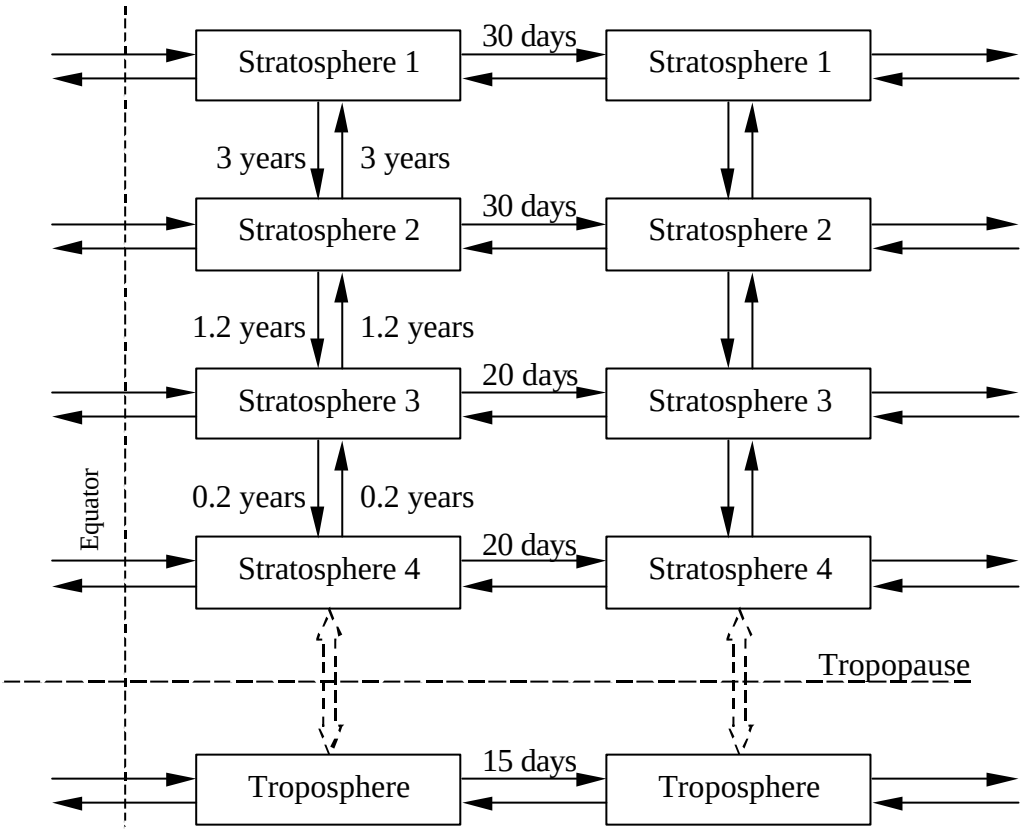

Figure 11 Exchange times, which correspond the best agreement of experimental data and simulation. The data are shown for the equatorial latitudinal belt only. The exchange rates at other latitudinal belts can be recalculated (see description in the text)

The latitudinal dependence of the annual ^{90}Sr deposition between 1958 and 1966 is given in [98]. The results of multiple measurements and the assumption that the efficiency of the fallout is similar over the ocean and over the continents were used in this work.

The data on ^{90}Sr concentration in the atmosphere at various altitudes on the latitude 30°N between April 1963 and January 1966 was published in [81]. The corresponding distribution of ^{14}C concentration can also be found there. However, the data do not represent the results of direct measurements. The experimental points were used to build the contour plots, which were later interpreted numerically. In the same way, the latitudinal dependences of stratospheric ^{14}C in the years 1963, 1964, and 1965 were obtained. Accordingly, the usage of these data implies the possibility of a large uncertainty and only the general tendency can be used for the modeling.

2.4.4. Parameters of the model

The vertical and horizontal exchange rates were obtained by optimization of the output of the model compared to the experimental data. The residence times T_{Ver} and T_{Hor} of the boxes of

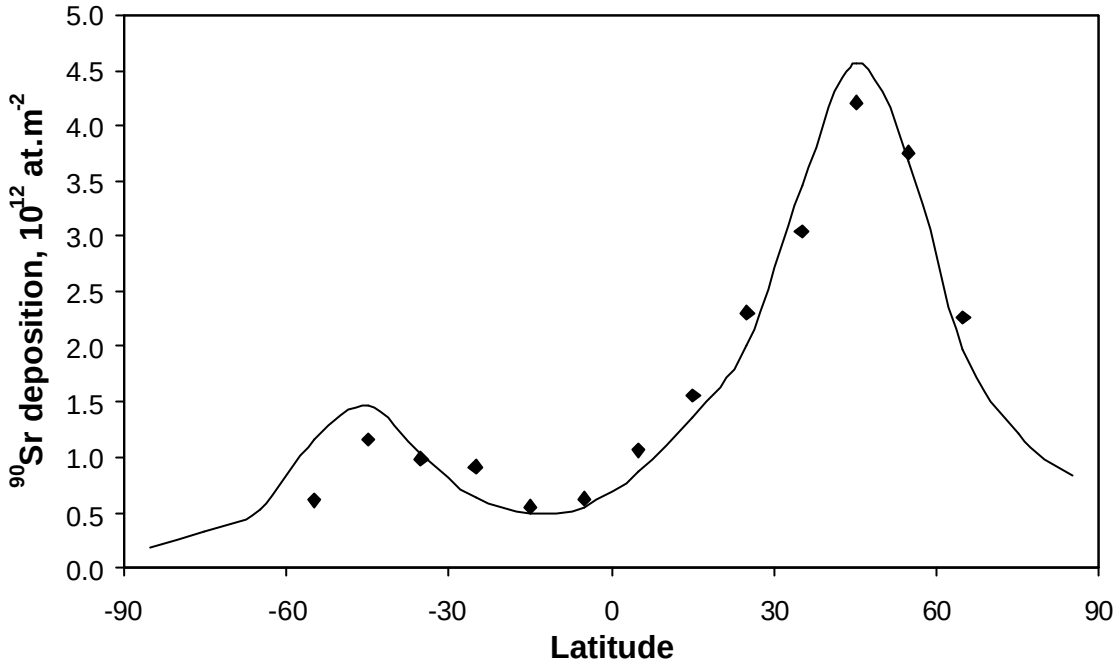

Figure 12 Latitudinal distribution of fluence of bomb-produced ^{90}Sr. The solid line represents the simulated data and the points show experimental data [89].

the equatorial latitudinal belt are shown in Figure 11. The corresponding exchange rates for other latitudes were calculated according to the formulas (5)-(7).

The attenuation coefficients of the exchange rate within tropic barrier tb_i and the relative amplitudes of the seasonal variations in the surf zone sz_i are presented in Table 9. The airflow from the summer hemisphere to the winter hemisphere is continues in the high stratosphere [99]. Thus, no tropic barrier exists there.

The parameters of the advection v_{St1}, v_{St4}, and v_{Tr} are collected in Table 10. The time of 60 days in the upper stratosphere is in good agreement with the upward flux of $32.4 \cdot 10^8$ kg·s^{-1} for each hemisphere [73] and the mass of the box of $1.63 \cdot 10^{16}$ kg. After the bifurcation at mid-latitudes, a part κ=60% of the flux in the upper atmosphere moves farther polewards and the rest sinks to the troposphere.

The diffusive exchange through the tropopause takes place with a rate STE_0 = 0.18 days^{-1} and an amplitude a=0.9. This corresponds to the diffusive flux through the tropopause of about $580 \cdot 10^8$ kg s^{-1}, which is much higher than the flux of advection.

The best agreement of the simulated and experimental ^{90}Sr deposition was obtained with an aerosol radius r of 0.2 μm.

Figure 12 shows the comparison of the simulated and experimental latitudinal distribution of ^{90}Sr deposition. It can be seen that the northern hemisphere is described well

	Attenuation coefficients within tropic barriers, *tb*	Amplifying coefficients in the surf zone (max value), *sz*
Stratosphere 1	1.0	3
Stratosphere 2	0.5	3
Stratosphere 3	0.5	5
Stratosphere 4	0.5	5
Troposphere	0.5	1

Table 9 Coefficients, which were used in the model to take into account non-uniform diffusion (see section 2.3.2)

	Troposphere, v_{Tr}	Stratosphere 4, v_{Sr4}	Stratosphere 1, v_{Sr1}
Advection time, days	45	120	60

Table 10 Removal times by horizontal advection at the latitudinal belt 10°-20°

while slight differences are observable in the southern hemisphere. This can be attributed to the uncertainty in the altitudinal distribution of the ^{90}Sr injection. The largest test series were performed in the latitudinal belts 10°-20° and 70°-80° in the northern hemisphere. Strong upward and downward flows in the stratosphere are present there. Thus, the altitude distribution of ^{90}Sr is formed by the atmospheric circulation and not by the injection only. However, the absence of the evidence of strong local fallout shows that even ^{90}Sr injected by small bombs did not remain in the troposphere and reached the stratosphere. This effect was not described by the model. In order to take it into account the radioisotopes injected into the troposphere were assigned to the low stratosphere. This proved to be a good assumption for the average case. However, it could be wrong for some local test places. For example, a number of tests were performed at the latitude - 22°S. If the ^{90}Sr released in them remained in the troposphere, it would increase the fluence in the tropic zone and reduce it at higher latitudes.

A similar conclusion can be driven from the annual ^{90}Sr deposition in the northern and southern hemispheres (see Figure 13). In the northern hemisphere, the results of the simulation differ from the experimental data in years 1947 and 1950 and later in the 80s. In the 40s, it is due to the input to the stratosphere instead of input to the troposphere, which has a shorter residence time. The last reported atmospheric nuclear test took place in China in 1980. Afterwards, the exponential washout from the atmosphere is simulated. The increased fallout in 1983-1985 and its fast drop after 1986 cannot be explained by the model.

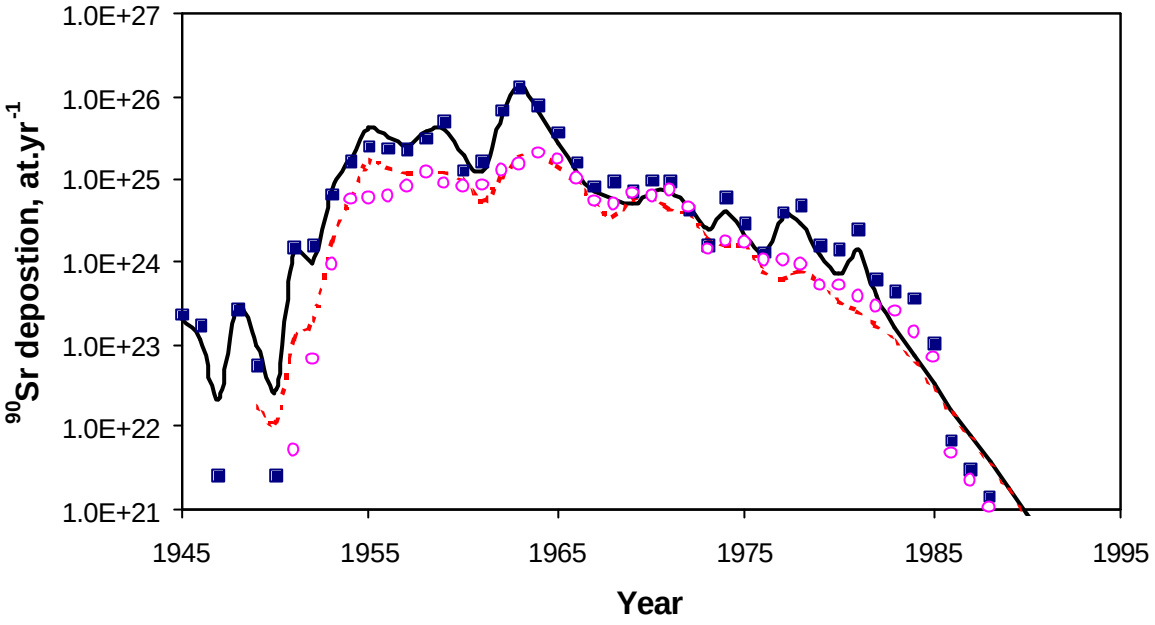

Figure 13 Annual total deposition of ^{90}Sr in the northern and southern hemispheres. The squares and the circles represent the experimental data [89], the solid and dashed lines represent the results of the calculation in the northern and southern hemispheres, respectively.

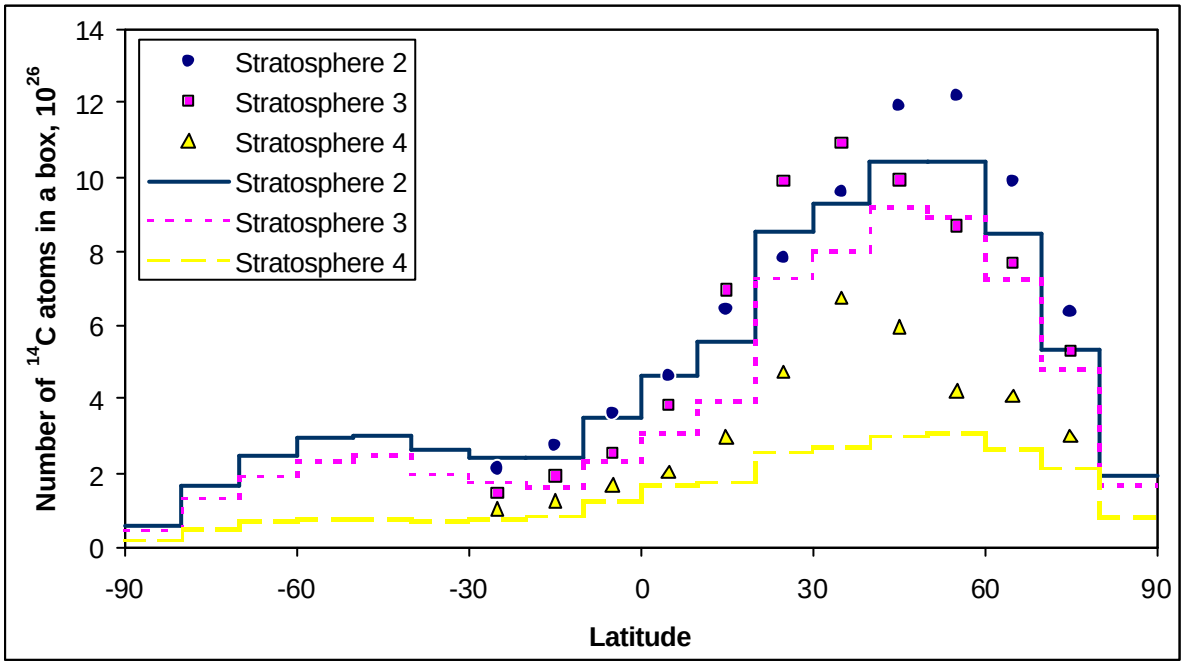

Figure 14 Latitudinal dependence of ^{14}C distribution in the stratospheric boxes in January 1964. The calculated values for the boxes Stratosphere 2, Stratosphere 3, and Stratosphere 4 are represented by solid, dot, and dashed lines correspondingly. The experimental values for them [81] are shown with circles, squares, and triangles correspondingly.

Because most of the nuclear bomb tests were performed in the northern hemisphere, the deposition in the southern hemisphere is sensitive to the transport parameters. In Figure 13

it can be seen that the deposition from the largest test series of 1961 and 1962 were described well. The largest difference to the experimental data is within years 1954-1958. This difference could be explained if ^{90}Sr of the series 1954 were injected into the high stratosphere. In this case, ^{90}Sr would be deposited with a longer delay and over a longer time. Thus, no peak around 1955 would be observable.

The latitudinal distribution of the ^{14}C stratospheric concentration in January 1964 is shown in Figure 14. The data in January 1963 and 1965 have a similar structure and do not need to be discussed separately. It can be seen that the largest discrepancy between the experimental and simulated data is at the middle latitudes in the low stratosphere. In the region 30°-50° the height of the tropopause changes rapidly (see Table 1). At these latitudes, the isentropes do not follow the tropopause and cross it (see Figure 8). Thus, the assumption of the fast diffusion along a stratospheric level and slow diffusion across is not valid there. Consequently, in the model the high radiocarbon concentration of the polar upper stratosphere does not increase the content of ^{14}C in the lower stratosphere of middle latitudes. However, this problem is of importance for the low stratosphere only. At higher altitudes and if the averaged global transport is considered this effect does not lead to a large error and can be neglected.

2.5. *Recycling*

2.5.1. Methyl chloride and OH radicals

The recycling of ^{36}Cl was firstly suggested in [9]. Though the volatilization of organochlorides was mentioned in this work, the main subject of the discussion was a delayed input of bomb-produced ^{36}Cl into the lakes. In this model, the deposited chlorine was not immediately transported to the aquifer but captured by the vegetation and litter, released to soil and transferred to the ground and surface water. This mechanism could explain the measurements in Laurentian Great Lakes [64] and high ratios of ^{36}Cl/Cl (up to a few 10^{-11}) in the growing vegetation and soil pore water [100]. However, this model was not able to predict high fluxes of ^{36}Cl in modern precipitation. The idea of chlorine reemission to the troposphere from the biosphere in form of methyl chloride was proposed by [8] and the first numerical estimates of this effect were performed in [27].

Methyl chloride is the most abundant chlorine containing organic gas (see Table 30). Its main sources are emission from the ocean and biomass burning. Thus, the high content of ^{36}Cl in the biosphere should lead to high ratios of ^{36}Cl/Cl in methyl chloride and high

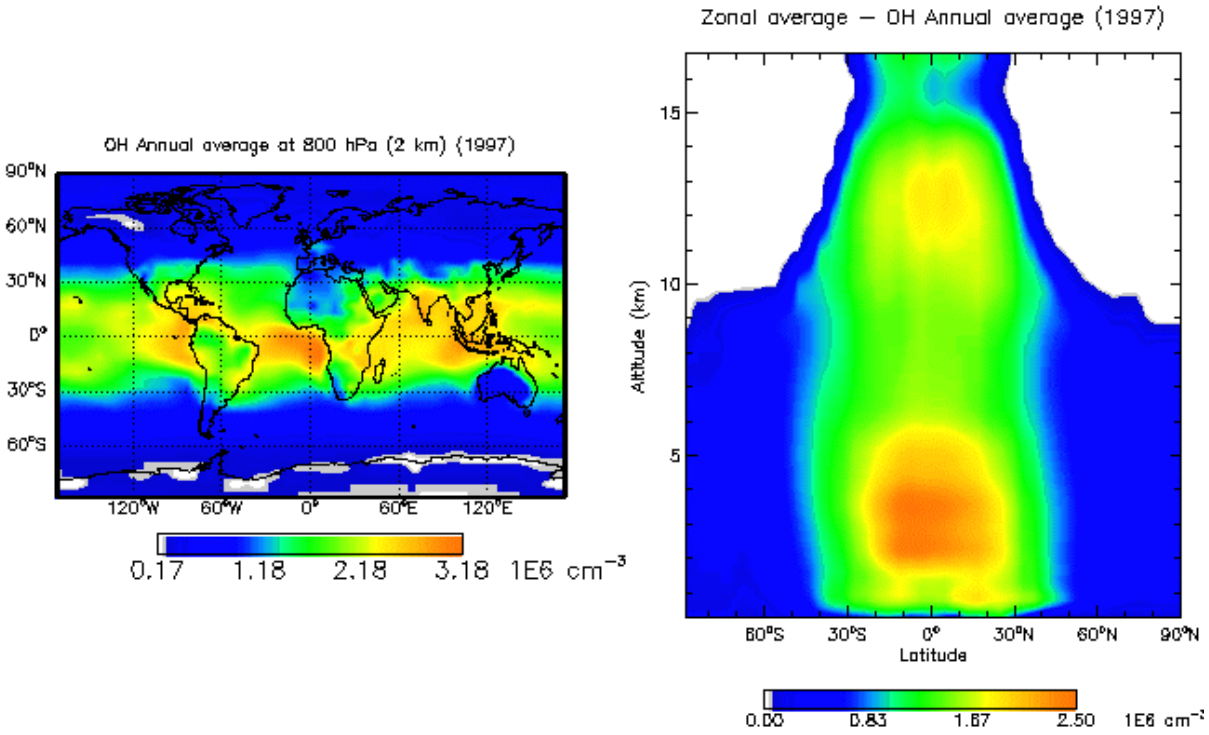

Figure 15 Distribution of OH radicals over the globe. The left picture shows the simulated annual average OH distribution at the altitude of about 2km. The right picture shows annual and latitude average distribution. The plots are taken from http://www-as.harvard.edu/chemistry/trop/geos/

circulation fluxes of ^{36}Cl. Methyl chloride has a residence time in the troposphere of 1.1 years and it is mainly removed in reactions with OH radicals. Accordingly, the deposition of chlorine recycled by CH_3Cl has a few features:

- OH is unevenly distributed in the troposphere with a maximum in the equatorial region and a minimum in the polar regions (see Figure 15). This explains why no recycling ^{36}Cl was found in Greenland and why the discrepancy between measured and calculated ^{36}Cl fluxes is larger at low latitudes then near the poles. Another reason for this effect is that vegetation is poor at high latitudes and little of ^{36}Cl reemission due to methyl chloride is possible there.
- The same concerns the difference between the northern and southern hemispheres. The percentage of land relatively to ocean is higher in the northern hemisphere than in the southern one. Thus, the effect of the recycling is expected to be higher in the northern hemisphere than in the southern.
- According to [101], less than 0.1% of the global surface may be responsible for about 10% of the total flux of atmospheric CH_3Cl. Moreover, strong time variations have been observed. Thus, the reemission of chlorine has a pronounced non-uniform distribution and the deposition of the recycled chlorine has significant fluctuations.

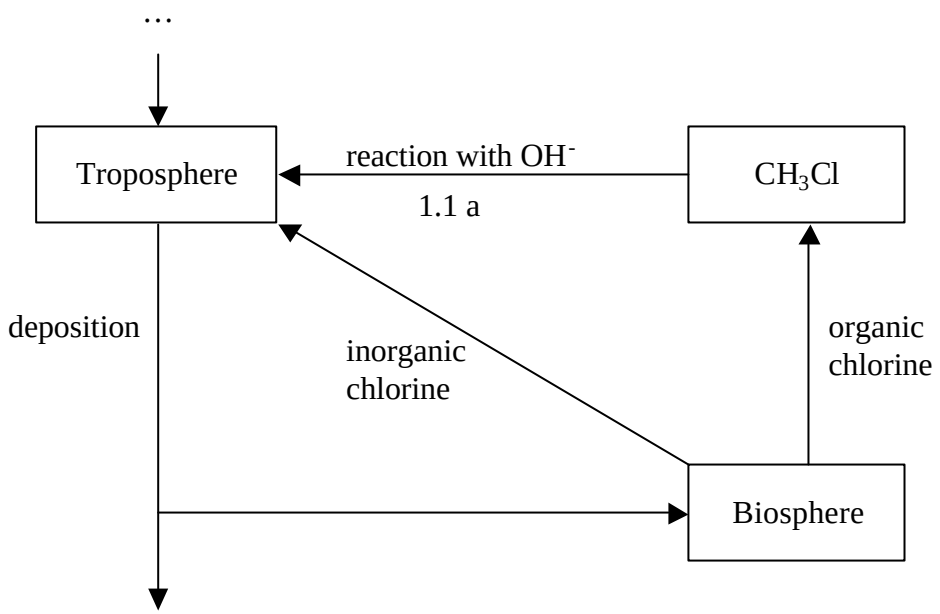

Figure 16 Recycling scheme of ^{36}Cl. A part of the deposited ^{36}Cl is captured by the biosphere. The biosphere releases chlorine in both organic and inorganic forms. The most abundant organic chlorine-containing composition CH_3Cl decays in reactions with OH^-. Inorganic chorine is washed out of the troposphere.

All these effects can be found by comparison of the measured and calculated ^{36}Cl fluxes (see Figure 7).

2.5.2. Incorporation of the recycling into the transport model

To take into account the recycling two additional boxes were included to every latitudinal belt: *biosphere* and *methyl chloride* (Figure 16). A part of chlorine deposition is captured by the biosphere. No correction has been done to take into account the difference of biological species at different latitudes. However, it was assumed that no biologic activity was present at latitudes above 70°. Moreover, the rate of chlorine capture by the biosphere was taken proportional to the ratio of land area at the latitudinal belt to the entire area of this belt (see Table 11). The biosphere releases chlorine in form of methyl chloride, which is transported in the same way as the tropospheric air. With a rate proportional to the OH column concentration in every latitudinal belt, chlorine is transported from the *methyl chloride* box to the box of the troposphere. The column concentration of OH was obtained by integration and averaging of the data from [102] for January, April, July, and October (see Table 11).

According to [86] the biosphere releases about 20 times more chlorine in inorganic form than as methyl chloride. Most of the inorganic chlorine has a short residence time in the biosphere and its contribution to the recycling is negligible. However, that part of chlorine, which is stored in the biosphere for a long time, is released in both organic and inorganic

	Latitudinal belt	Area, 10^{12} m^2	Percentage of ocean, %	Percentage of land, %	Tropospheric OH column, 10^{16} m^{-2}
North hemisphere	90-80	3.90	91	9	0.23
	80-70	11.59	70	30	0.27
	70-60	18.91	30	70	0.43
	60-50	25.61	43	57	0.60
	50-40	31.49	48	52	1.01
	40-30	36.41	57	43	1.49
	30-20	40.20	62	38	1.75
	20-10	42.78	73	27	2.12
	10-0	44.09	77	23	2.35
South hemisphere	0-10	44.09	76	24	2.47
	10-20	42.78	78	22	2.35
	20-30	40.20	77	23	1.97
	30-40	36.41	89	11	1.44
	40-50	31.49	97	3	0.93
	50-60	25.61	99	1	0.54
	60-70	18.91	90	10	0.36
	70-80	11.59	36	64	0.23
	80-90	3.90	12	88	0.18
	Total	510.0	71	29	1.52

Table 11 Area, ratio ocean-land, and OH^- column concentration at different latitudinal belts.

forms. In this case, organic gases with a long residence time in the troposphere are responsible for the global effect of the recycling and inorganic chlorine and the organic gases with short residence time produce local effects.

In order to take the inorganic part of the chlorine into account the possibility of the direct transition of chlorine from biosphere to troposphere was left in the model. Thus, the recycling model was described by 3 free parameters:

- part of the chlorine fallout onto the land, which is captured by the biosphere,
- mean residence time of chlorine in the biosphere,
- ratio of chlorine release in form of methyl chloride and in inorganic form. Other chlorine containing compounds were neglected. It should be noticed that the box of

the biosphere in the model consists only of that part of the biosphere, which keeps chlorine for a long time (more than a few years). Thus, this ratio is not equal to 1/20.

2.6. *Lakes with different flushing times*

Rainwater falls onto the land and produces runlets and rivers, which flow into the lakes, the seas, and the ocean. The area, from which the rainwater enters a lake, is called *catchment area* of this reservoir. In the stationary case, the volume of a lake does not change with time and the sum of the inflows is equal to the outflow plus evaporation rate. If N rivers flow into a lake with the surface S and the mean precipitation rate over the catchment area is Φ^w, the water balance can be written as

$$\sum_{i=1}^{N} F_i^w + \Phi^w \cdot S = Q + l \cdot S \qquad (11)$$

where

F_i^w - the water flow of the river number i,

Q - the outflow of the lake,

l - the thickness of the layer, which evaporates per unit of time

The rivers inflow can be found as the precipitation rate over the catchment area A minus the precipitation over the lake and the part of the water η that is lost due to evaporation. With these denominations the input into the lake can be written as

$$\sum_{i=1}^{N} F_i^w + \Phi^w \cdot S = \Phi^w \cdot \left(A \cdot (1-\eta) + S \cdot \eta\right) \qquad (12)$$

The chloride contained in rainwater is well soluble. It flows with the water into the lake and its input can be described by an equation similar to (12). The only difference is that it is not evaporated and only if some rivers dry out η might be equal 1. In all other cases η=0 and the input of the chloride into the lake is:

$$F_{in} = \Phi_0 A$$

where Φ_0 is the flux of the chloride deposition. The outflow of the chloride from the lake is:

$$F_{out} = c \cdot Q$$

where c is the concentration of the chloride in the lake. For the stationary conditions

$$\Phi_0 \cdot A = c \cdot Q \qquad (13)$$

and the stationary chloride concentration

$$c_0 = \frac{\Phi_0 A}{Q} = \frac{\Phi_0 A\, T}{V} \tag{14}$$

where

V - volume of the water in the lake,

$T = \frac{V}{Q}$ - *flushing time* of the lake,

For the studies of ^{36}Cl, the equation (14) can be used if only natural sources contribute to the system. In fact, these natural sources should be ideal in order to allow neglecting the variations of the production rate and the transport conditions.

Of a special interest is a situation, when the input function Φ depends on time (e.g. due to nuclear bomb tests the flux of ^{36}Cl varies strongly, see Figure 6). In this case, the balance equation (13) should be written in dynamical form

$$\frac{dc}{dt} = -\frac{c}{T} - \frac{c}{\tau} + \frac{\Phi(t)A}{V} \tag{15}$$

where

τ - life-time of ^{36}Cl.

The general solution of the equation (15) looks like

$$c(t) = c(0) + \int_0^t \frac{A}{V}\Phi(t')\, e^{\frac{t'-t}{\tilde{T}}} dt' \tag{16}$$

where

$\tilde{T} = \frac{T \cdot \tau}{T + \tau}$ - residence time of ^{36}Cl in the lake.

It can be seen that a lake plays a role of an integration system with a parameter $\tilde{T}$, which determines the period of averaging of the incoming signal. The lakes with long residence time $\tilde{T}$ attenuate short variations and are suitable for measurements of the mean ^{36}Cl fluxes. Because of the long life-time of ^{36}Cl, in most cases $\tilde{T}$ is equal to the flushing time of the lake T and typically we do not distinguish them. Only if the flushing time is longer than a few hundred thousand years or the lake does not have any outflow, the ^{36}Cl decay should be taken into account. In this case, the stationary natural ^{36}Cl concentration is often not reached yet and (14) should be modified:

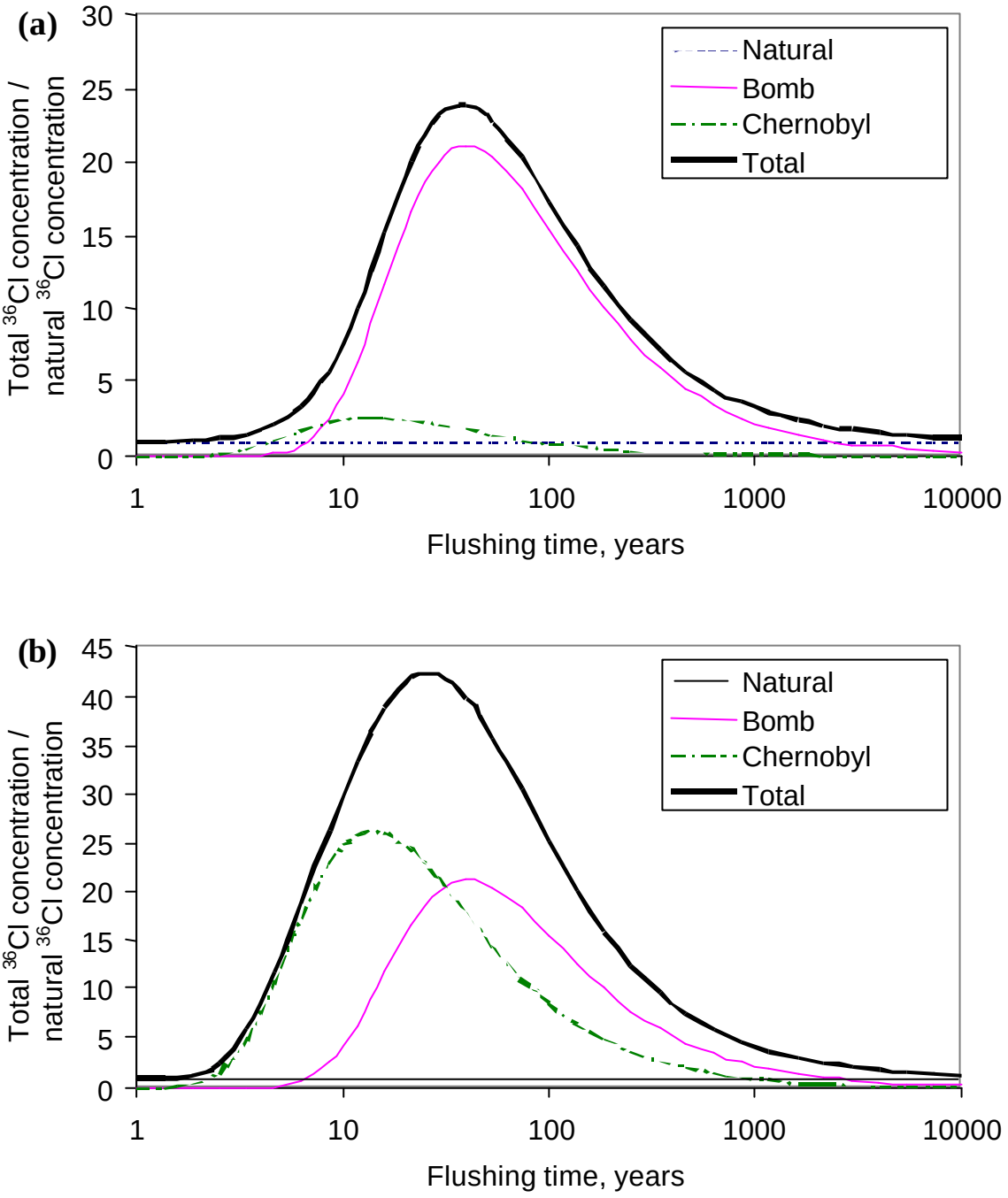

Figure 17 Ratio of total to natural ^{36}Cl concentration for lakes with different flushing times. The bomb input was assumed to be 2300 years of natural production. The input of Chernobyl ^{36}Cl was taken as 100 years (a) and 1000 years (b) of natural production.

$$c_0 = \frac{\Phi_0 A \tilde{T}}{V}\left(1 - e^{-\frac{t}{\tilde{T}}}\right),$$

where t is the closure age of the lake.

An important case of the functional dependence $\Phi(t)$ is a permanent source Φ_0 with a short additional source $\Delta\Phi$, which appears at the moment t=0 and lasts time Δt. Using the solution (16) it can be found that after the input (at the time $t>\Delta t$) the concentration of the salt in the lake can be calculated as

$$c(t) = c_0 + \frac{A}{V}\Delta\Phi \cdot T\left(e^{\frac{\Delta t}{T}} - 1\right)e^{-\frac{t}{T}}$$

where c_0 is the stationary concentration according to (14).

If the duration of the additional source is small compared to the flushing time ($\Delta t << T$) this formula can be simplified

$$c(t) = c_0 + \frac{A}{V}\Delta\Phi \cdot T\ \frac{\Delta t}{T}e^{-\frac{t}{T}} = c_0 + \frac{F \cdot A}{V}e^{-\frac{t}{T}} \qquad (17)$$

where F is fluence of ^{36}Cl.

When a real substance is investigated, the relative changes are more important than the absolute ones. Thus, in the case of ^{36}Cl the ratio of its concentration to its natural level can be estimated as

$$\frac{c(t)}{c_0} = 1 + \frac{F}{\Phi_0 \cdot T}e^{-\frac{t}{T}} \qquad (18)$$

Equation (18) expresses the main idea of the ^{36}Cl measurements in lakes with different flushing times. Because the moment of the sampling is limited by 2 or 3 years (the duration of a typical scientific project) t is fixed. However, T can be varied and the maximum of the ratio (18) is reached, when $T \approx t$. Thus, in the year 2000 the influence of the bomb produced chlorine is mostly expressed in the lakes with the flushing time of about 40 years and the influence of Chernobyl chlorine – in the lakes with the flushing time of about 14 years. With the help of the lakes with $T << t$ it is possible to make conclusions about the ^{36}Cl fluxes at present and if $T >> t$ the information on the natural fluxes in the past can be obtained.

If the geographical distribution of the fallout of ^{36}Cl produced by different sources were similar, it would be convenient to determine the magnitude of the source in terms of years of natural production: $\Delta T = \frac{F}{\Phi_0}$. For the magnitudes of the bomb peak 2300 years and Chernobyl – 100 and 1000 years the dependence (18) is shown in Figure 7(a) and (b) correspondingly. It can be seen that small inputs of Chernobyl chlorine (about 100 years of

natural production) dominate in the lakes with flushing times about 8 years only. In the regions, strongly contaminated with Chernobyl ^{36}Cl (about 1000 years of natural production) the bomb influence can be determined only in the lakes with flushing times more than 50 years. The information about modern fallout of ^{36}Cl can be obtained only in the lakes with flushing times shorter than 2-5 years.

In some water systems, there is an additional reservoir within the catchment area of one lake. This reservoir (ground water or another lake) is able to keep the rainwater and the dissolved in it chlorine for some time. For this kind of systems, the relation "*mother-daughter*" should be considered. If a brief source caused the fluence F at the moment t=0 the ^{36}Cl output of the "mother" reservoir can be described as

$$I(t) = \frac{F\ A_m}{T_m} e^{-\frac{t}{T_m}} \tag{19}$$

where

A_m - catchment area of the additional reservoir,

T_m - flushing time of the additional reservoir.

For the "daughter" lake the change of the number of ^{36}Cl atoms is equal to the difference of the input (19) and the output

$$V\frac{dc}{dt} = -\frac{V}{T}c + I(t) \tag{20}$$

Only chlorine from the part of the catchment area of the "daughter" lake, which does not belong to the catchment area of "mother", reaches the "daughter" reservoir immediately after fallout. Thus, the initial condition can be written in the form

$$c(0) = \frac{F\left(A - A_m\right)}{V} \tag{21}$$

The solution of the equation (20) with the initial condition (21) plus the natural concentration of ^{36}Cl can be written as

$$c(t) = c_0 + \frac{FA}{V} e^{-\frac{t}{T}} + \Delta c(t) \tag{22}$$

where

$$c_0 = \frac{\Phi_0 TA}{V}$$

$$\Delta ?(t) = \frac{FA_m}{V} \frac{1}{\frac{T_m}{T} - 1} \left(e^{-\frac{t}{T_m}} - \frac{T_m}{T} e^{-\frac{t}{T}} \right)$$

Comparing the expressions (22) and (17), it can be seen that the additional reservoir decreases the ^{36}Cl concentration on the short time scale ($t << T, T_m$). As time goes on, this difference is getting smaller and at the moment

$$t = \frac{T_m T}{T_m - T} \ln\left(\frac{T_m}{T}\right)$$

it disappears completely. Afterwards the water delay increases the observed ^{36}Cl concentration in the "daughter" lake and its difference compared to a simple system reaches its maximum at the moment

$$t = 2 \frac{T_m T}{T_m - T} \ln\left(\frac{T_m}{T}\right)$$

This effect is especially important for the lakes with short (few years) flushing times. The ground water with the flushing time of a few years can significantly change the ^{36}Cl concentration in the lake and course a wrong interpretation of the measurements.

CHAPTER 3. Experimental setup

3.1. *AMS measurements of chlorine –36 in Garching*

3.1.1. Ion extraction and acceleration

The scheme of ^{36}Cl AMS at the accelerator laboratory in Munich is shown in Figure 18. The sample made of silver chloride and pressed in a holder is placed into the ion source (see Figure 19). By the heating of the cesium container Cs vapor is created. The molecules of gaseous Cs diffuse through the pipe and through the valve and reach the spherical tantalum ionizer, where positive ions Cs^+ are formed. These ions accelerated by voltage of 6 kV bombard the target and initiate the sputtering process. Due to the low electron affinity, Cs condensed on the surface of the target also assists the extraction of negative ions. The extraction voltage (28 kV) is chosen in such a way that a superposition of the extraction and the sputter fields pumps the negative particles out of the source with the maximum efficiency.

The primary mass selection is performed by the injector magnet. The electrostatic deflector is used for switching between the injector of AMS (18 degrees) and the injector for other applications made in the laboratory (0 degrees). Additionally, it plays a role of an energy filter. Before the ions enter the tandem, they are preaccelerated by a voltage of 150 kV. In order to reach high energies, a pelletron tandem accelerator with terminal potential U=10 MV is used. In the first half of the tandem the negative ions of $^{36}Cl^-$ are accelerated to the energy $E=eU$, where e is the elementary charge. A thin carbon foil in the middle of the tandem strips off a few electrons. The ions become positively charged and undergo the second step of acceleration. Thus, ions with charge state Z are accelerated up to the energy $E=(Z+1)eU$. If a molecule of mass M enters the tandem, its molecular bounds are destroyed in the stripper and a single compound of mass m with charge state Z has the energy $E = \left(Z + \frac{m}{M} \right) eU$ at the exit of the accelerator. The ^{36}C ions with charge state +8 and energy of 2.5 MeV/nucleon are selected by the analyzing magnet. The ions with other charge

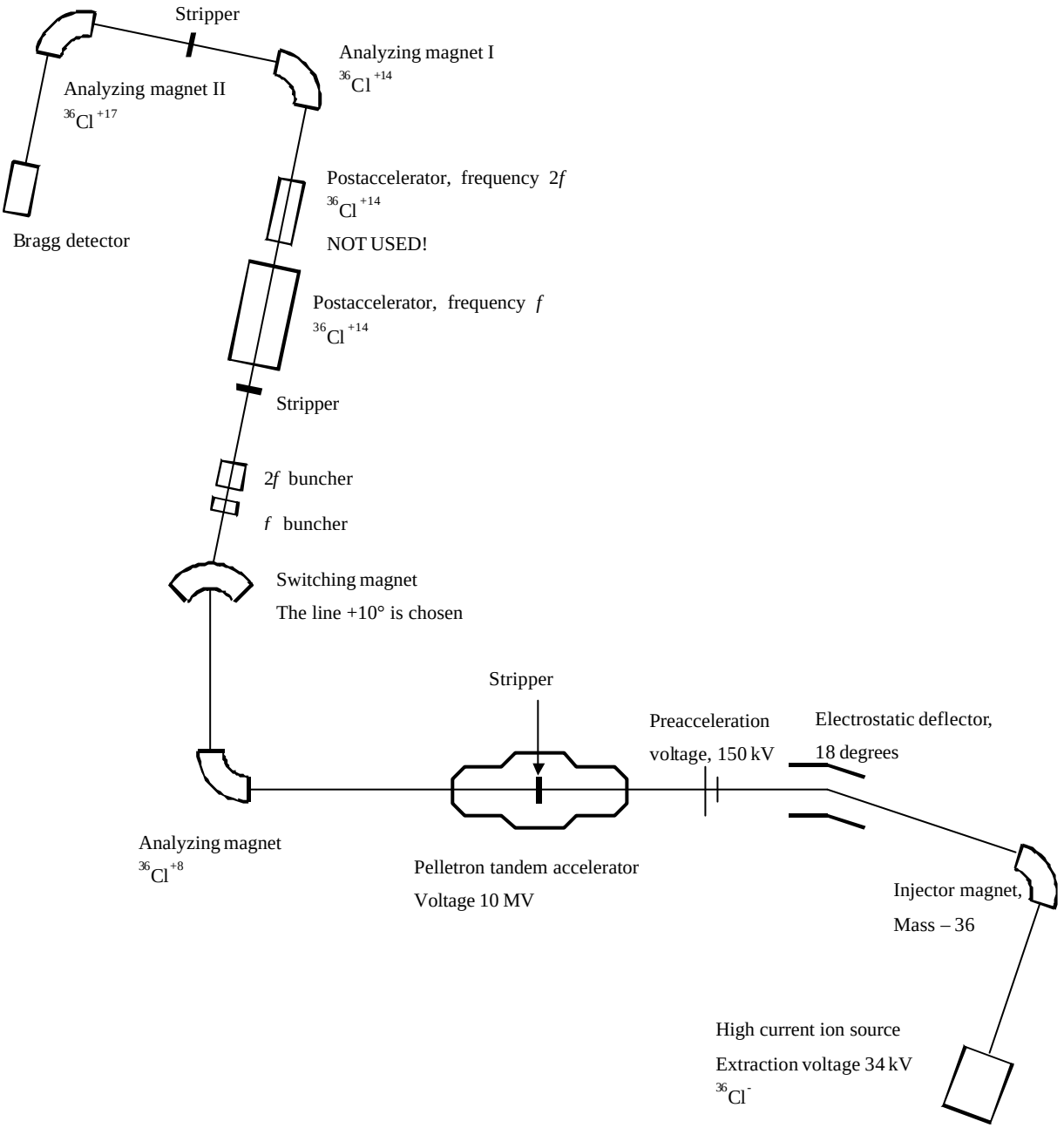

Figure 18 Beamline for ^{36}Cl AMS in Garching

states and energies are strongly suppressed. Only the ions with similar rigidity can pass through the magnet. The accelerator is used for different applications performed by different groups. In order to separate them, the beam line is divided into several channels. For the ^{36}Cl measurements, the line +10° is chosen by the switching magnet.

3.1.2. Radio-frequency accelerator

One of the main difficulties in the ^{36}Cl measurements is the separation of ^{36}Cl from its stable isobar ^{36}S. In most of the existing AMS facilities, this problem is solved by extremely clean

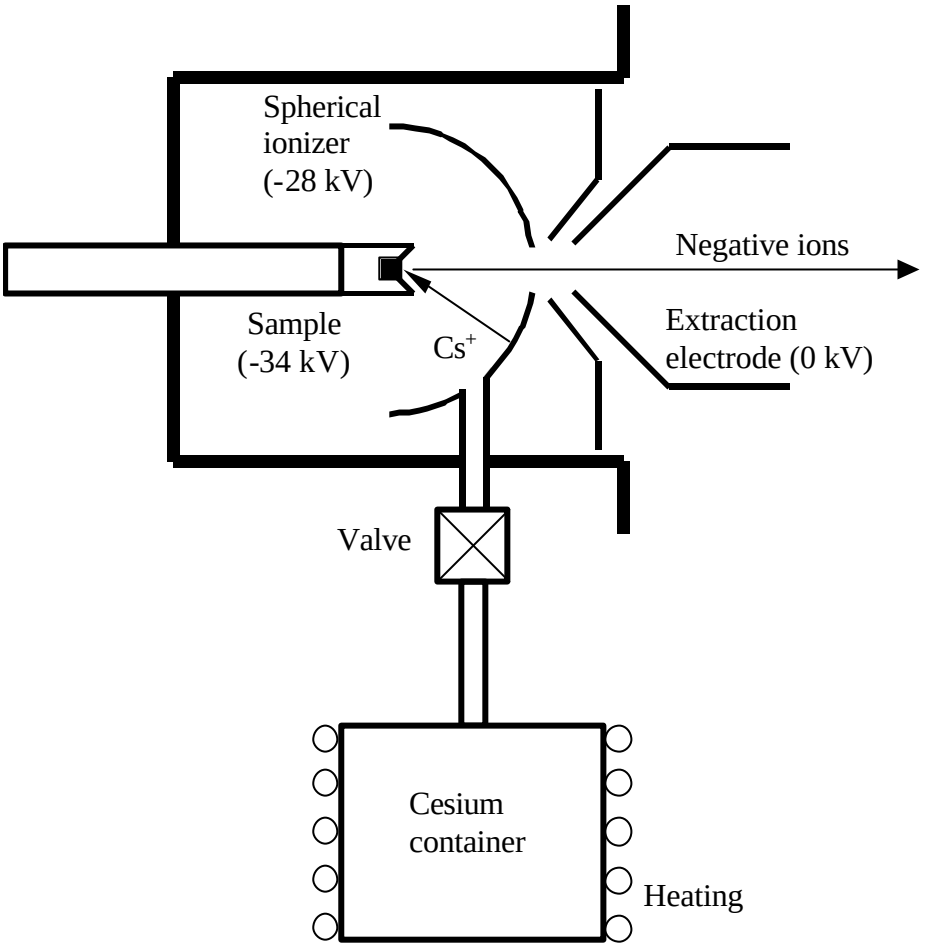

Figure 19 Schematic drawing of the high current ion source

and laborious chemical treatment of the sample and with the help of a high resolution ΔE-E detector. Good results were achieved with the gas-filled magnet [103]. The complete ionization is used to separate ^{36}Cl and ^{36}S at the AMS facility in Garching. In this case, chlorine ions have charge state +17 while the charge state of sulfur cannot exceed +16 and isobar separation becomes simple and reliable [104, 105].

According to Bohr, the probability to strip an electron is significant if the orbital speed of the electron is smaller than the velocity of the ion in medium. For complete ionization, the velocity of the ion should become comparable with the speed of the electron on the K-shell. The acceleration to very high energies became possible when the additional radio-frequency postaccelerator SchweIN (Schwer Ionen Nachbeschleuniger) was built [106]. The developed IH structure had a number of advantages compared to the older schemes of Wideröe [107] and Alvarez [108].

Standing waves are created in a cylindrical resonate cavity. The *TE* mode (H-mode) is used, that means that no electric field along the axis of the cylinder would exist if there were

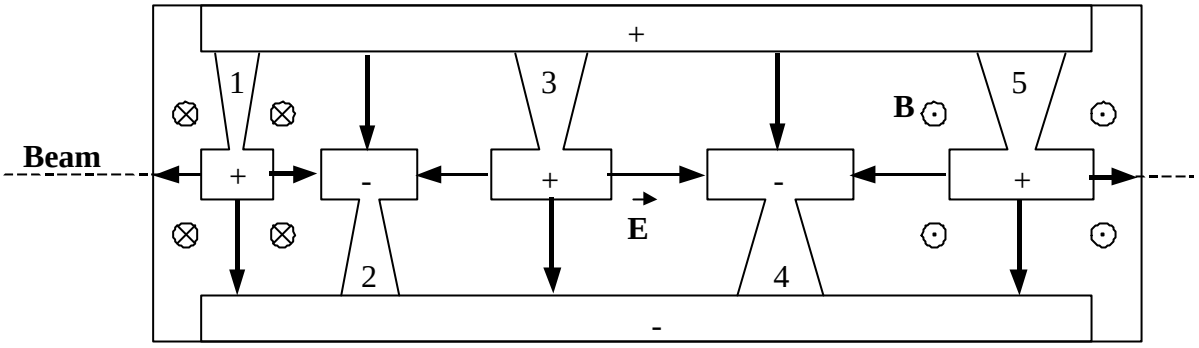

Figure 20 IH structure realized in the radio-frequency accelerator in Garching

no drift tubes. The last ones distort the field and a component of the electric field along the beam line appears (see Figure 20). In the shown configuration, positive ions are accelerated between the drift tubes 1 and 2. While they are inside the tube 2, the direction of the electrical field is changed. No force acts on the ions at that time because of the shielding by the drift tube. In the new field configuration, the ions are accelerated between tubes 2 and 3, then between 3 and 4 and so on. While the kinetic energy of the ions increases, they cover larger distances within half of the period. Accordingly, the lengths of the drift tubes and the distances between them increase along the beam.

If the beam is continuous, only a small part of the ions, which lies within a small range of the phase shifts, can be fully accelerated. The other particles get out of the resonance and become less energetic or even decelerate. In order to increase the phase acceptance a buncher synchronized with the RF accelerator is put in front of it. This buncher decelerates the advanced ions and accelerates those, which are late in phase. Thus, the particle parcels are formed. For the ideal time focusing, the phase dependence of the additional energy should be a linear function within the range $[-\pi, \pi]$. This dependence can be well approximated by a linear combination of harmonic functions with frequencies f (the frequency of the standing waves in the RF accelerator, f=78 MHz) and $2f$. Thus, a transmission of more than 50% through the system buncher-accelerator is reached (theoretically it is possible to reach a transmission of about 70%). Ions with masses different from 36 have much lower transmission. Thus, the postaccelerator is also an efficient isotopic filter.

For an additional increase of energy, the second RF accelerator operating with the frequency $2f$ of standing waves was build. However, for ^{36}Cl measurements, the gain by the increased stripping probability is lower than the losses by the reduction of the optical transmission and it is not in use.

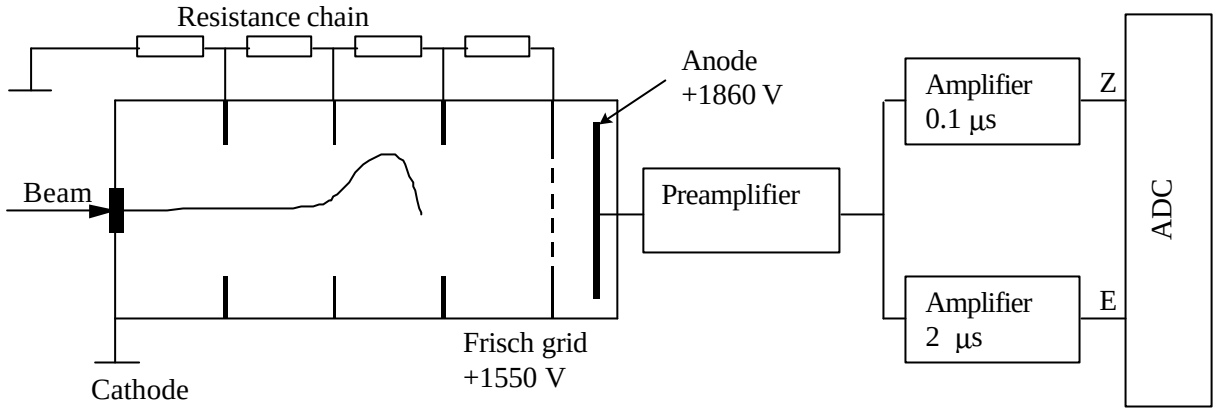

Figure 21 Schematic drawing of the Bragg ionization detector

For a larger efficiency of the postaccelerator, a stripper is placed directly before it. The analyzing magnet I after the postaccelerator selects the ions with charge state +14 and energy 155 MeV and the following stripper provides the complete ionization.

3.1.3. Bragg detector

The ions of ^{36}Cl with the charge state +17 selected by the analyzing magnet II are registered by a Bragg detector [109]. The ions enter the detector through an aluminized mylar foil, which separates the high vacuum of the beam line and the gas P10 under the pressure 578 mbar in the chamber. Drifting through the medium, the charged particles ionize the gas. The energy loss in the high-energy region can be described by the Bethe-Bloch formula (4). At small velocities, the shielding by the electron shells becomes important and the dependence changes [110]:

$$\frac{dE}{dx} = -8\pi Z^{\frac{1}{6}} e^2 a_0 \frac{z\,Z}{\left(z^{\frac{2}{3}} + Z^{\frac{2}{3}}\right)^{\frac{3}{2}} AM} \cdot \frac{\beta}{\beta_0}. \qquad (23)$$

Here a_0 and b_0 are parameters, which characterize the medium. The other parameters are taken from the denomination of (4). The range at the limits of applicability of (4) and (23) corresponds to the maximum differential energy loss and is called Bragg peak.

The electric field between the entrance window (cathode) and the anode (see Figure 21) forces the created electrons to move to the anode with a drift velocity of a few cm/s and the positive ions to the cathode with a drift velocity less than 10^{-3} cm/s. While the charged particles change their position, the signal ΔU on the detector is produced.

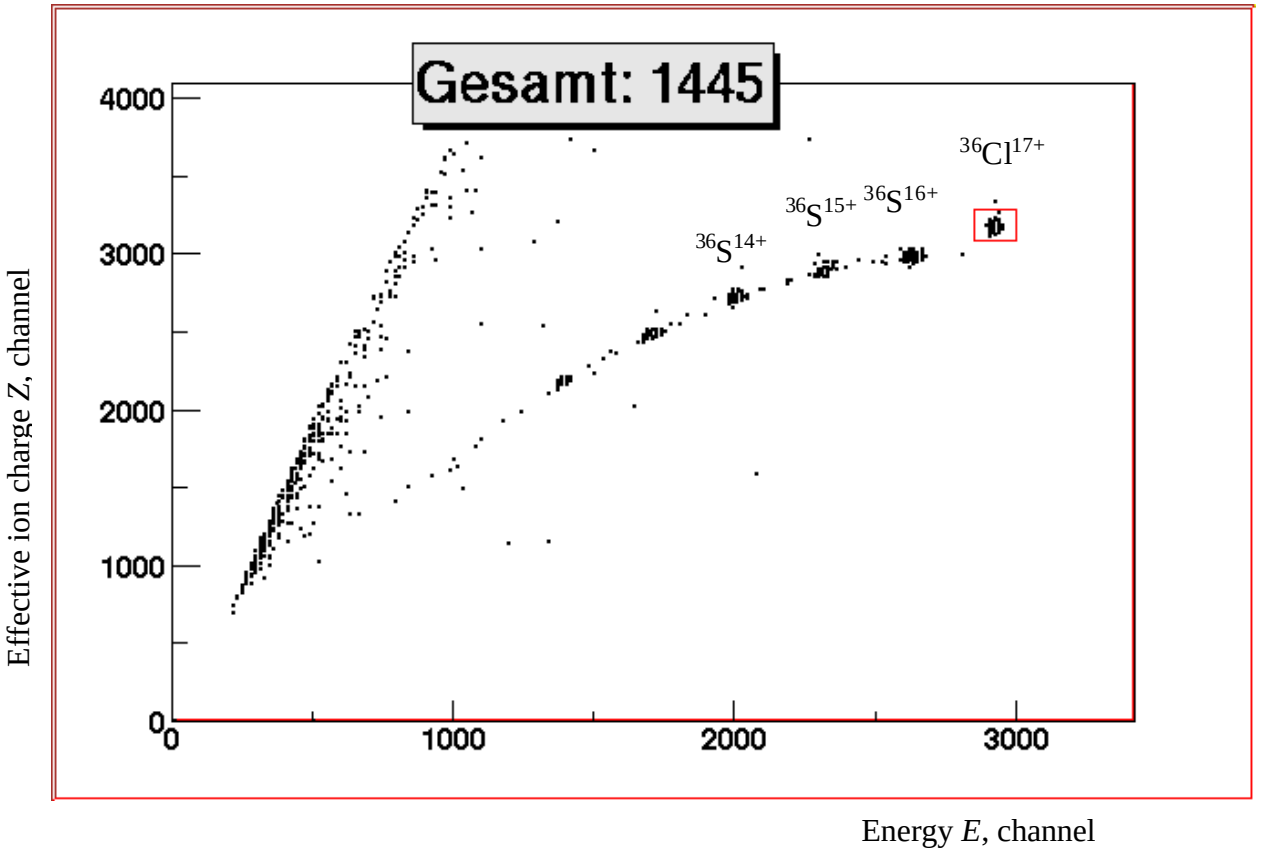

Figure 22 Typical spectrum Z vs E obtained with the Bragg detector. ^{36}Cl events are marked with a box. The X-axis has the meaning of energy; the Y-axis has the meaning of effective ion charge. The values stand for the sequence numbers of channels.

$$\Delta U(t) = \frac{N\,e}{C\,l}\left(v_{ion} + v_e\right) t$$

where

N	-	number of created free electrons,
l	-	distance between the positive and negative electrodes of the detector,
v_{ion}, v_e	-	drift velocities of the positive ions and electrons correspondingly,
$?$	-	effective capacitance between the electrodes of the detector.

In order to avoid the dependence of the signal on the position of the ionization, a shielding Frisch grid is installed close to the anode. The *RC* time of the detector is chosen in such a way that the fast electron signal is not disturbed and the slow ion signal is strongly attenuated. Thus, the anode signal repeats the dependence of the ionization losses along the beam direction. The integrated signal characterizes the energy of the entered ion and its inclination in the beginning – the charge of the ion. To obtain these two parameters the same anode

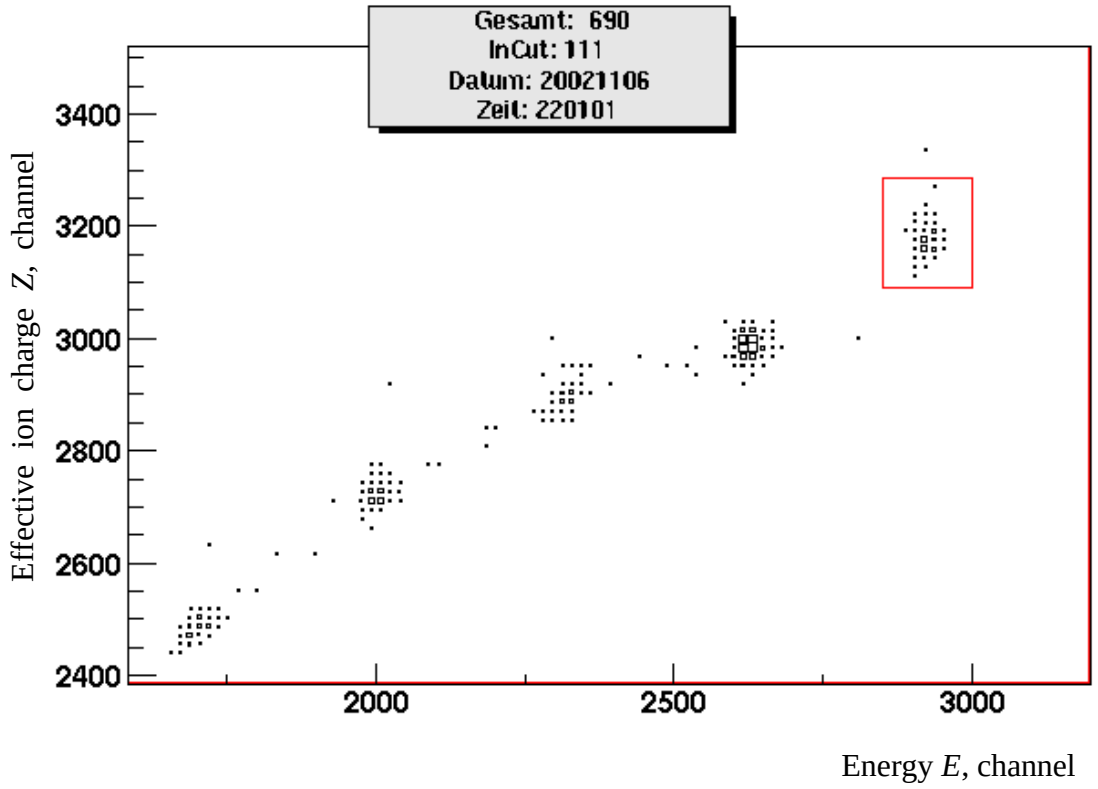

Figure 23 Expanded spectrum Z vs E of a standard sample ($^{36}Cl/Cl = 10^{-11}$) obtained with the detector. The panel on the top shows the number of ^{36}Cl events, which are marked with a box.

signal is integrated once over a long time of about 2 µs and once over a short time of about 0.1 µs. This information is sufficient to separate ^{36}Cl from ^{36}S.

The obtained spectrum of a standard sample with $^{36}Cl/Cl$ ratio of 10^{-11} is shown in Figure 22.

3.1.4. Measuring procedure

In order to determine the transmission of the system, a standard sample with known $^{36}Cl/Cl$ ratio X_{st}, is measured. With the source analyzing magnet, the extracted ions of the mass 35 (or 37) are selected. The current I of the stable chlorine isotopes is measured directly before the entrance into the tandem accelerator. The correct ratio $\frac{I_{35}}{I_{37}} = \frac{75.77}{24.23}$ shows that no interfering molecules disturb the experiment and that the adjustment of the system is reasonable. Then the source magnet is switched to the mass 36 and N ^{36}Cl events are registered in the detector within the time t (see Figure 23). If e is the charge of the electron, the number $\frac{I_{36}\, t}{e}$ of ^{36}Cl ions entered the accelerator within the same time. The current of

^{36}Cl can be estimated as $I_{36} = \frac{I_{35}}{\eta_{35}} \cdot X_{st}$ where η_{35}=0.7577 is the isotopic ratio of ^{35}Cl. Thus, the transmission (the part of ^{36}Cl ions from cup 1 in front of the accelerator, which reaches the detector) can be calculated

$$T_{C1-D} = \frac{\eta_{35} N e}{I_{35} t X_{st}}. \quad (24)$$

When an investigated sample is measured, the sequence of the operations remains the same. Assuming the stability of the conditions the transmission is known. Thus, equation (24) can be used to find the isotopic ratio X of ^{36}Cl/Cl:

$$X = \frac{\eta_{35} N e}{I_{35} t T_{C1-D}} \quad (25)$$

For a better accuracy and in order to account a possible change of experimental conditions the current of a stable isotope is always evaluated before and after the measurements of ^{36}Cl and the average value is used for the calculations. For the same reason, the average value of the transmission is used in (25), which is calculated before and after the measurements of the sample.

In order to check out the possibility of contamination either during the chemical preparation or during the AMS measurement, blank samples are measured a few times within the experiment. These blank samples are prepared under the same conditions as the others and have the ratio of ^{36}Cl/Cl below 10^{-15}. Typically, no ^{36}Cl events were registered during blank measurements. That means that a possible chemical contamination was below 10^{-14} – the sensitivity of the AMS facility. The cross talk within one experimental run was determined to be below 10^{-3} of the measured ratios ^{36}Cl/Cl. That allows the usage of a standard with ^{36}Cl/Cl ratio of 10^{-11}.

3.2. *Sample preparation*

The sampling was performed by the hydrological institutes situated in the regions, close to the lakes, the ^{36}Cl concentration in which was measured. These institutes possessed the necessary knowledge about the particularities of the specific lake to deliver representative samples. The volumes of water between 1 and 10 liters were hermetically closed in plastic bottles and sent

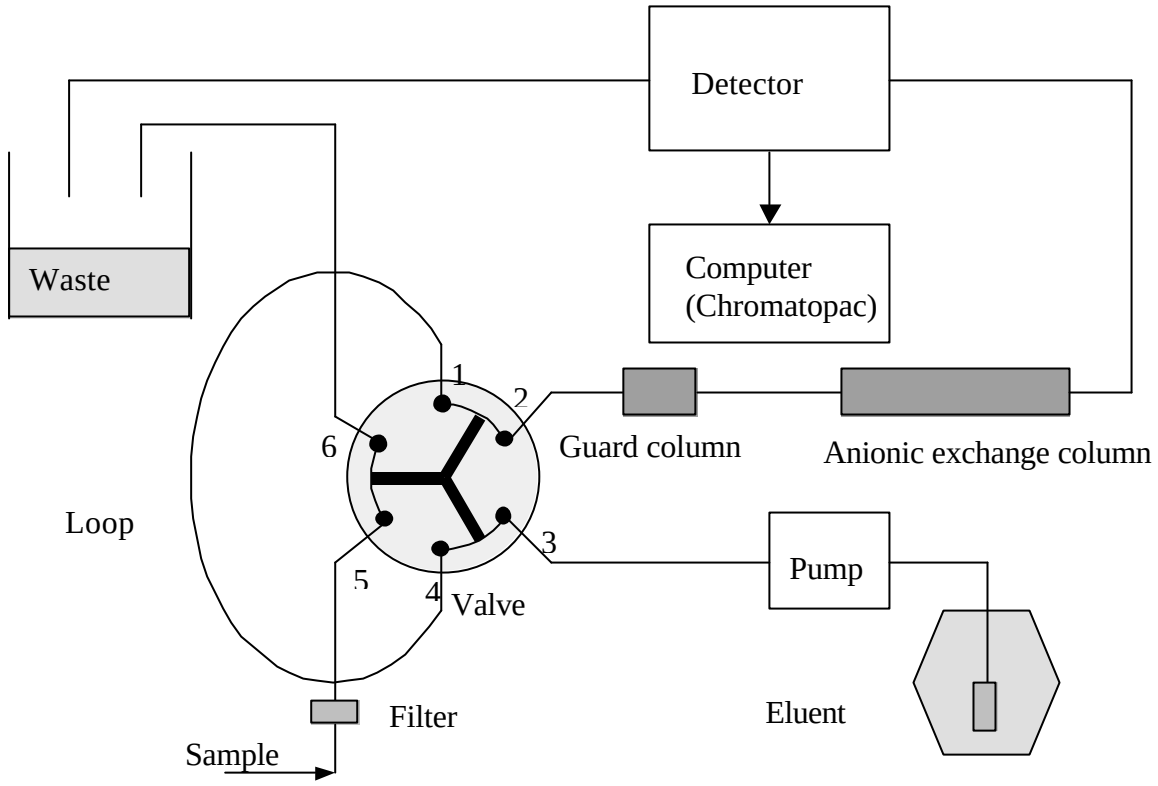

Figure 24 Scheme of HPLC used for stable chlorine measurements

to Technische Universität München for the measurements[1]. In order to eliminate the biological activity, 5 ml of hydrogen peroxide[2] were added to every liter of water.

The volume of about 5 ml from each sample was used for the measurements of the stable chlorine concentration and the rest remained for the AMS measurements.

3.2.1. Measurements of the stable chlorine concentration

The concentration of the stable chlorine in the samples was determined using High Performance Liquid Chromatography method (HPLC). The scheme of the method is shown in Figure 24. The eluent is pumped through a filter into the measuring system with a constant rate of about 1.0 ml min^{-1}. In the valve position shown on the picture, the eluent washes the loop and flows through the columns and detector into the waste container. The entire system is put into a thermostat so that stable conditions can be reached soon. In order to perform a measurement the valve is switched in such a way that the exits 2-3, 4-5, and 6-1 are connected. The sample is injected into the entrance 5, it fills the loop between 4 and 1 and

[1] Water from lakes Baikal, Ladoga, Onega and Ilmen was preliminary delivered to Saint-Petersburg State Technical University. There a part of the water was left without changes as aliquots for stable chlorine measurements and the rest was concentrated by rotating evaporation method to the volume of 50-100 ml. The obtained samples and the aliquots were sent to Technische Universität München for the measurements

[2] Merck Eurolab GmbH, Suprapur, 35%

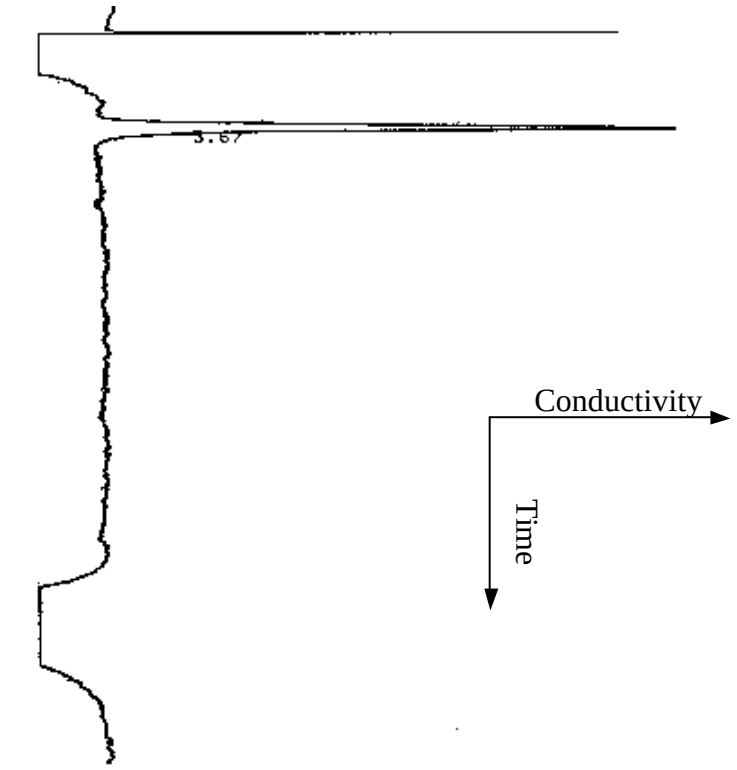

CHROMATOPAC C-R6A FILE 4
SAMPLE NO 6 METHOD 2941
REPORT NO 797

PKNO	TIME	AREA	MK	IDNO	CONC	NAME
1	5.67	970628			100	
		49176hi				
TOTAL		979628			130	

Figure 25 Chromatogram of a standard solution with chlorine concentration of 2.83 ppm

through the output 6 the rest of it flows into the waste. Then the protocol is started and the valve is switched back. The eluent pushes the fixed volume of the sample in the loop (100 µl) through the columns to the detector.

One of the most sensitive and important elements of HPLC is anionic exchange column[3]. Different ions need different time to pass through it and by the moment, when the ion reaches the detector, it is possible to determine what kind of species it is. In order to protect the expensive exchange column from damage a guard column is placed in front of it. The guard column is made in the same way as the main one but it is much shorter and cheaper.

The detector measures the conductivity of the solution and sends an analog signal to the computer (chromatopac), which presents the signal graphically and calculates the area

[3] For chlorine measurements the anionic exchange column *Polyspher IC AN-1, Merck KGaA* was used

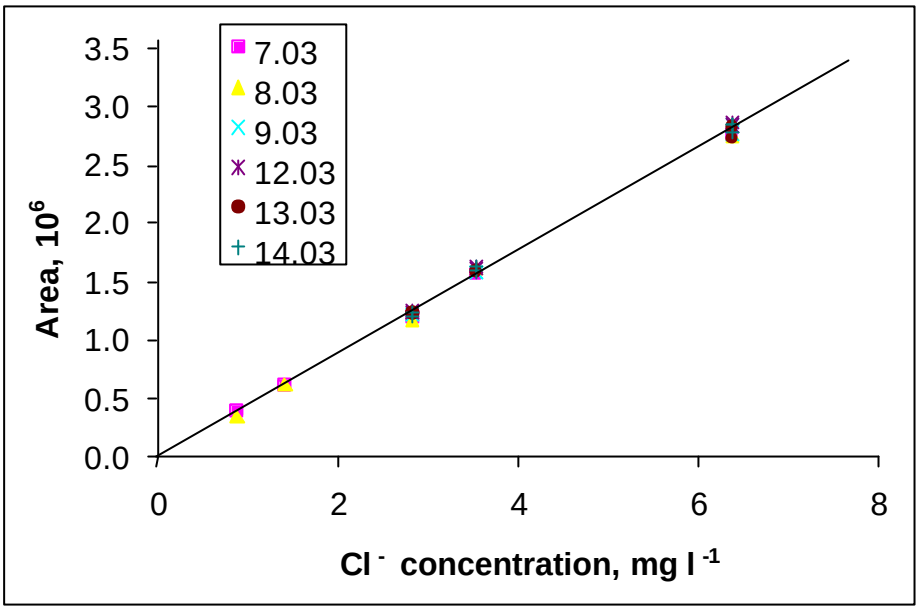

Figure 26 Chromatopac calibration within the run of measurements in March 2001. The marks of different forms stand for measurements performed within different days. The solid line shows the calibration curve.

under the found peaks (see Figure 25). The calibration of the chromatopac was performed with the help of standard solutions of different chlorine concentration. For the better accuracy, the calibration procedure was repeated for every sample though normally the conditions remained stable (see Figure 26). The sample measurements had higher divergence and they were repeated 3-5 times for the water from each lake. This gave the overall accuracy of about 3% (dependent on the sample).

3.2.2. Chemical preparation of the samples

About 3 mg of stable chlorine are necessary for the AMS measurements of ^{36}Cl. Using the results of the concentration measurements, the required volume of water, which contained enough chlorine, was calculated for each sample. With typical chlorine content in sweet water of about 1-7 ppm one or a few liters of water were sufficient.

The sample preparation included the removal of suspended particles by filtration through 0.45 µm Nuclepore® filters. For convenience and for a better yield every sample was decreased in a volume to 50-100 ml using the method of rotating evaporation. The pH factor was reduced to about 3-4 with a few drops of nitric acid. Silver nitrate of a very high purity was added. The required amount of $AgNO_3$ was calculated as

$$M_{AgNO_3} = M_{Cl} \cdot 4.8 \cdot a$$

where

M_{Cl} - mass of chlorine in the sample,

α - excess factor. For higher chlorine yield $AgNO_3$ was always taken in excess and α of about 2 was used.

The solution was left for agitation for about 6 hours at temperature between 60 and 80 °C. Due to the chemical reaction

$$AgNO_3 + NaCl \rightarrow NaNO_3 + AgCl \downarrow,$$

silver chloride fell out in form of white powder. Because the direct light destroys the chemical binding of AgCl the beaker with reactants was covered with aluminum foil. The residue was centrifuged during 20 min with 4000 rotations/min, washed with a weak solution of nitric acid, distilled water, and finally the remained powder was dried in a vacuum oven at temperature of about 80 °C. The dried powder was weighted and pressed into a target holder.

The comparison between the mass of extracted silver chloride and the volume of used water with known chlorine concentration indicated the efficiency of the chemical extraction. The typical yields were between 70 and 90%.

3.3. *Collection and treatment of methyl chloride*

3.3.1. Methyl chloride

It was suggested that the high ^{36}Cl fluxes measured in modern precipitation could be explained by the recycling of bomb-produced ^{36}Cl though the biosphere. The carrier of the recycling was expected to be chlorine containing organic molecules and mainly CH_3Cl.

In order to check the role of methyl chloride in ^{36}Cl transport the measurements of the ratio $^{36}Cl/Cl$ in CH_3Cl were performed. The sampling was carried out at the biological station of Tehnische Universität München in *Kranzberger Forst* [111]. This station is situated far from industrial plants but it has a developed infrastructure.

The concentration of methyl chloride in the troposphere is about 540 pptv [112]. This corresponds to about 665 ppt of chlorine content. If we sum up all reactive chlorine-containing species with residence time in the atmosphere less than 10 years, the chlorine content of about 1550 ppt is obtained (see Table 12). Together with 8.4 Tg of chlorine in reactive gases about 14.8 Tg of chlorine in non-reactive gases are present in the atmosphere. No natural sources are known for them [113] and little of ^{36}Cl is bound on them. However, they are important for the total chlorine content in the atmosphere, which is about 4250 ppt.

Chemical composition	Mass part in the budget of the reactive chlorine	Chlorine mass in the troposphere, Tg	Chlorine mass part in the troposphere, ppt
CH_3Cl	43%	2.8	665
CH_3CCl_3	29%	1.9	448
$CHClF_2$	8%	0.5	124
Inorganic Cl	7%	0.46	108
$CHCl_3$	4%	0.26	62
CH_2Cl_2	3%	0.2	46
C_2Cl_4	2%	0.13	31
Other compositions	4%	0.26	62
Total	100%	6.5	1546

Table 12 The most abundant chlorine containing chemical compositions with residence time in the atmosphere less than 10 years [112]

In order to perform the carrier-free AMS measurements about 3 mg of chlorine is necessary. Thus, the entire chlorine from a volume of

$$V = 22.4\frac{l}{mol}\cdot\frac{3\cdot10^{-3}g}{35\frac{g}{mol}}\cdot\frac{1}{4250\cdot10^{-12}}\cdot\frac{35}{29}\approx 5.5\cdot10^{5}l = 550\ m^3$$

had to be collected.

3.3.2. Experimental setup for the methyl chloride collection

The chlorine extraction from the air was performed according to the scheme in Figure 27. The air was sucked with a rate of about 30 l/min using a membrane pump. The capture of the methyl chloride and other chlorine-containing molecules was carried out by molecular sieve of types 13X and 5A[4], which was placed into two U-shape tubes of diameter 16 mm and the height of 300 mm. The tubes with zeolite were connected to each other with CF16 flanges and to prevent a contamination during the transportation the valves *SwageLok* were installed on their ends (see Figure 28). Before the experiment, the tubes with molecular sieve had been kept in an oven at temperature of 350 °C for a few hours under a vacuum and filled with nitrogen after cooling down. Thus, the molecules, which had been captured during the production of the zeolite, were released and the molecular sieve was ready for operation.

The efficiency of the substance capture by molecular sieve decreases while it is filled. For example, if water is being captured the saturation is reached when the water mass is about 20% of the mass of the molecular sieve. The zeolite in one tube has a volume of about 120 ml and density of 0.74 g/ml. Thus, 17.8 mg of water would overfill the capacity of the molecular

[4] Zeochem, 3.3901.41 and 3.3901.40

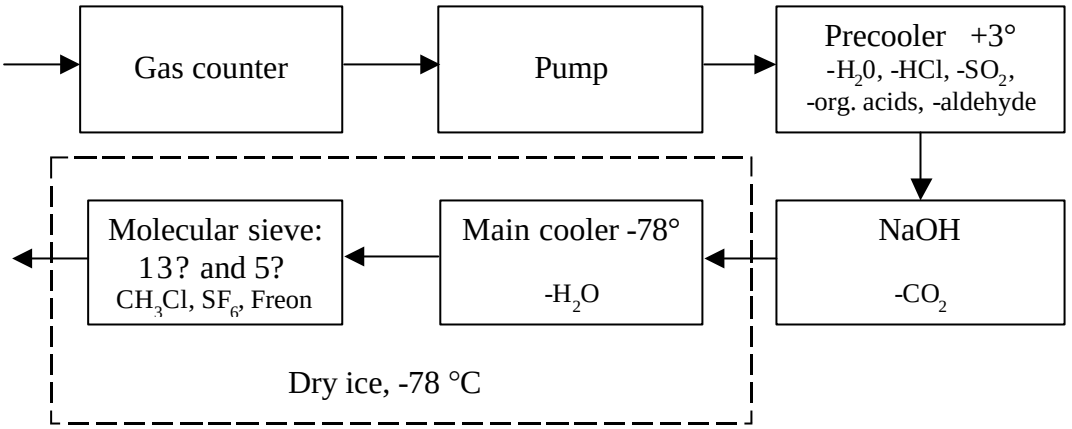

Figure 27 Scheme of the chlorine collection from the air

sieve. In order to keep the efficiency of the chlorine compounds capture the pumped air was preliminary cleaned from the most abundant "impurities": from water and carbon dioxide.

The freezing drying was used to remove the water. A precooler decreased the temperature of the air to +3 °C and the low temperature was reached by dry ice (see Figure 29). The thermostat (height 600, diameter 250) was filled with dry ice and isopropyl alcohol for the larger thermal conductivity. A heat exchanger of cylindrical form (height 400 mm, diameter 100 mm) with two exit tubes was placed into the thermostat. The air was cooled down in the heat exchanger and frozen on its walls. When the created ice hindered the free flow of the air, the heat exchanger was changed to another one, warmed up to melt the ice inside and dried. For the better capturing efficiency, also the molecular sieve was placed into the thermostat.

The removal of carbon dioxide was achieved with sodium hydroxide[5] according to the reaction:

$$2NaOH + CO_2 \rightarrow Na_2CO_3 + H_2O$$

Sodium hydroxide is dark and sodium carbonate is white. Thus, the change of the color indicated how much chemically active sodium hydroxide was still left.

The volume concentration of carbon dioxide in the air is about 0.03%. It means that about 13 mole or 570 g of CO_2 are within 1000 m^3 of the air. In order to neutralize this amount of CO_2 about 1 kg of NaOH is necessary. The producer of the sodium hydroxide guaranteed its efficiency to be not less than 50%. Thus, 1 kg of NaOH had to be enough to remove entire carbon dioxide from the volume of 550 m^3. However, NaOH absorbed water actively and it could not be operated for more than 3 or 4 days.

[5] Merck, 1.01567

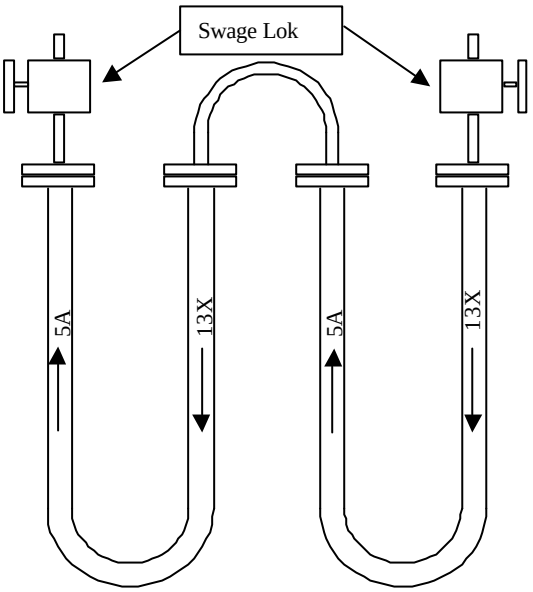

Figure 28 U-shape tubes with molecular sieve for the extraction of chlorine from the air

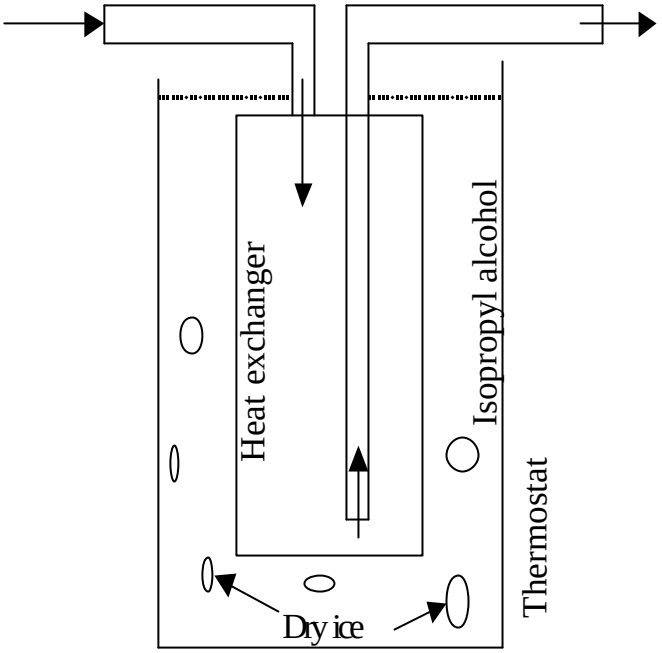

Figure 29 The scheme of the air cooling with help of dry ice

After enough air had been pumped through the system, the U-shape tubes with the molecular sieve were hermetically closed until the chemical treatment.

3.3.3. Chemical treatment of the molecular sieve

Because methyl chloride was assumed the main carrier of recycled ^{36}Cl the procedure of chemical treatment was developed and checked for CH_3Cl.

The molecular sieve was put into a flask and covered with methanol (see Figure 30). To avoid a loss of the chlorine during evaporation, the flask was closed with a lid. The solution was left for magnet agitation for one hour. Due to mechanical mixing, the molecular sieve was destroyed and CH_3Cl was dissolved in the methanol. The solution was purified by passing through a paper and then through a 0.45 µm Nuclepore® filter. To destroy the molecular bindings of CH_3Cl 1 g of dry KOH was added to the solution. The reaction

$$CH_3Cl + KOH \rightarrow CH_3OH + KCl\downarrow$$

takes place if the lattice energy of KCl can be used. Thus, no water should be present in the solution. Otherwise, KCl would be dissociated and the reaction rate would be drastically reduced. In order to prevent the loss of chlorine on the water vapor during the reaction, the flask was closed with a condenser, which was water-cooled.

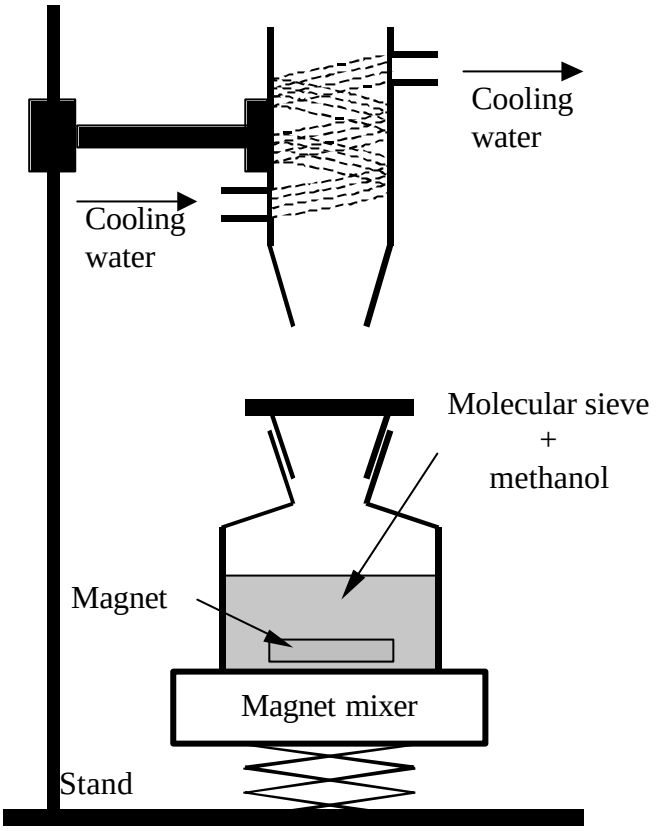

Figure 30 Chemical treatment of the molecular sieve

Distilled water was added to dissolve the potassium chloride. Nitric acid was used to reduce pH factor to 3-4. $AgNO_3$ was added in excess to precipitate chlorine. The solid phase was separated from the liquid one by centrifugation, washed with distilled water, separated from the liquid phase again, dried in a vacuum oven at temperature of 60 °C and pressed in a target holder.

3.3.4. The experiment

The experiment to collect methyl chloride from the air was carried out in October 1999. 701 m^3 of air were pumped though the system. Taking into account the weather conditions (mean temperature of 10.5 °C, mean pressure of 964 kPa) this volume corresponds to the volume V_s at standard conditions:

$$V_s = V\frac{P}{P_s}\frac{T_x}{T} = 701\frac{96.3}{101.325}\frac{273}{283.5} = 642\ m^3 \qquad (26)$$

After the chemical treatment, 17.5 mg of powder were extracted. This corresponds to 4.3 mg of chlorine, which is higher than expected 3.5 mg if the entire chlorine from all chlorine-containing molecules were extracted with 100% yield. This discrepancy can be explained by

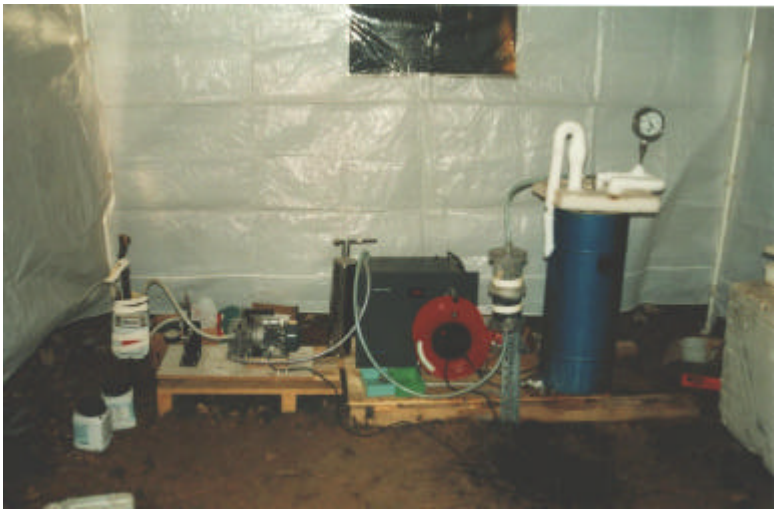

Figure 31 Experimental setup for the collection oft CH_3Cl from the air in Kranzberger Forst: (left to right) gas meter, pump, precooler, NaOH container, main cooler

the non-uniform distribution of the chlorine-containing species in the atmosphere. The divergence of local experiments within 25% seems to be quite probable. On the other hand, this discrepancy can indicate that the extracted sample consisted not only of AgCl but also of some impurities. The analysis made during AMS measurements showed high amount of carbon in the sample. Thus, it is possible that the sample was contaminated by organic molecules, which build carbon chains. However, the AMS method is not sensitive to impurities and the obtained results remain reliable in any way.

Besides the main sample the same chemical treatment was applied to the following samples:

- Molecular sieve, through which about 250 ml of chemically pure CH_3Cl were pumped. Taking into account the conditions (temperature 22 °C, pressure 95.4 kPa), this volume contains 0.35 g of Cl. The extracted 1 g of AgCl (0.25 g of Cl) proved the efficiency of the method even under adverse conditions. (The pumping rate of methyl chloride was high and released energy has warmed up the system. Thus, the efficiency of the CH_3Cl capture by the molecular sieve was reduced.)
- Molecular sieve of 120 ml in volume, which corresponds to the volume of the main sample, without any preliminary treatment. The extracted 4.4 mg of AgCl showed that molecular sieve itself contained chlorine and it should be taken into account in the final results.
- Blank sample without molecular sieve. The absence of precipitation at the end of the chemical treatment proved the purity of the used chemical agents: methanol, KOH, $AgNO_3$

CHAPTER 4. Interpretation of the results

4.1. *Natural and bomb-produced fallout of chlorine-36*

4.1.1. Cosmogenic chlorine-36

The daily input of ^{36}Cl (see Table 13) to the atmospheric boxes used in the transport model (Table 1) was computed by the code described in [9]. The model output describes the

	0°-10°	**10°-20°**	**20°-30°**	**30°-40°**	**40°-50°**	**50°-60°**	**60°-70°**	**70°-80°**	**80°-90°**
Stratosphere 1	2.3	3.1	5.8	15.2	44.2	88.5	99.0	66.4	23.0
Stratosphere 2	5.9	8.0	14.4	35.9	93.3	158.6	158.8	102.2	35.2
Stratosphere 3	8.8	11.9	21.0	48.7	109.0	159.0	144.2	90.0	30.7
Stratosphere 4	10.8	14.5	25.0	53.0	101.8	129.2	107.4	65.0	21.9
Troposphere	81.5	108.2	167.0	241.4	275.8	231.9	153.6	86.5	28.1

Table 13 Daily input of ^{36}Cl in 10^{17} at.day^{-1} to the atmospheric boxes used in the model.

South hemisphere:

Latitude, °	**85°**	**75°**	**65°**	**55°**	**45°**	**35°**	**25°**	**15°**	**5°**
Annual precipitation rate, mm	80	241	563	1207	1271	934	754	1162	1494
Average ^{36}Cl flux, at m^{-2} s^{-1}	7.2	11.9	16.4	27.8	29.9	20.9	13.0	9.0	5.6

North hemisphere:

Latitude, °	**5**	**15**	**25**	**35**	**45**	**55**	**65**	**75**	**85**
Annual precipitation rate, mm	1965	1139	700	772	830	755	469	239	155
Average ^{36}Cl flux, at m^{-2} s^{-1}	6.0	9.1	13.4	21.7	28.4	26.1	17.5	12.1	9.1

Table 14 Annual precipitation rate and average ^{36}Cl flux at the different latitudinal belts

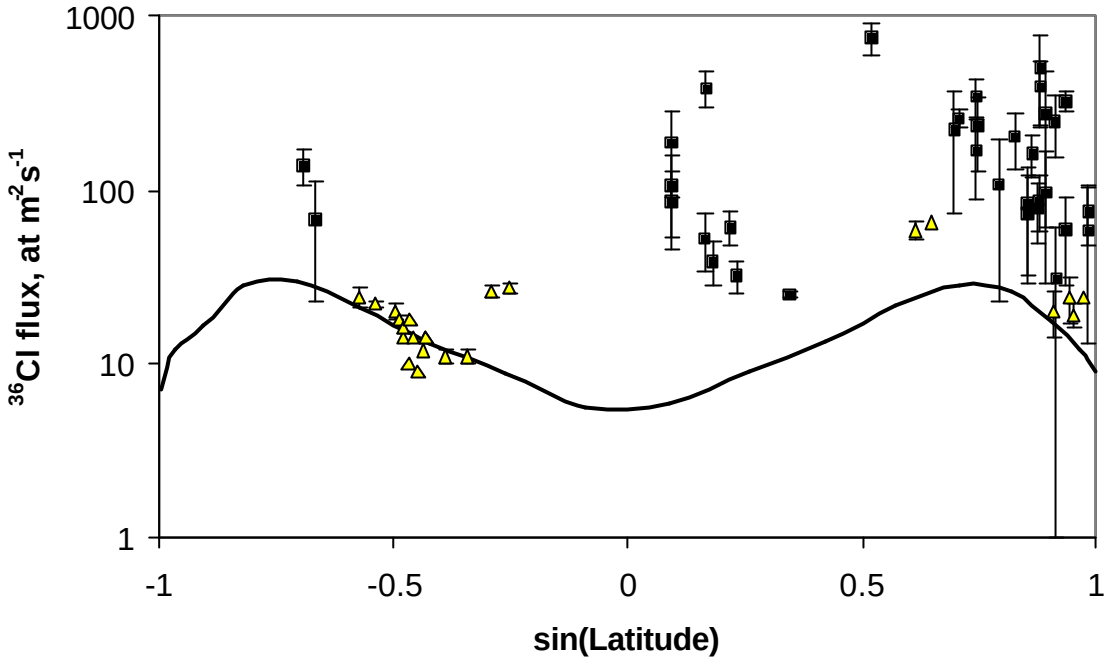

Figure 32 Calculated (solid line) and experimental ^{36}Cl deposition fluxes as function of latitude (squares - measurements of TUM [8], triangles – measurements, performed by other groups). Only cosmogenic production of ^{36}Cl was taken into account in the calculation

latitudinal dependence of annual ^{36}Cl fallout (Table 14). Though the simulated data are generally lower than those of [27] (the mean global production rate of ^{36}Cl is 16 at m^{-2} s^{-1} instead of 24 at m^{-2} s^{-1}) the main features described in [27] are reproduced (compare Figure 32 and Figure 7). The calculated fluxes in the southern hemisphere are in a good agreement with the experimental data, while a large discrepancy is observed in the northern hemisphere.

4.1.2. Bomb-produced chlorine-36

In order to estimate the bomb-produced ^{36}Cl fallout, the data on the nuclear explosions [89] were analyzed. In cases of underwater tests and the tests performed on the barges, the released

South hemisphere:

Latitude, °	**85°**	**75°**	**65°**	**55°**	**45°**	**35°**	**25°**	**15°**	**5°**
Average ^{36}Cl fluence, 10^{12} at m^{-2}	0.63	1.18	2.00	4.49	5.66	3.87	2.26	1.59	1.47

North hemisphere:

Latitude, °	**5**	**15**	**25**	**35**	**45**	**55**	**65**	**75**	**85**
Average ^{36}Cl fluence, 10^{12} at m^{-2}	2.21	3.77	5.14	8.44	11.01	8.58	4.42	2.48	1.61

Table 15 Latitudinal distribution of bomb-produced ^{36}Cl for a from section 2.4.2 equal to 1.

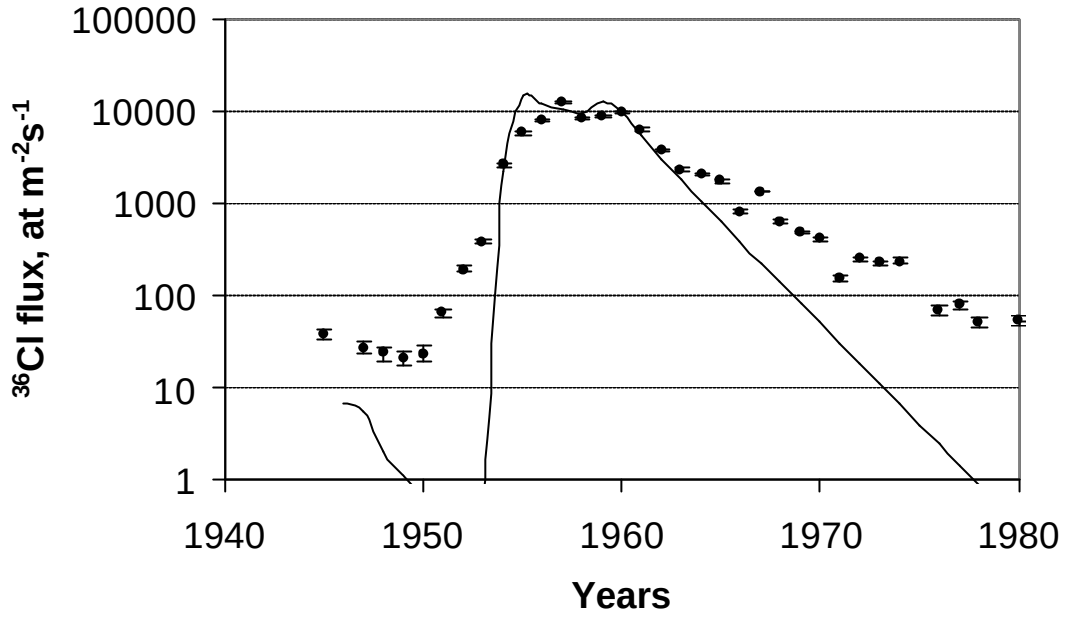

Figure 33 Comparison of the ^{36}Cl fluxes obtained from the ice measurements at Dye-3, Greenland, 65° N [5] (points) and the simulated time-dependence of the bomb-produced ^{36}Cl at the latitude 65° N (solid line). Here, it was assumed that 60% of the ^{36}Cl produced in the ocean entered the stratosphere

neutrons activated stable chlorine in the ocean. The summary of these tests and the corresponding calculated injection of ^{36}Cl to the atmospheric boxes for α=1 (see section 2.4.2) are gathered in Table 16.

The simulated latitudinal distribution of the ^{36}Cl fluence is shown in Table 15. In Figure 33 the time dependence of the calculated ^{36}Cl fluxes at latitude 65°N together with experimental points are presented. For the better comparability, the parameter α was put 0.6, which corresponds the equal heights of the calculated and measured at Dye-3 ^{36}Cl bomb peak. The simulated rate of decrease of ^{36}Cl fallout is lower than the experimental one. This difference is negligible within the first 4 years after the ^{36}Cl injection and it is strongly pronounced after 1970.

The low calculated ^{36}Cl fluxes could be explained by the cosmogenic ^{36}Cl, which fallout is about 17.5 at m^{-2} s^{-1} at the latitude 65° N (see Table 14). In the years 1951-1953, the increase of ^{36}Cl flux can be hardly attributed to the test of 03 October 1952, which was performed in the southern hemisphere. It is possible that the neutrons from the "near Earth's surface" explosions activated stable chlorine in the crust with its following release to the troposphere. The strength of this ^{36}Cl source is difficult to estimate with a reasonable accuracy. However, within the years 1954-1958 it should play a minor role compared to the tests performed near the surface of the ocean. Another possibility to explain

Date	Type of test	Latitude	Power, kt TNT		^{36}Cl input, 10^{23} at.				
			Fission	Fusion	Strato 1	Strato 2	Strato 3	Strato 4	Tropo
24-Jul-46	water	12	21	0	0.0	0.0	0.0	0.0	6.2
3-Oct-52	water	-22	25	0	0.0	0.0	0.0	0.0	7.4
26-Mar-54	barge	12	7300	3700	2754.3	512.7	0.0	0.0	0.0
25-Apr-54	barge	12	4600	2300	1157.6	761.9	129.8	0.0	0.0
4-May-54	barge	12	9000	4500	3701.6	307.9	0.0	0.0	0.0
13-May-54	barge	12	845	845	0.0	38.3	177.3	147.7	138.6
14-May-55	water	-5	30	0	0.0	0.0	0.0	0.0	8.9
21-Sep-55	water	73	4	0	0.0	0.0	0.0	0.0	1.0
11-Jun-56	barge	12	183	182	0.0	0.0	0.0	0.0	108.4
25-Jun-56	barge	12	550	550	0.0	0.0	39.6	99.1	188.0
8-Jul-56	barge	12	925	925	0.0	69.9	203.5	152.9	123.2
10-Jul-56	barge	12	1500	3000	329.8	672.5	279.5	54.6	0.0
20-Jul-56	barge	12	2300	2700	482.4	716.1	257.0	29.6	0.0
21-Jul-56	barge	12	167	83	0.0	0.0	0.0	0.0	74.3
10-Oct-57	water	73	10	0	0.0	0.0	0.0	0.0	3.0
11-May-58	barge	12	680	680	0.0	1.3	106.0	127.5	169.2
11-May-58	barge	12	81	0	0.0	0.0	0.0	0.0	24.1
16-May-58	water	12	9	0	0.0	0.0	0.0	0.0	2.7
20-May-58	barge	12	6	0	0.0	0.0	0.0	0.0	1.8
21-May-58	barge	12	25	0	0.0	0.0	0.0	0.0	7.5
26-May-58	barge	12	220	110	0.0	0.0	0.0	0.0	98.0
26-May-58	barge	12	57	0	0.0	0.0	0.0	0.0	16.9
30-May-58	barge	12	12	0	0.0	0.0	0.0	0.0	3.4
31-May-58	barge	12	92	0	0.0	0.0	0.0	0.0	27.3
2-Jun-58	barge	12	15	0	0.0	0.0	0.0	0.0	4.5
8-Jun-58	barge	12	8	0	0.0	0.0	0.0	0.0	2.4
10-Jun-58	barge	12	142	71	0.0	0.0	0.0	0.0	63.3
14-Jun-58	barge	12	212	107	0.0	0.0	0.0	0.0	94.7
14-Jun-58	barge	12	725	725	0.0	6.8	128.1	134.5	161.2
18-Jun-58	barge	12	11	0	0.0	0.0	0.0	0.0	3.3
27-Jun-58	barge	12	275	137	0.0	0.0	0.0	0.0	122.4
27-Jun-58	barge	12	440	440	0.0	0.0	4.9	62.1	194.4
28-Jun-58	barge	12	3000	5900	1933.7	680.8	28.8	0.0	0.0
29-Jun-58	barge	12	14	0	0.0	0.0	0.0	0.0	4.2
1-Jul-58	barge	12	5	0	0.0	0.0	0.0	0.0	1.5
2-Jul-58	barge	12	150	70	0.0	0.0	0.0	0.0	65.3
5-Jul-58	barge	12	265	132	0.0	0.0	0.0	0.0	117.9
12-Jul-58	barge	12	3200	6100	2090.7	654.0	17.4	0.0	0.0
17-Jul-58	barge	12	170	85	0.0	0.0	0.0	0.0	75.7
22-Jul-58	barge	12	65	0	0.0	0.0	0.0	0.0	19.3
22-Jul-58	barge	12	135	67	0.0	0.0	0.0	0.0	60.0
26-Jul-58	barge	12	1000	1000	0.0	105.4	224.0	155.7	108.9
23-Oct-61	water	73	5	0	0.0	0.0	0.0	0.0	1.4
27-Oct-61	water	73	16	0	0.0	0.0	0.0	0.0	4.8
11-May-62	water	-5	20	0	0.0	0.0	0.0	0.0	5.9
22-Aug-62	water	73	6	0	0.0	0.0	0.0	0.0	1.8
2-Jul-66	barge	-22	28	0	0.0	0.0	0.0	0.0	8.3
24-Sep-66	barge	-22	125	0	0.0	0.0	0.0	0.0	37.1
2-Jul-67	barge	-22	22	0	0.0	0.0	0.0	0.0	6.5

Table 16 Input of ^{36}Cl due to nuclear bomb tests performed near the ocean. For the transport calculation, it was assumed that all tropospheric chlorine reached the lower stratosphere.

the form of the measured bomb-peak is the chlorine diffusion in ice. However, there is no data, which confirms this suggestion.

An interesting feature of the ^{36}Cl bomb-peak is its form at the top. There are two maximums: in years 1957 and 1960. The largest ^{36}Cl injections were in 1954 and 1958 with an additional peak in 1956. In order to explain the observed peaks, the removal time from the atmosphere should be larger than it was assumed. Moreover, the input in 1954 had to be significantly higher than in other years. Only in this case, the bomb chlorine from 1954 would add up with ^{36}Cl from 1956 and form a large peak in 1957.

After 1963, the decrease of ^{36}Cl flux was not as fast as it was modeled. Together with the influence of low-altitude nuclear explosions over the land and a possible diffusion of chlorine in ice, the reason for this discrepancy could be the recycling.

4.2. *Correction of the fallout for precipitation rate*

Local ^{36}Cl fluxes depend on the precipitation rate, which varies strongly. Although an exact correction for precipitation rate is hardly possible, a simple approach can be used to improve the comparability of the data.

In the model, the *wet* and *dry* forms of the tropospheric chlorine are distinguished. One third of the tropospheric chlorine falls out as a dry deposition with a typical time of 36 days. Two thirds of the chlorine is attached to the water vapor and its deposition is proportional to the precipitation rate. Thus, if N is the number of ^{36}Cl atoms in the column with unit area, the flux of ^{36}Cl can be determined as

$$F = N\left(\frac{P}{P_0}\frac{1}{18\ \text{days}} + \frac{1}{36\ \text{days}}\right),$$

where P_0=1 m·a^{-1} is the average precipitation rate and P is local precipitation rate. In the model, every latitudinal belt is characterized by one precipitation rate P_l and the corresponding ^{36}Cl flux is F_l. These two parameters allow the estimation of N and the ^{36}Cl flux at the place with local precipitation rate P (in m·a^{-1}):

$$F = F_l \frac{\frac{P}{18} + \frac{1}{36}}{\frac{P_l}{18} + \frac{1}{36}} \qquad (27)$$

Accordingly, if local flux F was measured, a corrected flux F_{corr} comparable with the model output can be found:

Lake	Latitude	Catchment area, km^2	Volume, km^3	Flushing time, a	Reference
Alpine glacial lakes					
Lake Constance	47° N	10900	48.5	4.1 (4.5)	[114,115]
Geneva	46° N	7975	88.9	11.8	[115]
Garda	45.6° N	2628	51.8	26.7	[116]
Como	46° N	4516	23.4	4.7	[116]
Lugano	46° N	615	6.5	8.19	[117]
Maggiore	46° N	6599	37.5	4	[118]
Chiemsee	42° N	1398.6	2.048	1.26	[119]
Starnberger See	42° N	314.7	2.999	20.9	[119]
Ammersee	42° N	993.02	1.75	2.7	[119]
Walchensee	42° N	779.3	1.3	1.62	[119]
Great European lakes					
Onega	61° N	51540	280	16	[114]
Ilmen	58.4° N	66500	6.5	0.4 (3.8)	[114]
Ladoga	60° N	258600	837.9	12.3	[114]
African lakes					
Victoria	1.6° S	263000	2750	120	[120], [121]
Mweru	9° S		32		[114]
Malawi	12° S	100500	8400	750	[121]
Asian lakes					
Baikal	53° N	540000	23000	385	[122]
Khubsugul	51° N	7680	380	470	[123]
Balkash	45° N	413000	105	37000	[124]
Issyk-Kul	43° N	22080	1738		[125]

Table 17 Hydrological parameters of the lakes, where ^{36}Cl concentration was measured. If there is a difference in published data, the other estimates are shown in brackets.

$$F_{corr} = F \cdot \frac{\frac{P_l}{18} + \frac{1}{36}}{\frac{P}{18} + \frac{1}{36}} \tag{28}$$

4.3. *Results of the measurements in lakes*

In frame of the performed work ^{36}Cl concentration in a number of lakes (Table 17, Figure 34) was measured. The obtained results are shown in Table 18.

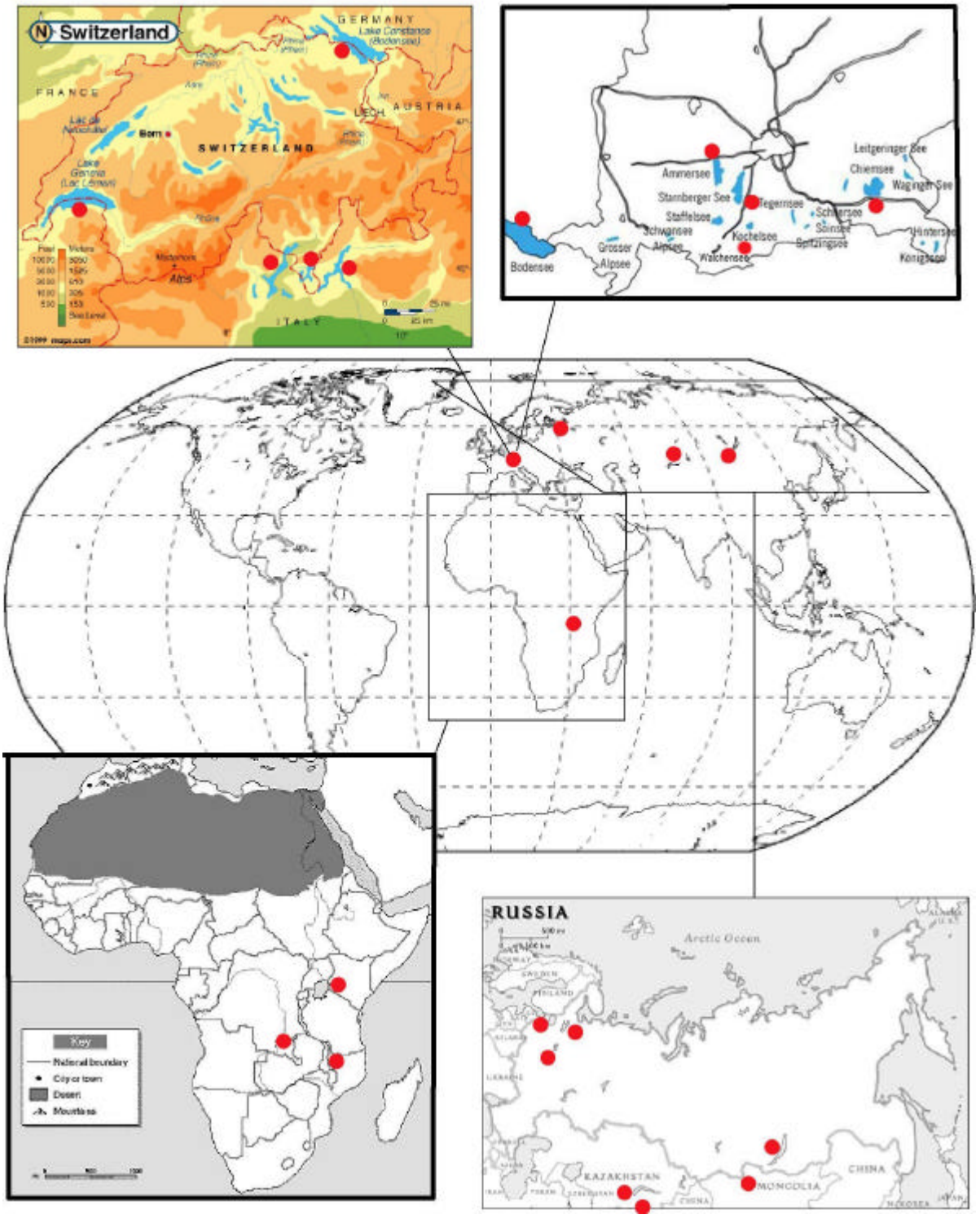

Figure 34 World map with expansions. The locations of sampling are shown with circles.

Only statistical error is shown for the results of the stable chlorine measurements, which were performed chromatographically. A systematic uncertainty caused by a limited resolution of the anionic exchange column, the uncertainty of the standard samples and a possible contamination of the samples during the transportation are difficult to estimate.

Though their influence is expected to be negligible, a contamination of aliquots was observed in case of Baikal Lake. The difference in chlorine concentration in samples taken from different parts of the lake was of order of 2. This contradicted the observed fast mixing within the lake. To check the obtained results, every sample was delivered in another container and the measurements were repeated. The new data were in good agreement with each other but the chlorine concentration was still too high compared to the measurements performed during the sampling: 0.44±0.03 mg/l [126]. The samples of the salty lakes (Balkash, Issyk-Kul) were preliminary dissolved in distilled water to reduce the chlorine concentration to 10 mg/l or less. The obtained concentration was corrected for the dissolving factor.

The ratio ^{36}Cl/Cl was measured at the AMS facility in Garching. Statistical uncertainty, fluctuations of the transmission, variations of the extraction current, and background (measured with a blank sample) were included in the calculations of the confidence interval. A typical uncertainty is between 10% and 20% and it is the main source of the error in determination of the concentration of ^{36}Cl in water.

^{36}Cl concentration was calculated as a product of stable chlorine concentration in at/l and ratio of ^{36}Cl/Cl measured in the same sample. Thus, in case of contamination of a sample with the stable chlorine, the obtained chlorine content and ratio ^{36}Cl/Cl contain an error whereas the ^{36}Cl concentration remains correct.

The extraction yield of chemical preparation was determined as ratio of dry mass of the produced material *m* to the mass of chlorine taken for the chemical treatment and corrected for attached silver:

$$Y = \frac{m}{cV \dfrac{M_{AgCl}}{M_{Cl}}},$$

where

- c - concentration of stable chlorine in the sample in mg/l,
- V - volume of the sample used for the chemical treatment,
- M_{AgCl}, M_{Cl} - molecular masses of AgCl (143.3 g/mol) and Cl (35.45 g/mol) correspondingly.

Because of the high selectivity of AMS, the presence of impurities in a sample does not disturb measurements of the ratio ^{36}Cl/Cl. Thus, no special precautions were done to eliminate other substances, which can fall out with silver. Typically, their concentration is negligible compared with chlorine and the yield can be estimated with a good accuracy. However, in

Lake	Date of sampling	Cl concentration, mg/l	Ratio ^{36}Cl/Cl, 10^{-13}	^{36}Cl concentration, 10^{7} at/l	Chlorine chemical yield, %
Alpine glacial lakes					
Lake of Constance	*Sep. 98*	5.2±0.1	4.3±0.5	3.8±0.4	75 – 84
Geneva	*Jan. 99*	7.3±0.2	5.0±1.8	6±1	84 – 89
Garda	*Oct. 98*	4.84±0.05	8.4±0.8	7±1	84 – 95
Como	*Oct. 98*	2.7±0.1	5.9±1.5	2.8±0.4	62 – 78
Lugano north	*March, 99*	2.1±0.1	22±2	8±1	66 – 97
Lugano south	*March, 99*	6.0±0.2	3.0±0.5	3.1±0.6	90 – 94
Maggiore	*Oct. 98*	2.6±0.3	4.5±0.8	1.9±0.2	
Chiemsee	*May 00*	5.5±0.1	3.8±0.4	3.6±0.3	88
Starnberger See	*Sept. 00*	8.1±0.1	5.0±0.4	6.9±0.6	79
Ammersee	*Sept. 00*	6.0±0.2	4.1±0.7	4.1±0.7	60
Walchensee	*Sept. 00*	1.00±0.02	14±2	2.4±0.3	72
Great Russian lakes					
Onega	*Aug. 01*	1.77±0.09	26±3	7.7±0.9	94
Ilmen	*Dec. 01*	33.5±0.4	2.1±0.4	12±2	67
Ladoga	*Sept. 99*	6.1±0.1	7.5±0.8	7.8±0.9	
Ladoga	*Jul. 00*	5.9±0.1	6.5±0.8	6.6±0.8	
African lakes					
Victoria	*Feb. 01*	3.8±0.1	4.7±1.5	3.0±0.9	
Mweru	*Feb. 01*	4.34±0.08	0.8±0.2	0.6±0.2	73
Malawi	*Feb. 01*	7.1±0.1	1.1±0.3	1.3±0.3	87
Asian lakes					
Baikal	*Aug. 98*	0.55±0.06	24±2	2.2±0.2	63 – 94
Khubsugul	*Oct. 01*	0.44±0.05	66±5	5.0±0.7	
West Balkash	*June. 01*	115±2	3.0±0.5	59±11	86
Issyk-Kul	*June 01*	1175±9	1.1±0.2	210±40	72

Table 18 Results of the measurements of stable chlorine and ^{36}Cl concentration in the lakes.

some samples, they cannot be neglected and the yield of chemical extraction cannot be calculated.

4.4. *Input of chlorine-36 in Chernobyl accident*

In many European lakes with flushing times below 20 years the observed ^{36}Cl concentration cannot be explained by natural and bomb production only. Recycling can increase the expected concentration but it is not sufficient to describe the measurements.

High ^{36}Cl fluxes in rainwater (ratio ^{36}Cl/Cl of about $5.3 \cdot 10^{-10}$, chlorine concentration 17.9 mg/l) were observed a few days after the accident in Chernobyl on 26. April 1986 [127]. Radioactive elements released by the accident did not enter the stratosphere and were not

mixed globally. Their transport was determined by the wind structure and by the precipitation rate within the next few days. The deposition of many elements was influenced by these parameters, and the fluxes of different radionuclides from Chernobyl should have correlated. Thus, ^{36}Cl fallout can be normalized to the fallout of Chernobyl ^{137}Cs, the distribution of which is known on a large scale [128].

For a few lakes, a detailed study of ^{137}Cs deposition and distribution was completed. The fluence of Chernobyl ^{137}Cs on lake Constance was determined to be 17±3 kBq m^{-2} [129]. A similar fluence of 17.5±4.5 kBq m^{-2} was measured in the soil around the lake [130]. The ^{137}Cs deposition over lake Lugano was reported to be 24 kBq m^{-2} [131]. Although lakes Maggiore and Como are situated close to it (distance is about 20 km), the ^{137}Cs deposition varies strongly on their watersheds [128] and the same fluence of 24 kBq m^{-2} can not be used as the average one.

	Lake area, km^2	Catchment area, km^2	Volume, km^3	Outflow, km^3 a^{-1}	Flushing time, a
Northern part	27.5	297.2	4.69	0.38	12.3
Southern part	20.3	310.6 + 297.2	1.8	0.77	2.3

Table 19 Hydrological parameters of the northern and southern parts of lake Lugano

Lake Lugano is divided into two parts by an artificial dam. The hydrological parameters of these parts are shown in Table 19 [132]. Thus, three aquifers are suitable to normalize ^{36}Cl and ^{137}Cs fluxes of Chernobyl origin: Lake of Constance, the northern and the southern parts of lake Lugano.

Applying the calculated data on ^{36}Cl production (Table 14 and Table 15), correction procedure (27), formulas (14), (17), and (22), the natural and bomb ^{36}Cl concentrations in the lakes were computed (Table 20). The parameter α, which describes the amplitude of the bomb impulse, was chosen 0.6. This corresponds to the height of the ^{36}Cl bomb peak measured at Dye-3. Thus, the effect of the bomb-produced ^{36}Cl was slightly overestimated (see section 4.5). It does not influence significantly on the results for lake Constance. However, the remaining ^{36}Cl concentration, which was attributed to the Chernobyl accident, in lake Lugano and especially in its southern part was underestimated. The ratio of ^{36}Cl to ^{137}Cs released by the accident in Chernobyl was chosen so that the observed ^{36}Cl concentration in the lakes would be explained.

Besides the rough estimation of the bomb-produced ^{36}Cl, the high divergence of the ratio of the ^{36}Cl and ^{137}Cs fallouts originates from:

	Lake of Constance	**Lugano, north part**	**Lugano, south part**
Measured concentration of ^{36}Cl, 10^7 at/l	3.8±0.4	8±1	3.1±0.6
Estimated concentration of the natural ^{36}Cl, 10^7 at/l	0.11	0.12	0.12
Estimated concentration of the bomb-produced ^{36}Cl, 10^7 at/l	0.02	2.42	1.47
Concentration of ^{36}Cl due to Chernobyl accident, 10^7 at/l	3.7	5.5	1.6
Ratio of released ^{36}Cl and ^{137}Cs, 10^{11} at/kBq	1.43	1.0	0.04

Table 20 Normalization of ^{36}Cl and ^{137}Cs fallout of Chernobyl origin. The concentration of bomb-produced ^{36}Cl was calculated with parameter a = 1 (see Section 2.4.2)

- Lake of Constance has a short flushing time of about 4.5 years. Even a small amount of groundwater, which is not important for the water balance in the lake, can become a mother reservoir (see Section 2.6), which increases the effective flushing time. Neglecting the effect we obtain overestimated ratio ^{36}Cl/^{137}Cs.
- The flushing time of the south part of the lake Lugano is not known exactly. If it is 20% less than the value of 2.3 years used, the Chernobyl ^{36}Cl flux necessary for the explanation of the measurements increases by about 75%.
- Although the ^{137}Cs deposition on the lakes Constance and Lugano was measured fairly well, the average ^{137}Cs fallout over the catchment area could differ from the published values. On the watersheds of lake Constance and of the northern part of lake Lugano, regions an increased ^{137}Cs deposition was observed [128]. These regions could lead to the higher mean ^{137}Cs deposition than the assumed one. Accordingly, the obtained ratio of ^{36}Cl/^{137}Cs for the lakes Constance and Lugano north might be overestimated.

Taking into account the described above explanation for the high divergence, the average value of $9 \cdot 10^{10}$ at/kBq for the ratio of ^{36}Cl and ^{137}Cs deposition seems to be representative and contain an error below 50%.

With a total atmospheric release of ^{137}Cs during the accident of about 85 PBq [133] the total release of ^{36}Cl by Chernobyl nuclear power plant can be estimated to be about 0.5 kg.

4.5. *Input of bomb-produced chlorine-36*

The ^{36}Cl concentration in the lakes with flushing times more than 20 years depends strongly on the bomb input. This information was used to estimate the total amount of ^{36}Cl produced by the nuclear weapon tests and the parameter α from Section 2.4.2 in particular.

Lake	C_{meas}, 10^7 at/l	C_{nat}, 10^7 at/l	C_{Chern}, 10^7 at/l	C_{bomb}, 10^7 at/l	Fluence, 10^{12} at m^{-2}	Fluence corr, 10^{12} at m^{-2}	α
Garda	7±1	0.1	4.4	2.5±2.4	2.1±2	2.14±2	0.2±0.2
Victoria	3.0±0.9	0.2		2.8±0.9	0.43±0.14	0.55±0.18	0.28±0.09
Malawi	1.3±0.3	0.2		1.1±0.3	1.0±0.3	1.09±0.3	0.7±0.2
Starnberger	6.9±0.6	0.2	5.0	1.7±2.6	1.3±1.9	1.14±1.7	0.11±0.17
Baikal	2.2±0.2	0.5		1.7±0.2	0.8±0.1	1.13±0.15	0.12±0.02
Khubsugul	5.0±0.7	0.55		4.4±0.7	2.4±0.5	3.5±0.7	0.37±0.07
Michigan *	5.7±0.6	0.4		5.3±0.6	1.9±0.2	1.9±0.2	0.18±0.02
Superior *	3.4±0.4	0.26		3.0±0.4	2.1±0.3	2.2±0.3	0.21±0.03
Huron *	6.6±0.7	0.3		6.3±0.7	2.6±0.3	2.8±0.3	0.25±0.03

Table 21 Concentration of ^{36}Cl in lakes, calculated fluenes of bomb-produced ^{36}Cl over their catchment areas, and the calculated corresponding parameter α. C_{meas}, C_{nat}, C_{Chern}, and C_{bomb} stand for measured concentration, concentration of natural, Chernobyl and bomb-produced ^{36}Cl correspondingly. The measurements of Great Laurentian Lakes (Michigan, Superior, Huron) were performed in [7].

In a similar way as it was done in Section 4.4, the calculated concentration of natural ^{36}Cl in a lake was subtracted from the measured one. For European lakes, also the estimated concentration of Chernobyl ^{36}Cl was subtracted. The rest was assumed to originate from the nuclear tests and the corresponding ^{36}Cl fluence onto the catchment area of the lake was calculated (Table 21). The error bars include the experimental uncertainty of the ^{36}Cl measurements and the uncertainty of the determination of Chernobyl produced ^{36}Cl. The obtained results demonstrate a large divergence with a weighted average value α=0.18±0.07.

This can be compared with the results of the ^{36}Cl study in glaciers [5, 6, 134]. Although the divergence is large, the measurements in mountain glaciers are generally consistent with the determined value of α (Table 22). On the contrary, the measurements in Greenland ice demonstrate higher impact of the bomb-produced ^{36}Cl with an average value α=0.5. Available experimental ^{36}Cl fluxes together with the results of the simulation for α=0.5 and α=0.18 are summarized in Figure 35. Latitude of a local place, where a measurement was performed, might be different from the corresponding latitude in the transport model (see section 2.3.1). To show this, the experimental points contain horizontal

	Latitude	Altitude a.s.l., m	Fluence, 10^{12} at m^{-2}	Fluence corr, 10^{12} at m^{-2}	α
Greenland, Dye-3	65° N	2650	2.4	2.28	0.52
Greenland, B16	73.5° N		1.18	1.41	0.51
Greenland, B29	76° N		1.22	1.38	0.58
Greenland, B18	76.5° N		0.72	0.89	0.38
Greenland, B26	77° N		1.3	1.41	0.61
Greenland, B21	80.5° N		0.72	0.84	0.42
Alpes, Fiescherhorn	46° N	3850	2.37	1.66	0.15
Himalayas, Guliya	35° N	6710	0.43	0.83	0.1
Andes, Huascaran	9° S	6048	0.3	0.45	0.3

Table 22 Determination of the fluence of the bomb-produced ^{36}Cl in glaciers

error bars with a length of 5°. The difference between Greenland and lake normalization could have 3 different explanations:

- *The modeled curve does not describe the ^{36}Cl transport.* The model should be changed to have a maximum at about 55°N and to decrease rapidly to the south of this latitude. In this case, a very good agreement between most of the experimental data and the simulation would be established. Although the tropopause folds fluctuate in latitudes, the maximum of the STE is not expected to be at so high latitudes. Moreover, a rapid decrease of the ^{36}Cl bomb fluence between 50°N and 40°N contradicts the latitudinal distribution of the ^{90}Sr (Figure 12). Another strong evidence against a large peak of ^{36}Cl fluence at high latitudes is the low ^{36}Cl concentration measured in lake Baikal. However, a possibility of different latitudinal distribution of the bomb-produced ^{36}Cl and ^{90}Sr cannot be excluded. This can happen, for example, if the chlorine washout rate from the troposphere is much higher than one of strontium and the tropopause fold was closer to the North Pole in 1958 (maximum of ^{36}Cl fallout) than in 1963 (maximum of ^{90}Sr fallout).
- *Greenland normalization should be used; the balance of ^{36}Cl in lakes and in mountain glaciers is disturbed by its loss due to some unconsidered mechanisms.* For example, a part of snow with bomb-produced ^{36}Cl could have been blown away in the mountain glaciers. However, the measurements of $\delta^{18}O$ do not corroborate this hypothesis [6]. Neither a significant lack of ^{36}Cl in water systems seems to be probable. A part of chlorine fallen onto the watershed of a lake could be captured by the biosphere.

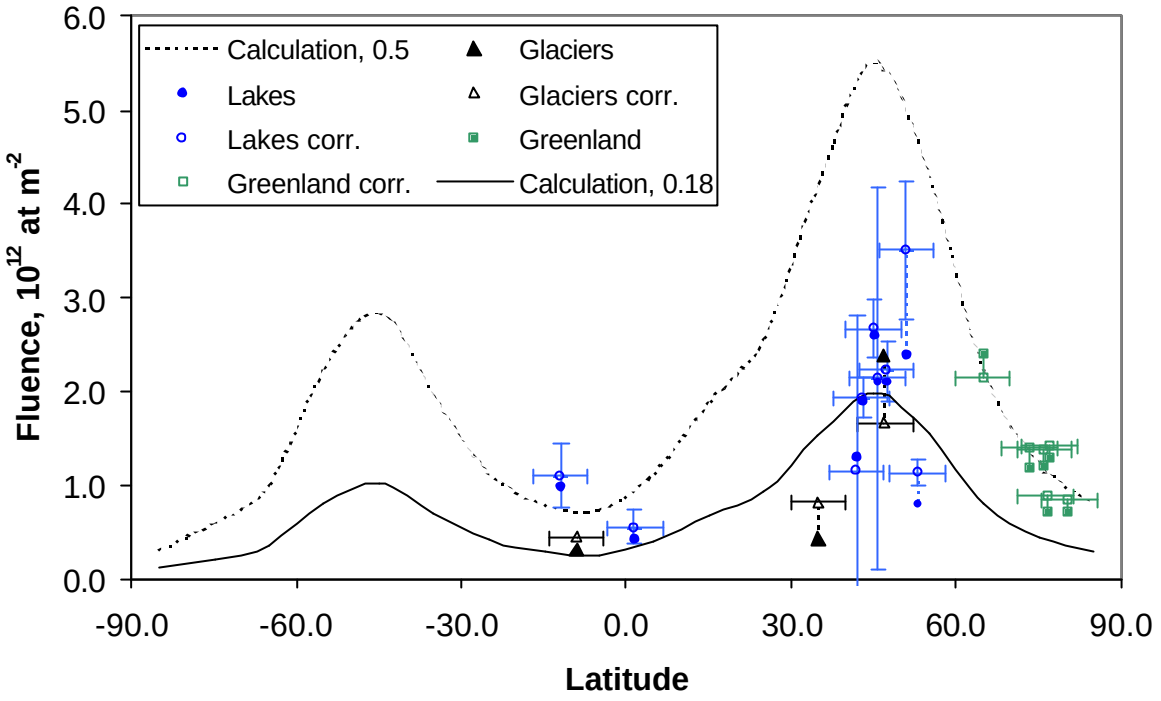

Figure 35 Fluence of the bomb-produced ^{36}Cl as function of latitude. The circles represent data, which are derived from the measurements of ^{36}Cl in lakes; squares are measurements in Greenland ice; triangles are the measurements in mountain glaciers. The filled symbols show the calculated fluence, unfilled symbols show the fluence, which is corrected for the precipitation rate. The dashed line shows the result of the calculation with a = 0.5, the solid line is the calculation with a = 0.18

However, because of its high solubility, most of chlorine should follow the water streams and be able to reach the reservoir. Only in case of the lake's stratification with a shallow layer of water above thermocline it is possible that a significant portion of chlorine would be removed before the chlorine is mixed over the entire volume of the lake.

- *The lake normalization should be used in the calculations, the atmospheric transport to Greenland is particular and the measurements their should be interpreted separately.* Three lakes do not fit the calculated latitudinal distribution: Malawi, Khubsugul, and Baikal. The hydrological parameters of lake Malawi are not known reliably and this lake should be interpreted carefully. High ^{36}Cl bomb fluence to lake Khubsugul arises after the correction for precipitation rate. This correction is not valid on the large areas, characterized by the low (or large) precipitation rate. Without the correction, the bomb ^{36}Cl fluence to the lake is about 30% less and close to those, measured in European and American lakes. Low fluence of the bomb-produced ^{36}Cl to lake Baikal is difficult to explain. However, a higher ^{36}Cl concentration of $(3.8\pm0.2)\cdot10^{7}$ at l^{-1} in the lake was reported by another group [65]. Using this value,

^{36}Cl bomb fluence of about $2.2 \cdot 10^{12}$ at·m^{-2} can be obtained. This value corresponds well the fluence derived from European and American lakes. To resolve the difference in results an additional sample from lake Baikal should be measured. Large amount of ^{36}Cl observed in Greenland can be explained by a fast atmospheric mixing with the air of lower latitudes. The area near Iceland in Greenland is known for the development of cyclones, which spread over the central Europe.

Before data on bomb-produced ^{36}Cl fluence in the latitudinal belt between 10°N and 40°N are available, it is difficult to determine, which of these three explanations is correct. In frame of this work the lake-based value of $\alpha=0.18\pm0.07$ (corresponds to about 24±9 kg of ^{36}Cl released to the stratosphere or 1600 years of natural production) was used. However, the possibility of a larger ^{36}Cl stratospheric release up to 65 kg (Greenland normalization) during the nuclear bomb tests is not closed yet.

4.6. *Bomb chlorine-36 in organic molecules*

The results of the AMS measurements of the ^{36}Cl/Cl ratio in the samples, described in the Section 3.3.4 are shown in Table 23. The content of ^{36}Cl in organic compounds exceeds the typical ratio of ^{36}Cl/Cl in modern precipitation, which is in the range between 10^{-15} [59] and a

Sample	Mass of AgCl, mg	Mass of Cl, mg	Ratio ^{36}Cl/Cl, 10^{-13}
Cl in the air	17.5	4.3	29±3
Chemical. CH_3Cl	1055	261	0.19±0.09
Molecular sieve	4.4	1.1	1.2±0.4

Table 23 Results of the measurements in samples used for the determination of ^{36}Cl in organic substances.

few 10^{-13} [80]. The high measured ratio of $2.9 \cdot 10^{-12}$ is difficult to explain in terms of the ^{36}Cl natural production. In fact, the ratio of ^{36}Cl/Cl in the methyl chloride emitted by the biosphere should be much higher.

- One of the main sources of the organic chlorine-containing compounds is ocean (see Table 30). However, a large amount of old chlorine dilutes ^{36}Cl there and CH_3Cl emitted by the ocean decreases the ratio ^{36}Cl/Cl of the biospheric methyl chloride.
- Another dilution effect has an experimental origin. From the Table 23 it can be seen that the molecular sieve used in the experiment contained some chlorine with low ratio of ^{36}Cl/Cl. The correction of this effect increases the measured ratio:

$$\frac{2.9 \cdot 10^{-12} \cdot 4.3\,mg - 1.2 \cdot 10^{-13} \cdot 1.1\,mg}{4.3\,mg - 1.1\,mg} = 3.9 \cdot 10^{-12}$$

- Only the biomass can play a role of long-term storage of the bomb-produced ^{36}Cl. However, the biomass burning is a dominant source of CH_3Cl and not of the other molecules (see Table 30). Thus, a number of chlorine-containing compounds captured by the molecular sieve decrease the $^{36}Cl/Cl$ ratio of the methyl chloride. The exact correction for this effect would be possible if the exact composition of the atmosphere in the place of sampling, yields and isotopic ratios of all species were known. Assuming that almost the entire measured ^{36}Cl originate from CH_3Cl and the other compounds were collected and extracted with the same yield it is possible to estimate the ration of $^{36}Cl/Cl$ in CH_3Cl:

$$3.9 \cdot 10^{-12}\,\frac{4250\ ppt}{665\ ppt} = 2.5 \cdot 10^{-11}$$

Using this value and the burden of chlorine in form of CH_3Cl of 2.8 Tg about 70 g of ^{36}Cl are incorporated in tropospheric methyl chloride. With the residence time of CH_3Cl in the troposphere of about 1.1 year, it means the global averaged flux of recycled ^{36}Cl of about 66 at $m^{-2}\ s^{-1}$. This is about 4 times larger than the global averaged flux of 16 at $m^{-2}\ s^{-1}$ estimated in [39].

4.7. *Recycling model of chlorine-36*

The model described in section 2.5.2 was applied to simulate the ^{36}Cl latitudinal distribution influenced by recycling. In the calculation, it was assumed that 16% of chlorine fallen onto land was captured by the biosphere and with a typical time of about 10 years was released to the troposphere: half in form of CH_3Cl and half as inorganic chlorine (NaCl and HCl). Figure 36 shows the comparison of the calculated fluxes in 1992 and the measurements in rainwater and in ice at about the same time. Three peaks can be distinguished: one in the equatorial region and two at the mid-latitudes. The first one is due to the destruction of methyl chloride by interacts with OH-radicals. The rest could be explained by the injection of the stratospheric ^{36}Cl into the troposphere and by the recycling of inorganic chlorine.

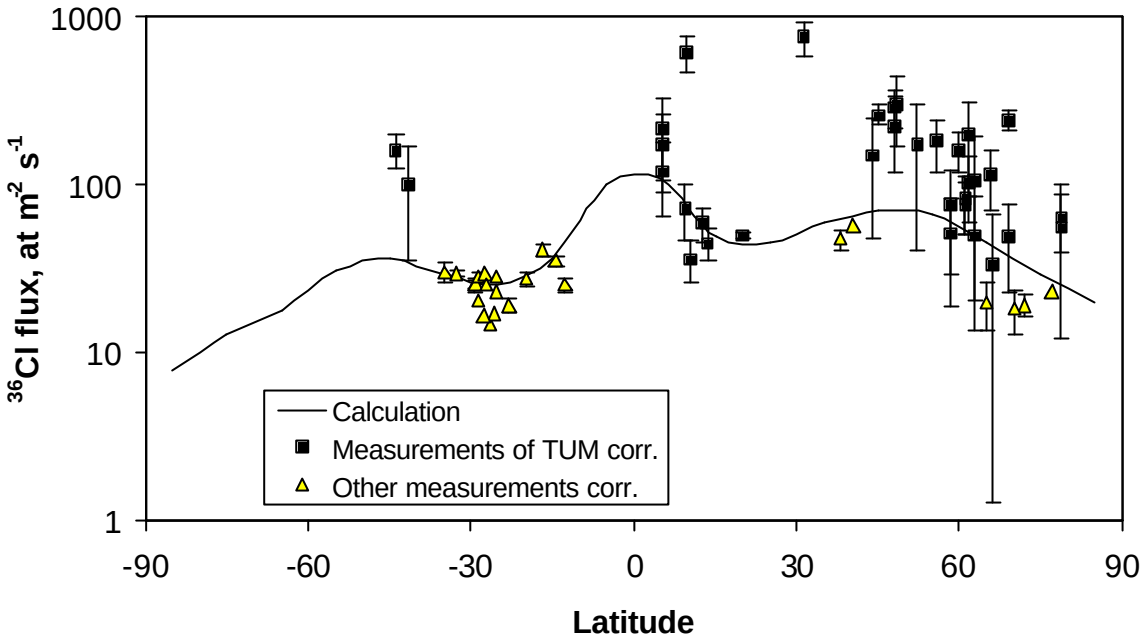

Figure 36 Influence of the chlorine recycling on the latitudinal distribution of the ^{36}Cl flux. The results of the measurements corrected for precipitation rate are presented by squares [8] and triangles [34, 61, 62]. The solid curve represents model calculations.

Because the tropospheric inorganic chlorine is rapidly washed out of the atmosphere, the maximum of its fallout is near its source. Recycled chlorine is stored in the biosphere on the land, and within one latitudinal belt, its deposition is larger over continents than over the ocean. This can be seen in Figure 36. The measurements between 65°N and 77°N in Greenland, where little of the biosphere is present, lie under the simulated curve whereas the experimental points of northern Europe are above it. The same can be attributed to the measurements in New Zealand between 41°S and 44°S. At these latitudes, only 3% of surface is covered with land. Thus, the ^{36}Cl recycling, which takes place in New Zealand, is strongly underestimated in the global model. The highest ^{36}Cl flux measured in Shanghai, 31°N could be explained by a close nuclear reactor.

The simulated model curve corresponds to mean global ^{36}Cl flux of 52 at m^{-2} s^{-1}. About one third of it is cosmogenic and the rest is due to the recycling of the bomb-produced ^{36}Cl. Methyl chloride carries a bulk of ^{36}Cl equal to the mean global flux of about 18 at m^{-2} s^{-1}, which is about 3.5 times less than the experimentally determined upper limit of 66 at m^{-2} s^{-1}.

In section 4.1.2, the simulated ^{36}Cl bomb flux after 1963 decreased too fast compared to the measurements in Greenland ice (Figure 33). In section 4.5, the ^{36}Cl bomb pulse in Greenland was discussed. It was stated that due to the fast mixing of Greenland and European

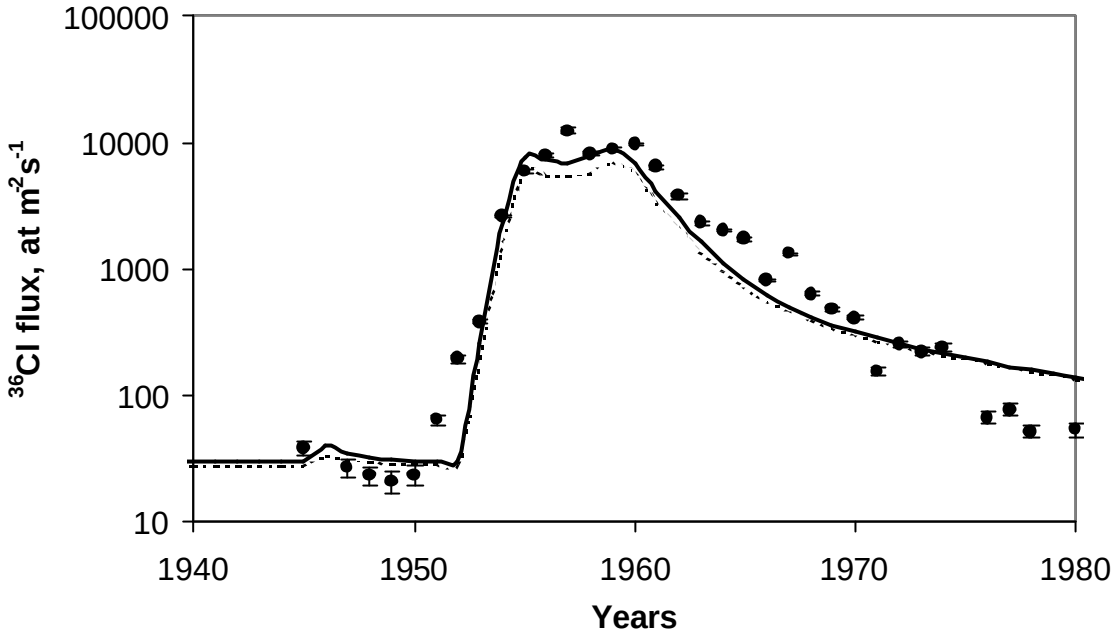

Figure 37 Bomb pulse of ^{36}Cl, calculated at latitudes 45°N (solid line) and 55°N (dashed line) and measured at Dye-3, Greenland, 65°N [5] (circules).

air, station Dye-3 (65°N) corresponds to lower latitude of the transport model. Figure 37 compares measured ^{36}Cl fluxes at Dye-3 with the simulation at 45°N and 55°N when the recycling is taken into account. It can be seen that the model describes the ^{36}Cl fluxes well until about 1965 and then the calculated decrease is too slow. This is because Greenland is far away from the regions with the developed biosphere and the fluxes of recycled ^{36}Cl there are suppressed, though they are still important. Thus, a model without recycling underestimates and a model with recycling overestimates the ^{36}Cl deposition in Greenland. This can be also seen in other glaciers [6] where the ^{36}Cl bomb peak decreases slower than in Greenland due to the recycling influence.

4.8. *Chlorine-36 in hydrology*

The measured ^{36}Cl concentration in the lakes was compared with the calculation (Table 24). The natural and bomb-produced components were simulated applying the recycling model. The values obtained with equation (17), which does not take recycling into account, are shown in brackets. The level of contamination due to Chernobyl accident on the watershed of European lakes was chosen so that

- the corresponding ^{137}Cs contamination was in the limits shown in [128]
- Chernobyl ^{36}Cl fallout was similar on the close areas

Lake	Mean precipitation rate, m/a	Recycled ^{36}Cl (bomb + natural), 10^7 at/l	Assumed Chernobyl ^{137}Cs fallout, kBq/m^2	Chernobyl ^{36}Cl, 10^7 at/l	Total estimated ^{36}Cl, 10^7 at/l	Measured ^{36}Cl, 10^7 at/l
Alpine glacial lakes						
Constance	1.08	0.3 (0.1)	17.5	2.4	2.7	3.8±0.4
Geneva	1.0	0.8 (0.6)	20	5.3	6.1	6±1
Garda	0.8	2.2 (2.4)	15	4.8	7.0	7±1
Como	1.7	0.4 (0.15)	20	2.6	3.0	2.8±0.4
Lugano north	1.7	1.1 (0.86)	24	5.1	6.2	8±1
Lugano south	1.7	0.9 (0.57)	24	3.2	4.1	3.1±0.6
Maggiore	1.7	0.3 (0.17)	20	1.8	2.1	1.9±0.2
Chiemsee	1.0	0.19 (0.08)	10		0.19	3.6±0.3
Starnberger	1.0	3.1 (3.1)	10	5.0	8.1	6.9±0.6
Ammersee	1.0	0.3 (0.15)	10	0.3	0.6	4.1±0.7
Walchensee	1.0	0.2 (0.1)	10		0.2	2.4±0.3
Great Russian lakes						
Onega	0.6	2.0 (1.5)	8	5.3	7.3	7.7±0.9
Ilmen	0.57	5.5 (2.7)	4	6.5	12.0	12±2
Ladoga	0.6	2.5 (2.3)	5	5.0	7.5	7.8±0.9
Ladoga	0.6	2.3 (2.1)	5	4.8	7.1	6.6±0.8
African lakes						
Victoria	1.3	4.2 (2.1)			4.2	3.0±0.9
Mweru	1.1	0.16 (0.02)			0.16	0.6±0.2
Malawi	1.1	0.7 (0.5)			0.7	1.3±0.3
Asian lakes						
Baikal	0.4	2.6 (3.0)			2.6	2.2±0.2
Khubsugul	0.38	2.5 (2.8)			2.5	5.0±0.7
West Balkash	0.19					59±11
Issyk-Kul	0.28					210±40

Table 24 Comparison of the calculated and measured ^{36}Cl concentrations in lakes

A good agreement between the calculations and the measurements is generally established. This proves that the applied method is suitable for the interpretation of the ^{36}Cl measurements.

4.8.1. Chernobyl pulse in European lakes

The ^{36}Cl concentration in European lakes is low sensitive to the ^{36}Cl bomb production and recycling. It depends mostly on the ^{36}Cl input from Chernobyl accident. If the hydrological parameters of a lake are known, the ^{36}Cl measurements provide information on Chernobyl contamination. On the opposite, if the ^{36}Cl (^{137}Cs) fallout is known, its modern concentration

allows quantitative determination of the water-exchange parameters in the lake. For example, lakes with short flushing times contain systematically more ^{36}Cl than it was expected (lake of Constance, Ammersee, Chiemsee). This is due to the groundwater, which plays a role of a mother reservoir within the catchment area of the lake and increases the effective residence time of dissolved substances. The effective residence time of a lake system should be clearly distinguished from the flushing time. The first takes into account a delayed input of the water to the reservoir. Thus, it is a property of both a lake and its watershed. The second is determined as a ratio of the volume to the outflow rate of the lake, and it is a property of the lake only. For example, lake Ilmen has a volume of 6.5 km^3 and a river outflow of 580 $m^3\ s^{-1}$. The calculated flushing time is of about 0.36 a while a known published value is 3.8 a. This is due to a number of marshes on the catchment area of Ilmen, in which the water is kept for a few years.

	Ammersee	Chiemsee	Constance	Ilmen
Flushing time, a	2.7	1.26	4.5	0.4
Eff. residence time, a	5.4±1.4	4.7±1.1	5.3±1.4	3.8±0.7

Table 25 Effective residence time of lake systems with short flushing times

The measurements of ^{36}Cl were used to determine effective residence time in European lakes with short flushing times (Table 25). Because the Chernobyl component is dominant in these cases, (17) can be modified in form:

$$T = \frac{t}{\ln\left(\frac{F \cdot A}{V \cdot c}\right)} \tag{29}$$

Here, F is fluence of Chernobyl ^{36}Cl and it is the main source of uncertainty, which is about factor of two. If T_0 is the expected value of T, a relative uncertainty can be found as

$$\sigma_\tau^{rel} = \frac{T_0}{t} \cdot \ln(2)$$

Because the time t between Chernobyl accident and the sampling is of about 14 years and the residence time found for the lakes with short flushing times is less than 6 years, the uncertainty of the residence time determination is below 30%. Thus, the method appears to be very sensitive even if the input fluence contains a high uncertainty.

In contrast to lakes Ammersee and Chiemsee, the Chernobyl ^{36}Cl peak cannot be used for study of water exchange on the watershed of Lake Walchensee. The area of its drainage basin was changed artificially and both inflow and outflow rates of the lake are regulated.

4.8.2. African lakes

Interpretation of the ^{36}Cl bomb pulse in sweat water lakes with long flushing times is not clear yet. If the recycling is taken into account, about 16% of the bomb ^{36}Cl fallout on the watershed of a lake does not reach the reservoir. On the other hand, the increased ^{36}Cl deposition after the 60s increases the ^{36}Cl concentration. The significance of these effects depends on the location of a lake, on the particularities of the biosphere on the watershed, and on the flushing time. Generally, the total contribution of the recycling to the ^{36}Cl concentration in a lake is low and comparable with the uncertainty of the measurements. However, the recycling plays an important role for equatorial lakes. If the recycling is taken into account, it increases the estimated ^{36}Cl concentration in lake Victoria by a factor of two. Unfortunately, the confidence interval of the measured value does not allow reliable determination, if the recycling is described correctly. Neither this problem can be solved by the ^{36}Cl measurement in lake Malawi. Although the measurements agree with the simulation within 2σ, the ^{36}Cl concentration in the lake can be assumed high. Large deposits of natural uranium were discovered on the area of Malawi. It could lead to the ^{36}Cl production by neutron activation of stable chlorine. Additionally, hydrological parameters of the lakes should be checked. Till now there are a number of contradictions in the literature.

Hydrological parameters of lake Mweru are not known reliably either. We have estimated the catchment area as 22700 km^2 and flushing time – 1.5 a. The ^{36}Cl concentration at present is shown in Table 24. Applying the recycling model and varying the flushing time, effective residence time of 5 a was found. This value could be less if recycling contributes more ^{36}Cl than it was assumed in the model.

4.8.3. Comparison of lakes Baikal and Khubsugul

An interesting pair of lakes to compare is Baikal and Khubsugul (Hövsgöl). They are situated close to each other. Both of them are old lakes with long flushing times. Both have similar ratios of the catchment area to the volume. However, the measured ^{36}Cl concentration differs by more than factor of two. Compared to the simulation, Baikal contains too little ^{36}Cl and Khubsugul contains too much. This is an indication that some particularities of at least one of the lakes were not taken into account. No information on additional anthropogenic ^{36}Cl input (e.g. due to nuclear power plants) to Khubsugul was found. The nearest known place of

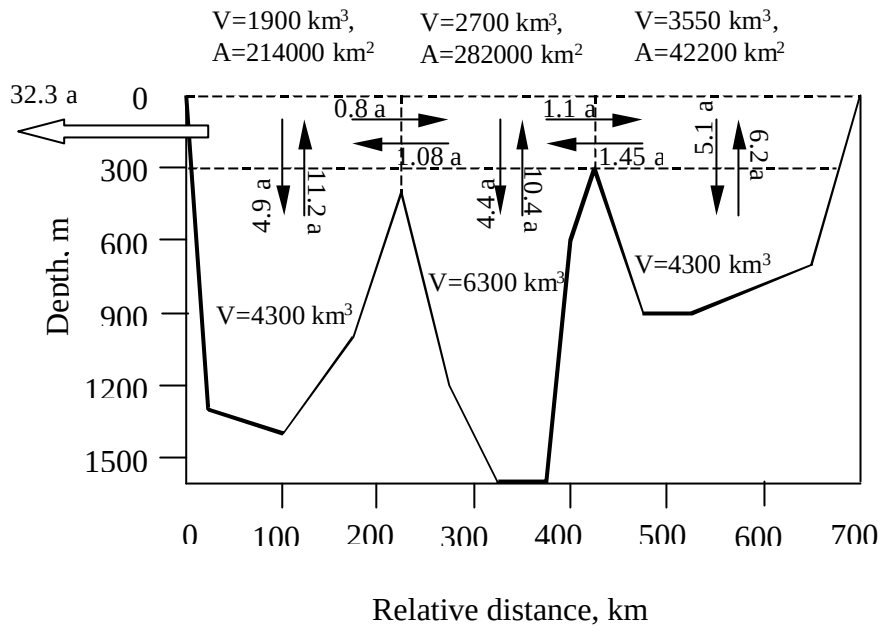

Figure 38 The mixing in Lake Baikal can be described by a 6-box model [136]

thermonuclear weapon tests Lop Nor is about 1500 km away and can be hardly responsible for the local increase of ^{36}Cl content. At least, the ^{36}Cl concentration in Baikal does not confirm this suggestion. The flushing time of lake Khubsugul was estimated between 470 and 740 years. It means that the main contribution of ^{36}Cl is due to the bomb-production. On the other hand, little of the bomb ^{36}Cl entered the lake, already left it. In this case, the ^{36}Cl concentration in Khubsugul depends weakly on the flushing time and its uncertainty cannot explain the ambiguity.

A promising interpretation of the increased ^{36}Cl concentration in Khubsugul is connected with the particularities of the air mixing. During winter, Mongolia is typically in a region of an anticyclone [71]. Generally, there is little precipitation in a high-pressure region. Moreover, the air expands outwards and little of radionuclides can enter the region. A temperature inversion is typical for the area of Khubsugul in winter months. Because the lake is surrounded by the mountains, almost an isolated basin of air is created in that region. The stratospheric air descends through the tropopause breaks and instead of being removed, it remains over the watershed of Khubsugul. Thus, the water of the lake should be enriched with stratospheric elements (e.g. with ^{36}Cl, which is transported in the stratosphere). On the other hand, the gases, which are broadening in the troposphere, should have a low concentration in the water. Indeed, the measurements of ^{129}I demonstrate significantly lower fallout onto Khubsugul than onto Baikal, which remains open for the air circulations [135]. In summer, north winds are typical for Central Asia. Thus, the air of high latitudes with low content of

	South Basin	Central Basin	North Basin
Surface layer	2.46	2.38	2.41
Deep water	2.53	2.45	2.46

Table 26 Calculated concentration of the bomb-produced ^{36}Cl in different compartments of lake Baikal in 1999, 10^7 at/l

Depth of the sampling, m			^{36}Cl concentration, 10^7 at l^{-1}		
			South Basin	Central Basin	North Basin
200	*200*	*200*	2.2±0.4	2.1±0.6	1.7±0.4
600	*800*	*500*	2.4±0.4	2.2±0.3	2.2±0.4
1300	*1500*	*800*	2.9±0.4	1.7±0.7	2.1±0.5

Table 27 Measured ^{36}Cl concentration at different locations of lake Baikal

^{36}Cl enters the region of Baikal. This reduces the ^{36}Cl fluxes on its watershed and the ^{36}Cl concentration in the lake. Khubsugul is separated from the northern air by the mountains and the ^{36}Cl fluxes should be typical for the latitude.

4.8.4. Mixing in Lake Baikal

Baikal is the deepest and the largest freshwater lake in the world. Though the lake was studied for a long time, the rate and mechanism of its water mixing are still under discussion. The mixing of the bomb-produced ^{36}Cl was supposed to be an important proof of the existing models. Nine samples of the water (10 liters each) were taken from the northern, central, and southern parts of the lake at different depths between 200 m and 1300 m in August 1998. The ^{36}Cl concentration there was measured as it was described in Chapter 3.

In [136], it was suggested to describe the lake as 6 boxes with characteristic exchange times (Figure 38). The upper 300 m of water undergo seasonal convective mixing whereas the deep water remains stationary. The sills reach up to the depth of about 300 m and separate deep water of North, Central, and South basins. The surface layers are coupled and horizontal mixing takes place there.

The model described in [136] was used to calculate the time dependence of the bomb ^{36}Cl distribution in the boxes. It was assumed that the ^{36}Cl fluence F of about $1.2 \cdot 10^{12}$ at m^{-2} fell onto the catchment area of each basin (shown with A in Figure 38) in 1960 and entered the surface layer of the basin immediately. Then an exchange between boxes and outflow (Lower Angara) from the surface layer of the South Basin took place. The natural component

of ^{36}Cl was neglected in this calculation. The equilibrium between the boxes was established at about 1975 so that the difference in the ^{36}Cl concentration in different parts of the lake was below 10%. The calculated ^{36}Cl concentration in 1999 is shown in Table 26. The largest difference (of about 6%) was expected between the deep water of the southern basin and the surface water of the central and northern basins. The measurements (Table 27) confirm higher ^{36}Cl content in deep water of the southern basin compared to the shallow water of the northern basin. However, because of the large uncertainty of about 20% they do not allow reliable conclusion on the determined in [136] exchange times.

4.8.5. Closure time of lakes

Lakes become salty if evaporation plays a dominant role in the water output. Precipitation and inflowing rivers contain salt in a small concentration. In the lake, the water evaporates and the concentration of salt increases. If a lake has a river output, a stable value of salinity is reached after period of about flushing time has passed (see section 2.6). In case of closed lakes without outflow (Figure 39), the salinity grows continuously and becomes comparable or even larger than the salinity of the ocean. If this process lasts longer than about million years, old ^{36}Cl decays and the ratio of ^{36}Cl/Cl becomes lower than the experimental sensitivity of AMS. The ^{36}Cl decay in lakes younger than about 300 ka is small and ^{36}Cl becomes a powerful tool to understand the lake's age and the exchange processes.

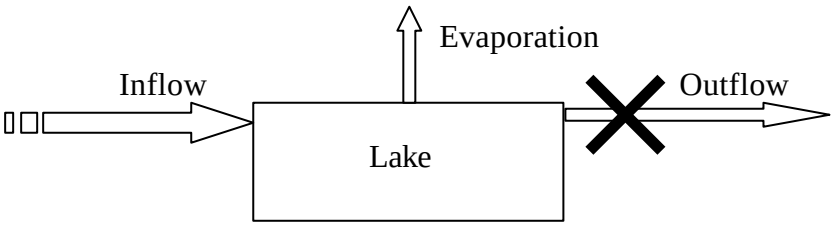

Figure 39 If outflow of a lake is stopped and the inflowing water evaporates completely, the lake becomes salty (e.g. Issyk-Kul)

Lake Issyk-Kul is the fifth deepest lake in the world and it has a mean absolute salinity of 6.06 g kg^{-1} [137]. The lake was formed in Lower Carboniferous and it was fresh at the beginning. In the Middle Pleistocene, the mountain ridges rose and the level of Issyk-Kul sank [125]. The water surface is at altitude of 1607 m at present and at elevation of about 1620 m the lake becomes open. The fluctuations of the lake's level led to temporal overflows [138], but these periods remained short.

A number of works were devoted to the esitmation of the lake's age (the period since Issyk-Kul became a closed basin). In [139] a closure age of about 6,900 years BP was

deduced on the base of the ratios of Sr/Ca, U/Ca, and Mg/Ca measured in the lake sediments. In [140] a comparison of methods using the input rate of a trace element and its modern concentration in the lake was done. It was shown that the method depends strongly on the chosen trace element and the obtained age varies from 2,100 a (Ca^{2+}) to 190,000 a (Cl^{1-}). Obviously, there are some mechanisms of geochemical or biochemical removal of the ions. Even the application of the most conservative element (Cl^{1-}) is difficult because only a present state of the surface water source function is known. If the groundwater is taken into account, the chlorine residence time decreases to 39,000 a [141].

The measurement of the ^{36}Cl concentration in the lake allows an independent estimation of the closure age. Multiplying the ^{36}Cl concentration with the lake's volume, a total amount of ^{36}Cl in the lake $N=(3.6\pm0.7)\cdot10^{24}$ at can be obtained. The estimated bomb-produced ^{36}Cl fluence on the watershed of Issyk-Kul is of about $1.1\cdot10^{12}$ at m^{-2} and the corresponding amount of ^{36}Cl is about $2.5\cdot10^{22}$. This is less than 1% of the total ^{36}Cl amount and can be neglected in the calculation. Because no other event is known, which could lead to a production of large amounts of ^{36}Cl (e.g. a nuclear explosion in the lake), almost the entire ^{36}Cl in the lake is cosmogenic. The production rate of the cosmogenic isotopes remained stable in the past and only under extreme conditions, it increased by about 50% [23]. Assuming a constant ^{36}Cl input Φ and ^{36}Cl decay with life-time t, a closure time

$$t_{cl.} = -\tau \cdot \ln\left(1 - \frac{N}{\Phi\tau}\right) \qquad (30)$$

can be calculated. With a natural ^{36}Cl flux at the latitude 42°N of 26 at m^{-2} s^{-1}, annual input $\Phi=1.8\cdot10^{19}$ at a^{-1} is obtained. Because the precipitation rate over Issyk-Kul changed many times within the last 100,000 a, no correction for it was done here. Thus, the ^{36}Cl content in lake Issyk-Kul corresponds to its closure age of about 270,000 a. It is hardly possible to determine the uncertainty of this estimate. Because Issyk-Kul is situated between mountains, the local meteorological conditions can influence the ^{36}Cl fallout. Assuming a possible ^{36}Cl flux enhancement of about 50%, the closure age can be reduced to 160,000 a. If the ^{36}Cl fluxes are too small, no upper limit for the lake's age can be obtained. On the contrary, the modern ^{36}Cl content in the lake sets a lower limit on the flux, which is of about 12 at m^{-2} s^{-1}.

The obtained time T should be interpreted as a closure age of the basin of the lake and not as a closure of the lake itself. It is possible that the lake still had an outflow but the ^{36}Cl fallout was stored in the glaciers on the watershed. After the closure of the lake, ^{36}Cl entered

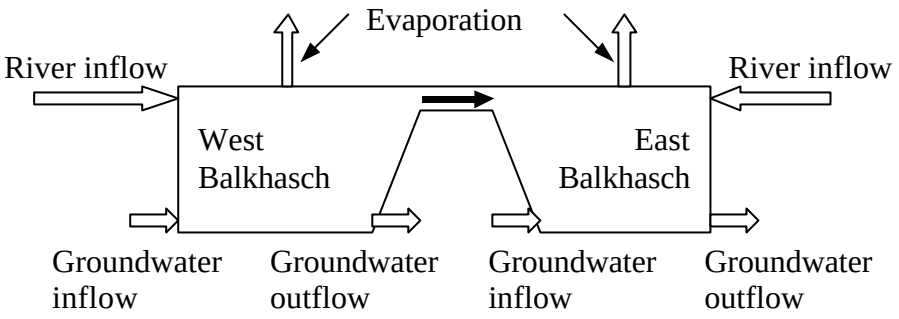

Figure 40 Lake Balhkash does not have any river outflow. The water balance is reached through the evaporation and groundwater outflow. Additionally, there is a flow from the western to the eastern part of the lake.

Issyk-Kul with melted water during a warm period (e.g. last full interglacial, 120-130 kyrs BP).

4.8.6. Groundwater outflow from terminal lakes

Lake Balkhash is another lake without surface outflow (Figure 40). However, its salinity remains in the range of $1 - 5$ g l^{-1} because of the groundwater. According to [124] its outflow exceeds its inflow by $0.38 - 0.39$ km^3 a^{-1}. This value contradicts the estimated absolute groundwater inflow of 0.08 km^3 a^{-1} and outflow of 0.028 km^3 a^{-1} [141]. Measurements of the ^{36}Cl concentration in the lake can deliver information on the flushing time and the outflow.

Lake Balkhash is divided by Say-Isek Peninsula into the western and eastern sectors. The water exchange occurs through a narrow and shallow channel. This allows consideration of the lake as two separate reservoirs. The water flow from the western part to the eastern part varied between 2.7 km^3 a^{-1} and 2.1 km^3 a^{-1} in the period from 1961 to 1999 [142]. Hydrological parameters of each sector are presented in Table 28. Precipitation rate over the watershed reaches 1.8 m a^{-1} in the southern mountain region and it varies from 0.15 to 0.25 m a^{-1} over most of the low land [124].

	West Balkhash	East Balkhash	Total
Mean depth, m	4.6	7.5	5.8
Surface area, km^2	10600	7600	18200
Volume, km^3	49	57	105
Catchment area, km^2	310000	103000 + 310000	413000

Table 28 Mean depth, surface area, volume, and catchment area of Lake Balkhash [114, 124, 142]

A precipitation rate of 0.2 m a^{-1} was adopted as a mean value and the content of bomb ^{36}Cl in West Balkhash was calculated. In order to explain the observed ^{36}Cl concentration (Table 18) a reservoir's flushing time of about 17 years is required. This corresponds to the outflow from West Balkhash of about 2.9 km^3 a^{-1}. The obtained value is slightly higher than one indicated in [142]. This difference could arise due to the influence of the groundwater outflow or due to model uncertainties.

East Balkhash does not have any surface outflow and the ^{36}Cl measurements in its water could be used successfully to study the groundwater balance.

Conclusion

The contribution of cosmogenic and anthropogenic sources to the ^{36}Cl content in environmental compartments was studied in this work. The global mean production rate of the cosmogenic ^{36}Cl is about 16 at m^{-2} s^{-1}. This value can differ by a factor of two when solar modulation or geomagnetic field undergoes large fluctuations.

Due to the "near water" nuclear weapon tests, a large amount of ^{36}Cl was released to the atmosphere. The peaks of this release were in 1954, 1956, and 1958. A significant part (of about 18%) of the bomb-produced ^{36}Cl reached the stratosphere and thus became mixed globally. The latitudinal distribution of the ^{36}Cl fallout is not clear yet. However, the results obtained with an atmospheric transport model show that about two thirds of the bomb ^{36}Cl fell down in the northern hemisphere and one third in the southern hemisphere. This corresponds to the deposition of about 2200 years and 1000 years of natural production in the northern and southern hemispheres, respectively.

The ^{36}Cl washed out of the troposphere is not lost. A part of it (up to 16% in average) can be caught by the biosphere. The plants decay with a typical time of 10 years and the chlorine stored in them is released to the troposphere: half in form of inorganic chlorine and half as methyl chloride. The ^{36}Cl released in inorganic form is washed out of the troposphere having a residence time of 18 days for wet deposition and of 36 days for dry deposition. Methyl chloride is mixed globally and it decays in the reactions with OH^- radicals at equatorial latitudes mostly. Thus, though more than 40 years have passed since the bomb ^{36}Cl injection into the atmosphere, the fallout of bomb ^{36}Cl can be still observed in the modern precipitation. The effect of the recycling is larger over land than over the ocean and in the northern hemisphere than in the southern one. Large fluxes of the recycling bomb ^{36}Cl are at the equatorial latitudes where the OH^- concentration hat maximum.

While the nuclear power plants are functioning, the stable chlorine contained in the nuclear fuel and moderator captures neutrons and produces ^{36}Cl. This ^{36}Cl enters the environment in liquid phase at the region of reprocessing plants. Only a minor part of it is

released in gas form, producing local ^{36}Cl contamination. During the nuclear accident in Chernobyl in 1986 about 0.5 kg of ^{36}Cl was released into the troposphere. This ^{36}Cl is unequally distributed over Europe so that a typical fluence over Germany or Switzerland is of a few 10^{12} at·m^{-2}, which is comparable to the deposition of bomb ^{36}Cl.

The ^{36}Cl of all types discussed above can be observed in the world lakes with different flushing times. In the lakes with flushing times longer than a few thousand years cosmogenic ^{36}Cl dominates. In the lakes with flushing times from about 15 years to a few thousand years most of the ^{36}Cl is of bomb origin. European lakes with flushing times longer than 5 years contain large concentrations of Chernobyl ^{36}Cl. The lakes with short flushing times below 5 years are influenced by the recycling and groundwater.

Due to its hydrophilic properties, ^{36}Cl can be successfully used as tracer to investigate water exchange processes. In European lakes with flushing times shorter than 5 years, a part of Chernobyl ^{36}Cl entered the groundwater. Because of the slow flow rate of the groundwater this ^{36}Cl is still continuously injected into the lakes. Thus, the characteristics of the groundwater flow into the lake can be obtained measuring the ^{36}Cl concentration. In Balkhash Lake, the bomb-produced ^{36}Cl leaves the lake with the groundwater. Thus, the temporal ^{36}Cl concentration in the lakes shows the flow rate out of the lake. Lake Issyk-Kul does not have any outflow and its ^{36}Cl concentration shows how long the lake has been storing natural ^{36}Cl or how long the lake has been remaining closed.

Appendixes

The data on chlorine-36 fluxes

Time of sampling	Latitude	Precipitation rate, m/a	^{36}Cl flux, at m^{-2} s^{-1}	Ref.	Comment
8/10/91-28/1/92	38.2		49 ± 9	[61]	Total flux
29/1/91-5/8/92	38.2		67 ± 6	[61]	Total flux
6/8/92-6/10/92	38.2		51 ± 9	[61]	Total flux
Averaged (8/10/91-6/10/92)	38.2		59 ± 8	[61]	Total flux
8/10/91-28/1/93	38.2		29 ± 10	[61]	Chlorine in water
29/1/91-5/8/93	38.2		5 ± 9	[61]	Chlorine in water
6/8/92-6/10/93	38.2		38 ± 4	[61]	Chlorine in water
Averaged (8/10/91-6/10/92)	38.2		44 ± 9	[61]	Chlorine in water
1979	-75.9	0.5	140	[58]	Estimation in a glacier
	77.2	0.27	24	[34]	Camp Century
	72.6	0.23	18	[34]	Summit
	70.3	0.49	24	[34]	Milcent
	65.2	0.59	20	[34]	Dye 3
11/93 - 10/94	-43.9	0.102	139 ± 33	[8]	
01/94 - 12/94	-41.7	0.684	68 ± 45	[8]	
11/89 - 12/90	5.3	0.975	106 ± 52	[8]	
09/93 - 08/94	5.3	1.633	188 ± 97	[8]	
01/95 - 12/95	5.3	1.234	86 ± 41	[8]	
01/95 - 12/95	9.45	1.279	53 ± 19	[8]	
11/89 - 10/90	9.6	1.054	389 ± 92	[8]	
04/93 - 03/94	10.4	1.26	39 ± 11	[8]	
05/94 - 04/95	12.65	1.183	61 ± 14	[8]	
05/94 - 04/95	13.5	0.669	32 ± 7	[8]	
05/94 - 04/95	20.2	0.099	25 ± 1	[8]	
01/89 - 12/89	31.2	0.762	755 ± 169	[8]	
01/93 - 12/93	44.07	1.46	222 ± 149	[8]	
12/93 - 11/94	45.08	0.801	258 ± 32	[8]	
03/93 - 02/94	48.13	1.081	347 ± 83	[8]	
02/96 - 06/96	48.16	0.506	170 ± 82	[8]	
04/96 - 06/96	48.4	0.52	235 ± 106	[8]	

Time of sampling	Latitude	Precipitation rate, m/a	^{36}Cl flux, at m^{-2} s^{-1}	Ref.	Comment
3-5, 10-11/90	52.27	0.29	109 ± 86	[8]	
03/90 - 02/91	55.75	0.895	202 ± 70	[8]	
03/91 - 02/92	58.4	0.73	74 ± 45	[8]	
03/89 - 02/90	58.4	1.555	83 ± 51	[8]	
3-4/90, 01/91	59.9	0.757	161 ± 44	[8]	
03/91 - 02/92	61	0.426	79 ± 30	[8]	
03/91 - 12/91	61.15	0.607	88 ± 31	[8]	
03/89 - 02/90	61.6	3.197	395 ± 160	[8]	
03/91 - 12/91	61.6	1.949	504 ± 279	[8]	
03/89 - 02/90	62.8	1.392	97 ± 68	[8]	
03/91 - 02/92	62.8	2.018	274 ± 213	[8]	
03/89 - 02/90	65.8	1.581	249 ± 95	[8]	
03/91 - 02/94	66	0.384	31 ± 31	[8]	
03/89 - 02/90	69.1	0.684	60 ± 32	[8]	
03/91 - 02/92	69.1	0.799	327 ± 43	[8]	
03/89 - 02/90	78.9	0.282	59 ± 46	[8]	
03/91 - 02/92	78.9	0.388	76 ± 28	[8]	
	-12	0.723	20 ± 2	[62]	
	-14	0.675	27 ± 2	[62]	
	-16	0.465	26 ± 2	[62]	
	-19	0.09	11 ± 1	[62]	
	-22	0.196	11 ± 1	[62]	
	-25	0.36	12	[62]	
	-25	0.09	14	[62]	
	-26	0.244	9	[62]	
	-27	0.242	18	[62]	
	-27	0.172	14	[62]	
	-27	0.228	10	[62]	
	-28	0.348	14	[62]	
	-28	0.179	16 ± 1	[62]	
	-29	0.48	20 ± 2	[62]	
	-29	0.356	18 ± 1	[62]	
	-32	0.552	22 ± 1	[62]	
	-34	0.612	24 ± 3	[62]	

Table 29 The available data on ^{36}Cl fluxes

Atmospheric chlorine in the environment

Chemical composition		NaCl	HCl	CH_3Cl	$CHCl_3$	$C_2H_3Cl_3$	C_2Cl_4	C_2HCl_3	CH_2Cl_2	$CHClF_2$
Total mass in troposphere, Tg		15	0.6	2.8	0.21	2.3	0.16	0.0053	0.25	0.65
Content in troposphere, ppt		3562	143	665	50	546	38	1.3	59	154
Life time in the atmosphere, years		0.0083	0.01	1.1	0.37	3.9	0.36	0.015	0.36	8.1
Sources, Tg / year	**Total**	**1806**	**65**	**1.33**	**0.564**	**0.583**	**0.328**	**0.223**	**0.7**	**0.08**
	Ocean	1785		0.46	0.32		0.016	0.02	0.16	
	Biomass burning	6.3	6.3	0.64	0.002	0.013			0.049	
	Industrial production			0.01	0.062	0.57	0.31	0.2	0.49	0.08
	Others	15	58.5	0.22	0.18		0.002	0.003		
Sinks, Tg / year	**Total**	**1803**	**62**	**2.6**	**0.412**	**0.39**	**0.44**	**0.35**	**0.5**	**0.04**
	Transport to stratosphere			0.2	0.002	0.05			0.01	0.01
	Chemical reactions			2.4	0.41	0.3	0.44	0.35	0.49	0.03
	Sorption by soil			0.18						
	Fall-out	1753	62							
	Others	49.6				0.04				

Table 30 The most abundant chlorine-containing chemical compositions. Their source and sink fluxes [86]

Acknowledgment

I had luck to come to the Technical University of Munich (Technische Universität München) to perform the Ph.D. study. Here I was surrounded by a number of friendly and highly competent people. Their help within and outside the university was essential for the success of my work.

- First of all I would like to say thank you to my supervisor Prof. Dr. Eckehart Nolte. He has invited me to TU Munich. He suggested an exciting theme to me. He was always interested in my achievements and ready to spend his time to discuss problems with me.
- I want to express my gratitude to Prof. Dr. A. Blinov, who supervised my diploma work and who took an active part in my following life as a scientist. During my Ph.D. study, I often consulted with him when I had any kind of doubts. He was also the first one, who thoroughly read my thesis and made a number of important comments.
- I am very grateful to my colleagues Dr. F. Kubo and Dr. Th. Huber who helped me to learn the experimental AMS. They were also the people who helped me not to be alone in the very beginning of my life in Germany. A special thank you I want to give to Herbert Reithmeier. He was the last who joined the AMS group but his pleasant attitude to people let him play one of the central roles in our team. Besides his help during experiments, I highly appreciate his readiness to assist when I was weather not sure about German grammar or standards of private life in Germany.
- I thank Dr. C. Stan-Sion and Dr. K. Knie for multiple useful discussions about ^{36}Cl measurements, AMS facility and for many suggestions, how I could improve my thesis.
- A special thank you I would like to give to Dr. F. Slemr and Dr. R. Stadler, how helped me to develop the experimental setup for CH_3Cl collection and the chlorine extraction procedure from the molecular sieve, respectively.
- I am grateful to Dr. G. Korschinek, Dr. G. Rugel, Dr. C. Wallner, Dr. A. Wallner, and Dr. W. Rühm for useful discussions and for the help during AMS measurements.
- Of a high importance was the help of technical personal: U. Heim, N. Gärtner, and W. Carli with the entire team of the accelerator laboratory.
- The work in the university would not be so pleasant if I were not able to relax with my friends in the spare time. In this regard, I give my thanks to Dr. A. Koptsevitch, A. Bernatz, K. Specht, C. Jocham, and S. Cristoforetti. I would like to express gratitude to Veronika Pull who has been supporting and encouraging me for the last two years.
- The last but not the least are my parents and sister. They always paid attention to my achievements and they did everything to help me all the time.

References

1 Finkel, R.C., M. Suter *AMS in the Earth sciences: technique and applications*. Advances in Analytical Geochemistry, V. 1, JAI Press Inc., 1993

2 Lal, D., B. Peters, *Handbuch der Physik*, V. 46:2, 1967, P. 551.

3 Bentley, H.W., F.M. Phillips, and S.N. Davis *Chlorine –36 in the terrestrial environment* Handbook of Environmental Isotope Geochemistry, Amsterdam, V. 2, 1986, P. 427-480

4 Elmore, D., B.R. Fulton, M.R. Clover, J.R. Marsden, H.E. Gove, H. Naylor, K.H. Purser, L.R. Kilius, R.P. Beukins, and A.E. Litherland, *Analysis of ^{36}Cl in environmental water samples using an electrostatic accelerator* Nature, V. 277, 1979, P. 22-25

5 Synal, H.-A., J. Beer, G. Bonani, M. Suter, and W. Wölfli *Atmospheric transport of bomb-produced ^{36}Cl* Nuclear Instruments and Methods, B52, 1990, P. 483-488

6 Synal H.-A., J. Beer, U. Schotterer, M. Suter, L. Thompson *Bomb produced ^{36}Cl in ice core samples from mountain glaciers*, Workshop Glaciers from the Alpes: Climate and Environmental Archives, Wengen, Switzerland, 1996

7 Milton, J.C.D., H.R. Andrews, L.A. Chant, R.J.J. Cornett, W.G. Davies, B.F. Greiner, Y. Imahori, V.T. Koslowsky, J.W. McKay, G.M. Milton, *^{36}Cl in the Laurentian Great Lakes basin* Nuclear Instruments and Methods, B92, 1994, P. 440.

8 Scheffel, C., A. Blinov, S. Massonet, C. Stan-Sion, H. Sachsenhauser, J. Beer, H.-A. Synal, P.W. Kubik, M. Kaba, and E. Nolte, *^{36}Cl in modern precipitation* Geophysical Reserch Letters, V. 26, N 10, 1999, P. 1401-1404

9 Cornett, R.J., H.R. Andrews, L.A. Chant, W.G. Davies, B.F. Greiner, Y. Imahori, V.T. Koslowsky, T. Kotzer, J.C.D. Milton, G.M. Milton *Is ^{36}Cl weapons' test fallout still cycling in he atmosphere*, Nuclear Instruments and Methods, B123, 1997, P. 378-381

10 Alvarez, L.W. and R. Cornog, *^{3}He in helium* Physical Review, V. 56, 1939, P. 379

11 Muller R.A. *Radioisotope dating with a cyclotron*, Science V. 196, 1977, P. 489-494.

12 Purser, K.H., R.B. Liebert, A.E. Litherland, R.P. Beukens, H.E. Gove, C.L. Bennet, M.R. Clover, and W.E. Sondheim, *An attempt to detect stable N- ions from a sputter ion source and some implications of the results for the design of tandems for ultra-sensitive carbon analysis* Rev. Phys. App, V. 12, 1977, P. 1487

13 Bennet, C.L., R.P. Beukens, M.R. Clover, H.E. Gove, R.B. Lievert, A.E. Litherland, K.H. Purser, and W.E. Sondheim, *Radiocarbon dating using accelerators: Negative ions provide the key*, Science, V. 198, 1977, P. 508

14 Van Holebeke, M. A. I., F. B. McDonald, and J. P. Meyer, *Solar energetic particle observations of the 1982 June 3 and 1980 June 21 gamma-ray/neutron events*, Astrophys. J. Suppl., V. 73, 1990, P. 285.

15 Schwabe, H. *Sonnen-Beobachtungen im Jahre 1843*. Astronomische Nachrichten, V. 20, N. 495, 1843, P. 233-236

16 Gleissber, W. *A table of secular variations at the solar cycle*. Terr. Magn. Atm. Electr., V. 49, 1944, P. 243
17 Gleissberg, W. *The eighty-year sunspot cycle*. J. Brit. Astr. Assoc., V. 68, 1958, P. 148
18 Damon, P.E., and C.P. Sonnett. *Solar and terrestrial components of the atmospheric ^{14}C variation spectrum*. In Sonnett, C.P., M.S. Giampapa, and M.S. Matthews, eds., The sun in time: Tucson, Ariz., The University of Arizona Press, 1991, P. 360-388
19 Stuiver, M., P. J. Reimer, E. Bard, J. W. Beck, G. S. Burr, K. A. Hughen, B. Kromer, F. G. McCormac, J. Plicht, and M. Spurk *Radiocarbon age calibration 24,000 - 0 cal BP*, Radiocarbon, V. 40, 1998, P. 1041-1083
20 Wagner, G., J. Beer, J. Masarik, R. Muscheler, P.W. Kubik, W. Mende, C. Laj, G.M. Raisbeck, F. Yiou *Presence of the solar de Vries cycle (~205 years) during the last ice age*, Geophysical Research Letters, V. 28(2), 2001, P. 303-306
21 Konstantinov A.N., Kocharov G.E., Levchenko V.A., Astronomy Lett., V. 16:9, 1990 (*in Russian*)
22 Baumgartner, S., J. Beer, J. Masarik, G. Wagner, L. Meynadier, and H.-A. Synal, *Geomagnetic Modulation of the ^{36}Cl Flux in the GRIP Ice Core, Greenland*, Science, V. 279, 1998, P. 1330-1332
23 Wagner G., J. Beer, C. Laj, C. Kissel, J. Masarik, R. Muscheler, H.-A. Synal *Chlorine-36 evidence for the Mono Lake event in the Summit GRIP ice core.* Earth and Planetary Science Letters, V. 181, 2000, P. 1-6
24 O'Brien, K., *Secular variations in the production of cosmogenic isotopes in the Earth's atmosphere*, Journal of Geophysical Research, V.84, 1979, P.423.
25 Masaric, J., J. Beer, *Simulation of Particle Fluxes and Cosmogenic Nuclide Production in the Earth's Atmosphere*, Journal of Geophysical Research, V. D104 (10), 1999, P. 12,099-13,012
26 Blinov A.V., Lazarev V.E., Bulletin of the Russian Academy of Sciences, Physics, V. 63/8, 1999, P. 1630 (*in Russian*)
27 Blinov, A., S. Massonet, H. Sachsenhauser, C. Stan-Sion, V. Lazarev, J. Beer, H.-A. Synal, M. Kaba, J. Masarik, E. Nolte *An excess of ^{36}Cl in modern atmospheric precipitation*, Nuclear Instruments and Methods, B172, 2000, P. 537
28 Blinov A.V., Lazarev V.E., Bulletin of the Russian Academy of Sciences. Physics, V. 61/6, 1997, P. 1460 (*in Russian*)
29 Dorman L.I. *Experimental and theoretical bases of astrophysics of cosmic rays*, Moscow, Nauka, 1975 (*in Russian*)
30 Endt P.M., Nuclear Physics, A521/1, 1990
31 Sleta L.A. *Chemistry. Handbook*, Kharkov, 1997 (*in Russian*)
32 Blinov, A.V. and Kremlevskii, M.N. *Formation of ^{36}Cl under the action of cosmic rays in the Earth's atmosphere*, Izv. Akad. Nauk SSSR, Ser. Fiz., V. 55, N. 10, 1991, P. 2066-68
33 Oeschger, H., J. Houtermann, H. Loosli, and M. Wahlen *The constancy of cosmic radiation from isotope studies in meteorites and on the Earth*, In Radiocarbon variations and absolute chronology, Nobel symposium, I.U. Olsen Ed.. Stockholm John Wiley. 1969.
34 Lukasczyk, C.E., *^{36}Cl im Groenlandeis*, ETH, Zurich, 1994
35 Baumgartner, S. *Kosmogene Radioisotope im Pleistozaen des Summit-GRIP-Eiskerns*, Dissertation, ETH, Zurich, 1995
36 Heisinger B., D. Lal, A. J. T. Jull, P. Kubik, S. Ivy-Ochs, S. Neumaier, K. Knie, V. Lazarev, and E. Nolte *Production of selected cosmogenic radionuclides by muons; 1. Fast muons*, Earth and Planetary Science Letters, V. 200/3, 2002, P. 345-355

37 Heisinger B., D. Lal, A. J. T. Jull, P. Kubik, S. Ivy-Ochs, K. Knie and E. Nolte *Production of selected cosmogenic radionuclides by muons: 2. Capture of negative muons*, Earth and Planetary Science Letters, V. 200/3, 2002, P. 357-369

38 Milton G.B., H.R. Andrews, S.E. Causey, L.A. Chant, R.J. Cornett, W.G. Davies, B.F. Greiner, V.T. Koslowsky, Y. Imahori, S.J. Kramer, J.W. McKay, and J.C.D. Milton *Chlorine-36 dispersion in the Chalk River area*, Nuclear Instruments and Methods, B92, 1994, P. 376

39 Lazarev V, Diploma work, SPSTU, St. Petersburg, 1998 (*in Russian*)

40 Castagnoli, G. and D. Lal, *Solar Modulation effects in Terrestrial Production of Carbon-14*, Radiocarbon, V.22, N. 2, 1980, P. 133-158

41 Störmer C, *The Polar Aurora*, Clarendon Press, Oxford, 1955

42 Barashenkov V.C., Toneev, V.D. *Interaction of high energy particles and atomic nuclei with nuclei*, Moscow, Atomizdat, 1972 (*in Russian*)

43 Carlson, R.F. Atomic Data and Nuclear Data Tables, V.63, 1996, P. 93

44 Sychev B.C., Serov A.Ya., Manko B.V. *Analytical approximations of differential cross-sections of secondary particles production in inelastic nucleon-nucleus reactions at the energies larger than 20 MeV*, Preprint 799, Moscow, 1979 (*in Russian*)

45 Bethe H.A., *Zur Theorie des Durchgangs schneller Korpuskularstrahlen durch Materie*, Annalen der Physik, V. 5, 1930. P. 325

46 Bloch F., *Bremsvermögen von Atomen mit mehreren Elektronen*, Zeitschrift für Physik, V. 81, 1933, P. 363

47 Janni, J., Atomic Data and Nuclear Data Tables, V.27. 1982, P.147

48 Rudstam, G., *Systematics of Spallation Yields*, Z. Naturforschung, V. 21A, 1966, P. 1027-1041

49 Silberberg, R., C.H. Tsao, *Partial Cross-Sections in High Energy Nuclear Reactions and Astrophysical Applications*, The Astrophysical Journal Supplement Series, V. 25, 1973, P. 315

50 Silberberg, R, C.H. Tsao, and A.F. Barghouty, *Updated Partial Cross Sections of Proton-Nucleus Reactions*, Astrophysical Journal, V. 501, 1998, P. 911

51 Stan-Sion, C., D. Huggle, E. Nolte, A. Blinov, M. Dumitru, *AMS Measurements of the production cross sectins of ^{36}Cl with protons up to 1 GeV*, Nuclear Instruments and Methods in Physics Research, B 117, 1996, P. 26-30

52 Reisbeck G.M. and F. Yiou, *Cross sections for the spallation production of ^{10}Be in targets of N, Mg, and Si and their astrophysical applications*, Physical Review, C9, 1974, P. 1385

53 Mashnik S.G., Sierk A.J. Bersillon O., Gabriel T., *Cascade-exciton model analysis of proton induced reactions from 10 MeV to 5 GeV*, Nuclear Instruments and Methods in Physics Research, A 414, 1998, P. 68-72.

54 Davis, R. Jr., and O.A. Schaeffer, *Chlorine-36 in nature*, Ann. NY Acad. of Sci., V. 62, 1955, P. 105-122

55 Ronyani, C. and Tamers, M.A. *Low-level chlorine-36 detection with liquid scintillation techniques*, Radiochem. Acta, V.6, 1966, P. 206-210

56 Bentley, H.W. *Some comments on the use of chlorine-36 for dating very old ground water: Workshop on dating old ground water*, S.N. Davis, ed., Subcontract 19Y-55412v, report to Union Carbide Corp., Nuclear Divisions, by Department of Hydrology and Water Resources, University of Arizona, 138 pp. 1978

57 Schaeffer, O.A., S.O. Thompson, and N.L. Lark, *Chlorine-36 radioactivity in rain*, Journal of Geophysical Research, V. 65, 1980, P. 4013-4016

58 Finkel, R.C., K. Nishiizumi, D. Elmore, R.D. Ferraro, H.E. Gove, *^{36}Cl in polar ice, rainwater and seawater*, Geophysical research letters, V. 7, N. 11, 1980, P. 983-986

59 Herut, B., A. Starinsky, A. Katz, M. Paul, E. Boaretto, D. Berkovits, *^{36}Cl in chloride-rich rainwater, Israel*, Earth and Planetary Science Letters, V 109, 1992, P. 179-183
60 Knies, D.L., D. Elmore, P. Sharma, S. Vogt, R. Li, M.E. Lipschutz, G. Petty, J. Farrell, M.C. Monaghan, S. Fritz, E. Agee, *^{7}Be, ^{10}Be and ^{36}Cl in precipitation*, Nuclear Instruments and Methods in Physics Research, B92, 1994, P. 340-344
61 Hainsworth, L.J., A.C. Mignerey, G.R. Helz, P. Sharma, P.W. Kubik, *Modern chlorine-36 deposition in southern Maryland, USA*, Nuclear Instruments and Methods in Physics Research, B92, 1994, P. 345-349.
62 Keywood, M.D., L.K. Fifield, A.R. Chivas, and R.W. Cresswell *Fallout of chlorine-36 to the Earths surface in the Southern hemisphere*, Journal of Geophysical Research, V. 103, D7, 1997, P. 8281-8286
63 Nolte, E., P. Krauthan, G. Korschinek, P. Maloszewski, P. Fritz, and M. Wolf *Measurements and interpretations of ^{36}Cl in groundwater Milk River aquifer, Alberta, Canada*, Applied Geochemistry, V. 6, 1991, P. 435
64 Milton, J.C.D., G.M. Milton, H.R. Andrews, L.A. Chant, R.J.J. Cornett, W.G. Davies, B.F. Greiner, Y. Imahori, V.T. Koslowsky, T. Kotzer, S.J. Kramer, J.W. McKay *A new interpretation of the distribution of bomb-produced chlorine-36 in the environment, with special reference to the Laurentian Great Lakes*, Nuclear Instruments and Methods in Physics Research, B123, 1997, P. 382
65 Beasley, T.M., L.W. Cooper, J.M. Grebmeier, L.R. Kilius, and H.-A. Synal *^{36}Cl and ^{129}I in the Yenisei, Kolyma, and Mackenzie Rivers*, Environ. Sci. Technol., V. 31, 1997, P. 1834
66 Synal H.-A., J. Beer, G. Bonani, Ch. Lukasczyk, and M. Suter. *^{36}Cl measurements at the Zürich AMS facility*, Nuclear Instruments and Methods in Physics Research, B92, 1994, P. 79
67 Kubo F. *Kosmogene Produktion von Radionukliden*, Dissertation, TUM, München, 2001
68 Grini A., G. Myhre, J.K. Sundet, and I.S.A. Isaksen. *Modeling the Annual Cycle of Sea Salt in the Global 3D Model Oslo CTM2: Concentrations, Fluxes, and Radiative Impact*, Journal of Climate, V. 15, N. 13, 2002, P. 1717-1730.
69 Calmet D., N. Coreau, P. Germain, F. Goutelard, P. Letessier, C. Frechou, D. Maro. *Chlorine-36 Measurement in the Near-field Environment of a Spent Nuclear Fuel Reprocessing Plant*, Radiochemical Measurements Conference in Honolulu, HI on 3-8 November 2001.
70 Graedel T.E., P.J. Crutzen *Chemie der Atmosphäre. Bedeutung für Klima und Umwelt*, Spektrum Akademischer Verlag, Heidelberg Berlin Oxford, 1994
71 Roedel W. *Physik unserer Umwelt: Die Atmosphäre*. Springer Vrlag, Berlin Heidelberg, 1994
72 Brewer, A.W. *Evidence for a world circulation provided by the measurements of helium and water vapor distribution in the stratosphere*. Quart. J. Roy. Meteor. Soc., V. 75, 1949, P. 351-363
73 Holton, J.R. *On the Global Exchange of Mass between sthe S|tratosphere and Troposphere*. Journal of the Stratospheric Sciences, V47, N3, 1990, P. 392-395
74 Holton J.R., P.H. Haynes, M.E. McIntyre, A.R. Douglass, R.B. Rood, L. Pfister. S*tratosphere-troposphere exchange*, Revs. Geophys., V. 33, 1995, P. 403-439
75 Raisbeck, G.M., F. Yiou, M. Fruneau, J.M. Loiseaux, M. Lieuvin, J.C. Ravel. *Cosmogenic ^{10}Be/^{7}Be as a probe of atmospheric transport processes*. Geoph. Res. Lett., V. 8, N. 9, 1981, P. 1015
76 Bentley, H.W., F.M. Phillips, S.N. Davis, S. Grifford, D. Elmore, L.E. Tubbs, and H.E. Gove *Thermonuclear ^{36}Cl pulse in natural waters*, Nature, V.300, 1982, P. 737

77 Mahlman J.D., H. Levy II, W.J. Moxim. *Three-dimensional tracer structure and behavior as simulated in two ozone precursor experiments*, J. Atmos. Sci., V. 37, 1980, P. 655-685

78 Mote P.W., Holton J.R., and Boville B.A., *Characteristics of stratosphere-troposphere exchange in a general circulation model*, J. Geophys. Res., V. 16, 1994, P. 16815-16829

79 Sachsenhauser, H., L Zerle, J. Beer, J. Masarik, and E. Nolte. *Atmospheric Transport of Cosmogenic Radionuclides.* Workshop Glaciers from the Alps: Climate and Environmental Archives, Wengen, Switzerland, 1996

80 Sachsenhauser H. *Atmosphärischer Transport von Radionukliden*. Diplomarbeit, TUM, München, 1996

81 Johnston, H.S., D. Kattenhorn, G. Whitten. *Use of Excess Carbon 14 Data to Calibrate Models of Stratospheric Ozone Depletion by Supersonic Transports.* Journal of Geophysical Research, V. 81, N. 3, 1976, P. 368

82 Johnston H. *Evaluation of Excess Carbon 14 and Strontium Data for Suitability to Test Two-Dimensional Stratospheric Models.* Journal of Geophysical Research, V. 94, N. D15, 1989, P. 18,485

83 McIntyre, M.E. *Atmospheric dynamics: some fundamentals, with observational implications*. In The Use of EOS for Studies of Atmospheric Physics, ed. J.C. Gille and G. Visconti, North-Holland, 313-386, 1992

84 Allam R.J. and A.F. Tuck. *Tranport of water vapour in a stratosphere-totposphere general circulation model I. Fluxes* Quart. J. Roy. Meteorol. Soc., V. 110, 1984, P. 321-356

85 Allam R.J. and A.F. Tuck, *Tranport of water vapour in a stratosphere-totposphere general circulation model II. Trajectories*, Quart. J. Roy. Meteorol. Soc., V. 110, 1984, P. 357-392

86 Keene, W.C., M.A.K Khalil., D.J Erickson III.,A. McCulloch., Th.E Graedel, J.M. Lobert, M.L. Aucott, S.L. Gong, D.B. Harper, G. Kleiman, P. Midgley, R.M. Moore, C. Seuzaret, W.T. Sturges, C.M. Benkovitz, V. Koropalov, L.A. Barrie, and Y.F. Li. *Composite global emissions of reactive chlorine from anthropogenic and natural sources: Reactive Chlorine Emission and Inventory*. Journal of Geophysical Research, V. 104, N. D7, 1999, P. 8429

87 Landsberg, H.E., J. Van Mieghem. *Proceedings of symposium on atmospheric diffusion and air pollution, held at Oxford, August 1958*. Advances in Geophysics, V. 6, 1959, P. 273.

88 Fabian, P., W.F. Libby, and C.E. Palmer. *Stratospheric Residence Time and Interhemispheric Mixing of Strontium 90 from Fallout in Rain*. Journal of Geophysical Research, V. 73, N. 204, 1968, P. 3611

89 UNSCEAR 2000. *Sources and effects of ionizing radiation*. Report to the General Assembly, V. 1, Annex C.

90 Shapiro, Ch.S., V.I. Kiselev, E.V. Zaitsev. *Nuclear Tests. Long Term Consequences in the Semipaoatinsk/Altai Region.* NATO ASI Series 2, Environment, Vol. 36, Springer. 1998.

91 Seifritz W. *Nukleare Sprengkörper – Bedrohung oder Energieversorgung für die Menschheit?* Thiemig, München, 1984

92 Adamskiy V.B., Smirnov Yu.N. *50-Megaton explosion over Novaya Zemlya*. The historical questions of natural sciences and technique, ? 3, 1995 (*in Russian*)

93 US-Japan joint reassessment of atomic bomb radiation dosimetry in Hiroshima and Nagasaki. Final Report. DS86. Radiation effects research foundation, V. 1, 1987.

94 Telegadas, K. and R.J. List. *Are Particulate Radioactive Tracers Indicative of Stratospheric Motions?* Journal of Geophysical Research, V. 74, N. 6, 1969.

95 England T.R. and B.F. Rider, LA-UR-94-3106, ENDF-349

96 Zerle, L., T. Faestermann, K. Knie, J. Beer, and E. Nolte. *The ^{41}Ca bomb pulse and atmospheric transport of radionuclides*. Journal of Geophysical Research, V. 102, N. D16, 1997, P. 19517

97 UNSCEAR Report to the General Assembly, UN Science Committee on the Effects of Atomic Radiation, New York, 1982

98 Joseph, A.B., P.F. Gustasson, I.R. Russel, E.A. Schuert, H.L. Volchok, A. Tamplin. *Radioactivity in the marine environment. Chapter 2: Sources of radioactivity and their characteristics*. National academy of Sciences, 1971.

99 Dunkerton, T. *On the Mean Meridional Mass Motions of the Stratosphere and Mesosphere*. Journal of the Atmospheric Sciences, V. 35, 1978, P. 2325-2333

100 Milton G.M., S.J. Kramer, T.G. Kotzer, J.C.D. Milton, H.R. Andrews, L.A. Chant, R.J. Cornett, W.G. Davies, B.F. Greiner, Y. Imahori, V.T. Koslowsky, J.W. McKay. *Cl36 – A potential paleodating tool*, Nuclear Instruments and Methods in Physics Research, B123, 1997, P. 371-377

101 Rhew R.C., B.R. Miller, R.F. Weiss, *Natuarl methyl bromide and methyl chloride emissions from coastal salt marshes*, Nature, V. 403, 2000, P. 292-295

102 Spivakovsky, C.M, J. A. Logan, S. A. Montzka, Y. J. Balkanski, M. Foreman-Fowler, D. B. A. Jones, L.W. Horowitz, A. C. Fusco, C. A. M. Brenninkmeijer, M. J. Prather, S. C. Wofsy, and M.B. McElroy. *Three-dimensional climatological distribution of tropospheric OH: Update and evaluation*, Journal of Geophysical Research, V. 105, 2000, P. 8931-80

103 Knie K. *Beschleunigermassenspektrometrie mit Isobarenseparation in einem dedizierten gasgefüllten Magneten*. Doktorarbeit, Technische Universität München, 1997

104 *Kubik, P.W., G. Korschinek, and E. Nolte.* Accelerator mass spectromentry with completely stripped ^{36}Cl ions at the Munich postaccelerator. Nuclear Instruments and Methods in Physics Research, B1, 1984, P. 51-59

105 Kubik, P.W., G. Korschinek, E. Nolte, U. Ratzinger, H. Ernst, S. Teichmann, and H. Morinaga. *Accelerator mass spectromentry of ^{36}Cl in limestone and some paleontological samples using completely stripped ions*. Nuclear Instruments and Methods in Physics Research, B5, 1984, P. 326

106 Nolte E., G. Geschonke, K. Berdermann, R. Oberschmid, R. Zierl, M. Feil, A. Jahnke, M. Kress, and H. Morinaga. *The Munich Heavy Ion Postaccelerator*. Nuclear Instruments and Methods, V. 158, 1979, P. 311

107 Wideroee, R. *Über ein neues Prinzip zur Herstellung hoher Spannungen*. Arch. Elektrotech., V. 21, 1928, P. 387

108 Alvarez. L.W., H. Bradner, J.V. Franck, H. Gordon, J.D. Gow, L.C. Marshall, F. Oppenheimer, W.K.H. Panofsky, C. Richman, J.R. Woodyard. Rev. Sci. Instr., V. 26, 1955, P. 111

109 Schiessl Ch., Wagner W., Hartel, P. Kienle, H.J. Koerner, W. Mayer, and K.E. Rehm *A Bragg-curve spectroscopy detector*. Nucler Instruments and Methods, V.192, 1982, P. 291

110 Lindhard J. and M. Scharff. *Energy dissipation in the keV region*. Phys. Rev., V.124, 1961, P. 128.

111 Lazarev V., A. Blinov, F. Kubo, Th. Huber, F. Slemr, and E. Nolte *Measurement of CH_3Cl in the atmosphere*. Jahresbericht, Beschleunigungslaboratorium der Universität und der Technischen Universität München, 1999, P.34

112 Khalil, M.A.K., R.M. Moore, D.B. Harper, J.M. Lobert, D.J.Erickson, V, Roropalov, W.T. Sturges, and W.C. Keene. *Natural emissions of chlorine-containing gases: Reactive Chlorine Emissions Inventory*. Journal of Geophysical Research, V. 104, N. D7, 1999, P. 8333

113 Khalil, M.A.K. *Reactive chlorine compounds in the atmosphere*, in The Handbook of Environmental Chemistry, edited by P. Fabian and O.N. Singh, Springer-Verlag, New York, 1998

114 International Lake Environment Committee Foundation (World Lake Database), http://www.ilec.or.jp/database/index/idx-lakes.html
115 Integrated Water Resource Management for Important Deep European Lakes and their Catchment Areas, http://pcs0.hydromod.de/Eurolakes/sites.html
116 Rossi G. *Il bilancio di massa del fosforo totale nei laghi di Como e di Garda,* Centro comune di Ricerca, 1993
117 Rossi G. *Modeling lake pollution*, Brussels-Luxemburg, 1991
118 *Ricerche sull'evoluzione del Lago Maggiore, Aspetti Limnologici*, Programma quinquennale 1993-1997, Campagna 1995 con sintesi degli anni 1993-1994. Commissione Internazionale per la protezione delle acque italo-svizzere.
119 Bayerisches Landesamt für Wasserwirtschaft.
120 Beadle L. C. *The inland waters of tropical Africa,* Longman, London and New York, 1981
121 Hecky H.E. et. al. In The Limnology, Climatology and Paleoclimatology of the East African Lakes ed. by Thomas C. Johnson and Eric O. Odada, Gordon and Breach Publishers, 1996
122 Shimaraev M.N., V.I. Verbolov, N.G. Granin, P.P. Sherstyankin. *Physical Limnology of Lake Baikal: a Review*, Baikal International Center for Ecological Research, Print No. 2, Irkutsk-Okayama, 1994.
123 Goulden, C. E. et al. *The Mongolian LTER: Hövsgöl National Park*. Korean J. Ecol., V. 23, 2000, P. 135-140.
124 Shaporenko S.I. *Balkhash lake*, in book Enclosed seas and large lakes of Eastern Europe and Middle Asia, pp. 155-197, ed. by A.F. Mandych, SPB Academic Publishing, Amsterdam, 1995
125 Tsigelnaya I.D. *Issyk-Kul' Lake*, in book Enclosed seas and large lakes of Eastern Europe and Middle Asia, pp. 199-229, ed. by A.F. Mandych, SPB Academic Publishing, Amsterdam, 1995
126 Shimaraev M. *Private communication*, 1999
127 Krauthan P. *Beschleunigermassenspektrometrie mit ^{36}Cl.* Diplomarbeit, Technische Universität München, 1988
128 *Atlas of caesium deposition on Europe after the Chernobyl accident*, Office for Official Publications of the European Communities, Luxembourg, 1998
129 Mangini, A., U. Christian, M. Barth, W. Schmitz, and H.H. Stabel. *Pathways and Residence Times of Radiotracers in Lake Constance*. In: Tilzer, M.M, and Serruya, C. (eds.): Large Lakes, Ecological Structure and Function.-Springer Verlad, Berlin, 1990, P. 245-264
130 Robbins, J.A., G. Lindner, W. Pfeiffer, J. Kleiner, H.H. Stabel, and P. Frenzel *Epilimnetic scavenging of Chernobyl radionuclides in Lake Constance*, Geochimica et Cosmochimica Acta, V. 56, 1992, P. 2339-2361
131 Konoplev A., Kaminski S., Klemt E. Konopleva I., Miller R., Zibold G. *Comparative study of ^{137}Cs partitioning between solid and liquid phases in Lakes Constance, Lugano and Vorsee*. Journal of Environmental Radioactivity, V. 58, 2002, P. 1-11.
132 *Ricerche sull'evoluzione del Lago di Lugano. Aspetti limnologici*. Programma quinquennale 1998-2002. Campagna 1999. Commissione internazionale per la protezione delle acque Italo-Svizere. LSA. 2000
133 Devell L., S. Güntay, and D.A. Powers *The Chernobyl reactor accident source term: development of a consensus view*, CSNI report of NEA/OECD, 1995
134 Synal, H.-A. *Private communications*, 2000
135 Reithmeier Herbert *Private communications*, 2002

136 Peeters F., R. Kipfer, R. Hohmann, M. Hofer, D.M.Imboden, G.G. Kodenev, and T. Khozder. *Modeling Transport Rates in Lake Baikal: Gas Exchange and Deep Water Renewal*. Environ. Sci. Technol, V. 31, N. 10, 1997, P. 2973-2982

137 Vollmer M.K., R.F. Weiss, R.T. Williams, K.K. Falkner, X. Qiu, E.A. Ralph, and V.V. Romanovsky. *Physical and chemical properties of the waters of saline lakes and their importance for deep-water renewal: Lake Issyk-Kul, Kyrgyzstan*, Geochim. Gosmochim. Acta, V. 66:24, 2002, P. 4235-4246

138 Romanovasky, V.V. *The Natural Complex of Lake Issyk-Kul*. Academy Nauk Kyrgyzstan, Frunze Ilim, 1990 (*in Russian*)

139 Ricketts R. D., T.C. Johnson, E.T. Brown, K.A. Rasmussen, V.V. Romanovsky. *The Holocene paleolimnology of Lake Issyk-Kul, Kygyzstan: trace element and stable isotope composition of ostracodes*. Palaeogeography, Palaeoclimatology, Palaeoecology, V. 176, 2001, P. 207 – 227

140 Lyons W.B., K.A. Welch, J.-C. Bonzongo, E.Y. Graham, G. Shabunin, H.E. Gaudette, R.J. Poreda *A preliminary assessment of the geochemical dynamics of Issyk-Kul Lake*, Kirghizstan, Limnol. Oceanogr, V. 46, N. 3, 2001, P. 713-718

141 Zekster I.S. *Groundwater discharge into lakes: a review of recent studies with particular regard to large saline lakes in central Asia*. International Journal of Salt Lake Research, V. 4, 1996, P. 233-249.

142 The regional Environmental Centre for Central Asia Ili-Balkhash Basin Sustainable Development Conception 7th International High-Level Seminar on Cleaner Production, Prague, Czeck Republic, April 29-30, 2002